

The impact of the corona measures on the air quality in Flanders

Justine Luca

Student number: 01604536

Promoters: Prof. Dr. Ir. Christophe Walgraeve, Prof. Dr. Ir. Jan Verwaeren

Tutor: Mr. Frans Fierens (Vlaamse Milieumaatschappij)

A dissertation submitted to Ghent University in partial fulfilment of the requirements for the degree of
Master of Science in Bioscience Engineering: Environmental Technology

Academic year: 2020-2021

Preface

I decided to do my master thesis on the impact of the corona measures on air quality in Flanders with the hope of getting some good news out of the corona crisis. After I had to return from my Erasmus experience in Bologna, due to corona, a lot of things changed. I think the pandemic affected many peoples life and we have long longed for the moment that our lives will start to get its normal rhythm again. Despite the bizarre year, I am very grateful that my thesis topic was approved and that it allowed me to learn a lot and get something insightful out of this crisis.

I would like to acknowledge Prof. Dr. Ir. Christophe Walgraeve for accepting my proposal with great enthusiasm and for guiding me so well in the beginning of the thesis and in the further progress of it. He made a lot of efforts to put me in contact with the VMM and thereby getting me started with the research. His expertise in air quality was a great support to achieve the proper results and conclusions.

Next, I would like to acknowledge Prof. Dr. Jan Verwaeren for helping me so well with the statistical part of the master thesis. I had never worked with random forest models and he helped me a lot with understanding the concept and applying it in the research. He also made the time to give feedback on my work and to guide me in the right direction.

I would also like to thank Frans Fierens. He was our contact person from the VMM and provided all the data necessary for this master thesis.

I also got a lot of support from my personal environment. Therefore, I would like to thank my parents and family for always encouraging me and giving me the chance to study in Ghent. I had to most amazing years in this city while completing my studies. I have met wonderful people in Ghent and I would also like to thank them this way for giving me so many beautiful moments, especially Maxim. Lastly, I would like to remember my beloved grandfather who lost the battle with corona this year. I hope that from some place he can, just as proud as he always was, witness me graduating.

Summary

The coronavirus was responsible for the introduction of a lockdown on 18 March 2020 in Flanders. This led to a lot of measures, the so-called corona measures, which prevented people from leaving their homes and they had to very strictly limit their social contact. The amount of traffic decreased on the roads in Flanders during the COVID-19 lockdown. Traffic is a source of various air pollutants and therefore it was aimed with this master thesis to investigate whether the corona measures had an influence on the air quality in Flanders. More specifically, it was aimed to investigate the impact on the concentrations of the traffic-related pollutants NO, NO₂ and O₃ at four different measuring stations. Each station is linked with another type of traffic situation. A background situation in Veurne, an urban-background situation in Ghent and finally two urban-traffic situations in Brussels, one in the city center and one in Sint-Jans-Molenbeek, were chosen. The same type of study was performed by the VMM in 2020 and this master thesis aims to build on their results. It is important when investigating the impact of an anthropogenic event, like the COVID-19 lockdown, on air quality that other influencing factors are also taken into account. One major factor in determining the air pollutant concentrations in the atmosphere is weather. The influence of the weather conditions was isolated by using a random forest model. The random forest model finds the relation between the weather parameters and the air pollutant concentrations from a training dataset. A specific model was constructed for each pollutant at each location. In order to construct these models, data were needed on the air pollutants concentrations and the weather variables. These were provided by the VMM. The training dataset for each model consists out of hourly data from 01/01/2015 – 31/12/2019. Predictions can then be made for the pollutants in 2020 based on data on the weather conditions in 2020. By comparing the predictions made for the period of the lockdown with the measured concentrations in that period, the impact of the corona measures may be observed. The results for the background station show no clear impact of the corona measures on the pollutant concentrations. The NO_x concentrations and the O₃ concentrations decreased in that station during the lockdown. This could be attributed to the less favorable weather conditions during the first month of the lockdown. At the urban-background and urban-traffic locations, an impact was seen on the air pollutant concentrations. The NO_x concentrations decreased during the lockdown due to the lower NO emissions coming from traffic in that period. On the contrary, the O₃ concentrations increased during the lockdown due to the lower NO concentrations, which are responsible for O₃ titration. In addition, the impact was investigated on the daily patterns of the pollutants. Again, no clear difference was seen in the background location. At the other locations, no clear difference was seen in the trend of the NO-profile that shows a peak at 7 a.m. related to the traffic peak hour and stable concentrations throughout the rest of the day. However, the peak was much smaller during the lockdown. The NO₂-profile at these stations in normal conditions shows a bimodal pattern with a peak in the morning and in the evening with the same magnitude, also related with the traffic peak hours. During the lockdown, this bimodal pattern was also seen but the last peak is smaller than the first peak, and both the peaks reach lower concentrations. The O₃-profile showed much higher peak concentrations in the afternoon compared with the previous years. It was also found that the daily patterns were different on a week day compared with a weekend day in Sint-Jans-Molenbeek but the impact of the corona measures on the daily patterns was the same, i.e. the same trends in the profiles but lower concentrations for NO_x and higher concentrations for O₃.

Samenvatting

Het coronavirus was verantwoordelijk voor de invoering van een lockdown op 18 maart in 2020 in Vlaanderen. Dit leidde tot heel wat maatregelen, de coronamaatregelen, waardoor mensen hun huis niet konden verlaten en hun sociale contacten uiterst moesten beperken. Tijdens de lockdown nam de verkeersdruk op de Vlaamse wegen af. Het verkeer is een bron van verschillende luchtverontreinigende stoffen. Het doel van deze masterproef was om te achterhalen of de coronamaatregelen invloed hebben gehad op de luchtkwaliteit in Vlaanderen. Meer specifiek werd de impact op de concentraties van de verkeersgerelateerde pollutanten NO, NO₂ en O₃ onderzocht in vier verschillende meetstations. Elk getypeerd door een verschillende verkeerssituatie. Er werd gekozen voor een achtergrondsituatie in Veurne, een stedelijke achtergrondsituatie in Gent en tenslotte twee stedelijke-verkeerssituaties in Brussel, één in het centrum en één in Sint-Jans-Molenbeek. Eenzelfde studie werd reeds uitgevoerd door de VMM in 2020. Deze masterproef zal voortbouwen op hun resultaten. Wanneer de impact van een antropogene gebeurtenis, zoals de COVID-19 lockdown, op de luchtkwaliteit wordt onderzocht, is het belangrijk rekening te houden met andere factoren die ook een invloed kunnen hebben. Een belangrijke factor die bepalend is voor de concentraties van de pollutanten in de atmosfeer is het weer. De invloed van weersomstandigheden kan geïsoleerd worden door gebruik te maken van een random forest model. Het model zoekt de relatie tussen de weersvariabelen en de concentraties van de luchtpolluenten uit een trainingsdataset. Voor elke pollutant op elke locatie werd een specifiek model geconstrueerd. Om dit te doen waren gegevens nodig van de concentraties van de pollutanten en de weersvariabelen. Deze werden verkregen door de VMM. De trainingsdataset voor elk model bestaat uit uurwaarden van de periode 01/01/2015 - 31/12/2019. Op basis van de weerscondities in 2020 kunnen vervolgens voorspellingen worden gemaakt voor de concentraties van de verontreinigende stoffen in 2020. Door de voorspellingen te vergelijken met de gemeten concentraties in de lockdown kan het effect van de coronamaatregelen worden waargenomen. De resultaten voor het achtergrondstation tonen geen duidelijk effect van de coronamaatregelen op de concentraties. De NO_x-concentraties en O₃-concentraties daalden in dit station tijdens de lockdown. Dit kan worden toegeschreven aan de minder gunstige weersomstandigheden tijdens de eerste maand van de lockdown. Op de andere locaties werd er wel een effect op de concentraties van de pollutanten vastgesteld. De NO_x-concentraties daalden tijdens de lockdown als gevolg van de lagere NO-emissies. Daarentegen stegen de O₃-concentraties tijdens de lockdown door de lagere NO-concentraties, die verantwoordelijk zijn voor O₃-titratie. Verder werd het effect op de dagelijkse patronen van elke pollutant onderzocht. Opnieuw werd geen duidelijke impact vastgesteld op de achtergrondlocatie. Op de andere locaties werd er geen verschil waargenomen in de trend van het NO-profiel. Dit is namelijk een piek om 7 uur 's ochtends, die gelinkt is met de ochtendspits, en stabiele concentraties gedurende de rest van de dag. Die piek was echter veel kleiner tijdens de lockdown. Het NO₂-profiel bij deze stations in normale omstandigheden vertoont een bimodaal patroon met een piek 's ochtends en 's avonds van dezelfde grootte, die opnieuw gelinkt zijn met spitsuren. Tijdens de lockdown was dit patroon ook aanwezig maar de laatste piek was kleiner dan de eerste en beide pieken bereikten lagere concentraties. Het O₃-profiel vertoonde veel hogere piekconcentraties in de namiddag in vergelijking met vorige jaren. De dagpatronen op een weekdag waren anders dan op een weekenddag in Sint-Jans-Molenbeek, maar het effect van de coronamaatregelen op de dagpatronen was hetzelfde. Namelijk dezelfde trends in de profielen maar lagere concentraties voor NO_x en hogere concentraties voor O₃.

List of Abbreviations

AAQ	Ambient Air Quality
API	Advanced Pollution Instrumentation
AQI	Air Quality Index
ATD-GC	Automated thermal desorption gas chromatography
BAU	Business As Usual
BeLAQI	Belgium Air Quality Index
BLH	Boundary layer height
BTEX	Benzene, toluene, ethylbenzene and xylenes
CMAQ	Community Multi-scale Air Quality
COVID-19	Coronavirus disease 2019
CTM	Chemical Transport Models
DID	Difference-in-difference
EAP	Environment Action Program
ECWMF	European Centre for Medium-Range Weather Forecasts
EEA	European Environmental Agency
EU	European Union
GEOS-5	Goddard Earth Observing System, Version 5
GMAO	Global Modeling and Assimilation Office
HPLC	High- performance liquid chromatography
HRAPIE	Health risks of air pollution in Europe
LRTAP	Long-Range Transboundary Air Pollution
MCC	Medium cloud cover
MSE	Mean squared error
NASA	National Aeronautics and Space Administration
NEC	National Emission Ceilings
NMVOG	Non-methane volatile organic compound
O(1D)	Excited oxygen
PM	Particulate matter
PM₁₀	Particulate matter with a diameter less than 10 μm
PM_{2.5}	Particulate matter with a diameter less than 2.5 μm
R²	R-squared
RH	Relative humidity
RMSE	Root mean squared error
RSS	Residual sum of squares
SARS-CoV-2	Severe Acute Respiratory Syndrome CoronaVirus-2
SD	Standard deviation
SDG	Sustainable Development Goal
STL	Seasonal and Trend decomposition using Loess
T	Temperature
T_{max}	Maximum temperature
T_{min}	Minimum temperature
TOFP	Tropospheric ozone forming potential
TS	Thermo Scientific
U.K.	United Kingdom
UN	United Nations
UNECE	United Nations Economic Commission for Europe
UPLC-UV	Ultra Performance Liquid Chromatography UV-absorption
US EPA	United States Environmental Protection Agency
UV	Ultraviolet
VMM	Vlaamse Milieumaatschappij
VOC	Volatile organic compounds

WD	Wind direction
WHO	World Health Organization
WS	Windspeed
WS_{max}	Maximum windspeed
WS_{min}	Minimum windspeed
λ	Wavelength
<i>h</i>ν	Sunlight

Table of Contents

PREFACE	I
SUMMARY	II
SAMENVATTING	III
LIST OF ABBREVIATIONS	IV
TABLE OF CONTENTS	VI
1. INTRODUCTION	1
1.1. CONTEXT AND MOTIVATION.....	1
1.2. OBJECTIVES.....	2
2. GUIDELINE VALUES FOR GOOD AIR QUALITY	3
2.1. EUROPEAN AIR QUALITY STANDARDS.....	3
2.2. GLOBAL AIR QUALITY STANDARDS	5
2.3. AIR QUALITY POLICY OF FLANDERS	6
3. IMPORTANT GASEOUS AIR POLLUTANTS	7
3.1. PRIMARY POLLUTANTS.....	7
3.1.1. VOC's.....	7
3.1.2. NO _x	8
3.1.3. SO ₂	9
3.1.4. NH ₃	10
3.2. SECONDARY POLLUTANTS.....	10
3.2.1. Ozone	11
4. MONITORING NETWORKS FOR AIR POLLUTANTS	15
4.1. MONITORING NETWORKS IN FLANDERS	15
4.2. ANALYTICAL METHODS	16
4.2.1. O ₃	16
4.2.2. NO _x	17
4.2.3. VOC's.....	17
5. DETERMINING THE IMPACT OF ANTHROPOGENIC EVENTS ON AIR QUALITY	19
5.1. BEFORE-AND-AFTER EVALUATION	19
5.1.1. Quantitative evaluation.....	19
5.1.2. Qualitative evaluation	21
5.2. MODEL-BASED APPROACHES TO ACCOUNT FOR WEATHER INFLUENCES.....	23
5.2.1. Influence of weather conditions	23
5.2.2. Machine learning: Random Forest.....	25
5.2.3. Deterministic models	28
6. DATA COLLECTION AND PRE-PROCESSING	29
6.1. DATA COLLECTION.....	29
6.1.1. Background location: Veurne.....	31
6.1.2. Urban-background location: Ghent, Baudelopark	31
6.1.3. Urban-traffic location: Brussels, Kunst-Wet.....	31
6.1.4. Urban-traffic location: Brussels, Sint-Jans-Molenbeek.....	32
6.2. DATA PRE-PROCESSING	32
6.2.1. Meteorological data.....	32
6.2.2. Air pollutant concentrations data.....	34
6.2.3. Traffic data.....	34
6.2.4. Final dataset	34
7. RESULTS AND DISCUSSION	36

7.1.	BEFORE-AND-AFTER EVALUATION	36
7.2.	MODEL VALIDATION AND INTERPRETATION	43
7.3.	RESULTS BASED ON MODEL SIMULATIONS	49
7.3.1.	<i>Background location: Veurne</i>	49
7.3.2.	<i>Urban-background location: Ghent, Baudelopark</i>	55
7.3.3.	<i>Urban-traffic location: Brussels, Sint-Jans-Molenbeek</i>	59
7.3.4.	<i>Urban-traffic location: Brussels, Kunst-Wet</i>	67
8.	CONCLUSION	71
9.	BIBLIOGRAPHY	73

1. Introduction

1.1. Context and motivation

Air quality is a widely discussed topic as it affects human health and the health of other living organisms and ecosystems. Air quality is a way of expressing how much the air is polluted, i.e. good air quality equals a low level of air pollution. Exposure to high concentrations of hazardous air pollutants on short term or low concentrations on long term are associated with various negative health effects including chronic and acute cardiovascular and respiratory diseases such as cancer and asthma. Exposure during pregnancy can even lead to birth defects (Kampa & Castanas, 2008). Routes of exposure are inhalation, through breathing of the contaminated air, and ingestion. After deposition of the air pollutants, humans and organisms may absorb the substances via contaminated water or food.

The WHO (2018) reports that in 2016, 91% of the world's population lived in areas where the air quality levels, that they provide as guidelines, had not been achieved. The European Environment Agency (EEA) (2013) states that ecosystems are threatened through damage of vegetation by high ozone concentrations, eutrophication and acidification due to high nitrogen dioxide and sulphur dioxide concentrations in the air. Lelieveld et al. (2019) estimated that air pollution was responsible for 8.8 million premature deaths due to effects of air pollution in 2015, using a statistical model and data from the WHO (World Health Organization). In their study the focus was on two pollutants, namely ozone (O₃) and particulate matter with a diameter less than 2.5 µm (PM_{2.5}). Because they are the ones that cause serious health effects. There are, however, other substances that are also responsible for the pollution of ambient air. Daly & Zannetti (2007) define an air pollutant as “any substance emitted into the air from an anthropogenic, biogenic, or geogenic source, that is either not part of the natural atmosphere or is present in higher concentrations than the natural atmosphere, and may cause a short-term or long-term adverse effect.”. Whereby biogenic sources are living organisms emitting harmful substances and geogenic sources include volcanic eruptions, forest fires, sandstorms, etc. The increasing emissions into the atmosphere by mankind caused a major increase in the problem of air pollution on local scale but also on global scale. In a world of globalization, poor local air quality is not only attributable to local emission sources. International trade has made air pollution a global problem and a variety of sectors are contributing to this. The largest emission sectors are industry, energy production, agriculture and transport, including traffic (Zhang et al., 2017).

Anthropogenic events may influence air quality. In 2020, with the appearance of the coronavirus, also known as SARS-CoV-2 (Severe Acute Respiratory Syndrome CoronaVirus-2), an exceptional anthropogenic event occurred around the entire world. The virus appeared in December 2019 in the city Wuhan in China. The virus is responsible for the coronavirus disease (COVID-19) which is highly infectious and causes respiratory illness (Lai et al., 2020). It spreads between humans, across all age classes, via droplets produced by talking, coughing or sneezing and via direct contact. On 11 march 2020, COVID-19 was declared a pandemic by the WHO (WHO, 2020). Serious measures were needed worldwide to stop or at least slow down the spread of the virus to make sure that health care can keep up with the number of infected people and that everyone can receive the appropriate medical support.

In order to guarantee this, many countries decided to go into lockdown. The city of Wuhan went into lockdown as early as January 2020 due to the huge number of infections at this epicenter of the pandemic (Ren, 2020). The first corona infection in Belgium was diagnosed on 3 February when 9 Belgians were repatriated from Wuhan, China. One person tested positive, the other 8 negative (Metro, 2020). On 29 February, a second infection appeared in Belgium, at that time the situation in Lombardy (northern Italy) was very serious, with several cities already quarantined (Guan et al., 2020). On 9 March 2020, Italy was the first country in Europe to announce a national lockdown (Gualano et al., 2020). Shortly after that, the presence of the virus in all of Belgium was a fact and its spread was extremely rapid. Experts feared that the number of infected people to be admitted to intensive care would exceed the capacity of the hospitals. To prevent this, the National Security Council decided that Belgium would go into lockdown on 18 March 2020. This decision involves many measures for the Flemish population, the so-called 'corona measures'. The main purpose of these measures is to limit social contact. This is done by introducing the prohibition on gathering together and closing borders, schools, restaurants, bars, non-essential shops and so many other things. Teleworking became the standard and it was forbidden to move over long distances. As a result of these measures, various activities of the emission sectors were halted in the period of the lockdown including a reduction of the amount of traffic. Teleraam, a Flemish platform that collects data from citizens on traffic in their own neighborhood, reports that in the first week of the lockdown there was a 50% drop in traffic on the local roads, this trend persisted in the following weeks (Beeckman, 2020). With this drop in traffic, the emissions of traffic-related air pollutants in the atmosphere decreased.

1.2. Objectives

This study aims to investigate the impact of the corona measures on the air quality in Flanders. More specifically, the focus will be on the impact of the reduction in traffic due to the COVID-19 lockdown on the concentrations in the air of the gaseous air pollutants related with traffic, i.e. NO_x (nitrogen oxides) and O_3 (ozone). In order to identify the influence related with the corona measures, other parameters that influence air quality have to be isolated. Weather conditions play an important role in air pollution and the influence of weather conditions can be isolated by using a random forest model. Predictions will be made of the concentrations of these substances for the period of the lockdown based on data on the weather conditions. These predictions will then be compared with the measured concentrations during that period to investigate the impact of the corona measures. In particular, it is aimed to find out if the measured concentrations of each pollutant are higher or lower than predicted with the model. Additionally, it is aimed to find out if the COVID-19 lockdown had influence on the daily patterns of these substances. The overall objective can be stated as: "Will air quality improve if the amount of traffic reduces abruptly due to anthropogenic events?". In order to perform this study, a lot of data on the concentrations of these pollutants and on the weather conditions is necessary. With the support of the *Vlaamse Milieumaatschappij, VMM* (The Flemish Environment Agency) it was possible to carry out the data collection on four different locations. Each location represents another type of traffic situation, including a background location and a location with a high amount of traffic. By including different types of locations in this study, it is aimed to compare the impact on the concentrations of the air pollutants during the lockdown for each location.

2. Guideline values for good air quality

Flanders is still facing the problem of premature deaths due to air pollution. The VMM (2020) estimated that in 2018 on average 4800 people died prematurely due to effects caused by PM_{2,5}, 1500 by NO₂ and 200 by O₃. Hence the importance of Flanders tackling the problem of bad air quality through legislation. As stated earlier, air pollution is a global problem. Therefore it needs to be tackled on local, regional, national and international level. Goals and guidelines for good air quality exist both on global level and on European level, these will be discussed in this chapter.

2.1. European air quality standards

Since the 1970s, the European Union (EU) has been tackling the problem of bad air quality by controlling the emissions of hazardous substances into the atmosphere, improving the fuel quality, and by integrating environmental protection requirements into the transport and energy sectors (European Commission, n.d.). The EU does this by defining targets and guiding the European environment policy with the Environment Action Programs (EAP). The European Commission (2019b) reports in their evaluation of the 7th EAP, which ended in 2020, that the programme provides a strategic framework that has successfully established the narrative of environment policy as a driver for green growth, a healthy planet and improved wellbeing for individuals. Additionally, general awareness of the fact that environmental protection goes hand in hand with a sustainable economic model that creates jobs and prosperity has increased.

The EU provides various directives and strategies for its Member States, including Belgium. The Directive 2001/81/EC, i.e. the National Emission Ceilings (NEC) Directive, was introduced in 2001 (Europese Unie, 2021). This directive contains specific ceilings, i.e. emission limits, for four pollutants (SO₂, NO_x, non-methane VOCs, and NH₃) for each country to be attained by 2010 in order to achieve a better air quality in Europe. The Member States have to develop a national programme to ensure the emission ceilings aren't exceeded and they have to make up emission inventories and report them every year to the European Commission and the EEA (European Parliament & Council of the European Union, 2001).

In 2004 and 2008, the European Commission additionally announced general air quality guidelines to be followed by all Member States with the Ambient Air Quality (AAQ) Directives, i.e. Directive 2004/107/EC and 2008/50/EC (EU, 2004; EU, 2008; Europese Unie, 2020)(EU, 2008). The former addresses the guidelines for arsenic (As), cadmium (Cd), nickel (Ni) and benzo[a]pyrene present in the fraction of PM₁₀. The latter discusses the guidelines for sulphur dioxide (SO₂), nitrogen dioxide (NO₂) and oxides of nitrogen (NO_x), particulate matter (PM), lead (Pb), benzene, carbon monoxide (CO) and ozone (O₃). These standards are given in Table 1. Also the conditions to be complied with when monitoring and assessing air quality are specified in these documents (DG Sante, 2015). Another aim of these directives is to make air quality information public. The Member States themselves must ensure compliance with the directives and provide sanctions in case of violation of the limits that have been imposed.

Table 1: European air quality standards for the different air pollutants (EU, 2004; EU, 2008)

Pollutant	Concentration	Averaging period
PM₁₀	50 µg/m ³	24 hours
	40 µg/m ³	1 year
PM_{2.5}	25 µg/m ³	1 year
SO₂	350 µg/m ³	1 hour
	125 µg/m ³	24 hours
NO₂	200 µg/m ³	1 hour
	40 µg/m ³	1 year
CO	10 µg/m ³	Maximum daily 8 hour mean
O₃	120 µg/m ³	Maximum daily 8 hour mean
Benzene	5 µg/m ³	1 year
Pb	0.5 µg/m ³	1 year
As	6 ng/m ³	1 year
Cd	5 ng/m ³	1 year
Ni	20 ng/m ³	1 year
Benzo[a]pyrene	1 ng/m ³	1 year

Despite the fact that SO₂ emissions were reduced with 82 %, NO_x emissions with 47 %, non-methane VOC emissions with 56 % and NH₃ emissions with 28 % in Europe between 1990 and 2010, poor air quality stays a serious problem. Therefore, the EU has decided to set up a Clean Air Policy package in 2013 to engage the Member States even more to achieve the objectives. This package includes a Clean Air Programme that should guarantee that by 2030, and compared to business as usual, 58 000 premature deaths are avoided, 123 000 km² of ecosystems and 56 000 km² protected Natura 2000 areas are saved from nitrogen pollution and 19 000 km² forest ecosystems are saved from acidification. The European Commission (2013) claims this will not only benefit the environment and human health but also the economic growth due to cost savings related to higher productivity of the workforce, lower healthcare costs, higher crop yields and less damage to buildings. The package also revises the NEC Directive and extends the horizon of this policy from 2010 to 2030. In 2016 the new NEC Directive was completed, with emission ceilings for each Member State to be achieved by 2030, also ceilings for PM_{2.5} are included. The emission reduction goals for Belgium are listed in Table 2 (European Parliament and Council, 2016).

Table 2: Emission reduction commitments for Belgium (European Parliament and Council, 2016).

SO₂ reduction compared with 2005		NO_x reduction compared with 2005		NMVOC reduction compared with 2005		NH₃ reduction compared with 2005		PM_{2.5} reduction compared with 2005	
For any year from 2020 to 2029	For any year from 2030	For any year from 2020 to 2029	For any year from 2030	For any year from 2020 to 2029	For any year from 2030	For any year from 2020 to 2029	For any year from 2030	For any year from 2020 to 2029	For any year from 2030
43%	66%	41%	59%	21%	35%	2%	13%	20%	39%

By 2050, the EU wants to be climate-neutral. For this purpose, an action plan has been developed, the Green Deal. All sectors of the economy must cooperate in order to make the full transition to a circular economy, restore biodiversity and reduce pollution. Financial and technical assistance will be provided by the EU (European Commission, 2020a). To achieve the objectives in the agenda of the Green Deal, on 14 October 2020 the European Commission (2020c) submitted a proposal for an 8th EAP to guide the environment policy until 2030. With all this, Europe wants to set an example for the rest of the world.

2.2. Global air quality standards

Reducing air pollution is part of the 2030 agenda for Sustainable Development of the United Nations (UN) (2020a). In 2015, the Sustainable Development Goals (SDG's) were implemented by all the UN Member States, including Belgium. The Decade of Action started in 2020. In this decade, all the nations should be encouraged to accelerate collective efforts to achieve the SDG's by 2030. Improving air quality to meet the guideline values established by the WHO contributes to several of the SDG's, these are given in Figure 1. Good air quality ensures a better quality of life and therefore contributes to the third SDG that covers good health and well-being. Air pollution is related to climate change through different processes. Some of the pollutants stimulate global warming while particulate matter improves global dimming. Therefore, the thirteenth SDG, i.e. climate action, is of relevance. Due to the atmospheric deposition of pollutants, land and water are negatively affected by air pollution. Hence the importance of SDG 6, 14 and 15, i.e. respectively clean water and sanitation, life below water and life on land. As mentioned before, the reduction of air pollution contributes to economic growth and thus the SDG 8.



Figure 1: SDG's that benefit from improving air quality (United Nations, 2020a).

The WHO (2005) has been providing standards to achieve a better global air quality since 1987 and these were last updated in 2005. The air quality guidelines include target values for particulate matter (PM₁₀ and PM_{2.5}), O₃, NO₂ and SO₂. These are given in Table 3. In 1979, Belgium signed up with the Long-Range Transboundary Air Pollution (LRTAP) Convention, as a UNECE (United Nations Economic Commission for Europe) member state. The Convention comprises 8 protocols and a biennial workplan is drawn up for the member states with activities to follow in order to reduce transboundary atmospheric pollution (ECE, 2019). The workplan for 2020-2021 contains priorities for the long-term strategy for 2020-2030 and beyond (ECE, 2019).

Table 3: WHO guidelines for PM, O₃, NO₂ and SO₂ (WHO, 2005)

<i>PM</i>		<i>O₃</i>	<i>NO₂</i>	<i>SO₂</i>		
<i>PM_{2.5}</i>	<i>PM₁₀</i>					
10 µg/m ³ annual mean	20 µg/m ³ annual mean	100 µg/m ³ 8-hour mean	40 µg/m ³ annual mean	200 µg/m ³ 1-hour mean	20 µg/m ³ 24-hour mean	500 µg/m ³ 10-minute mean
25 µg/m ³ 24-hour mean	50 µg/m ³ 24-hour mean					

2.3. Air quality policy of Flanders

Flanders has proved that its air quality policy has been successful over the years. Reductions of various gaseous air pollutants are observed compared with the concentrations in 1983, this is visualized in Figure 2 for NO, NO₂, SO₂, CO, O₃ and benzene. It can be seen that the annual O₃ concentrations increased over the years but that the O₃ maximum 8 hour values has decreased.

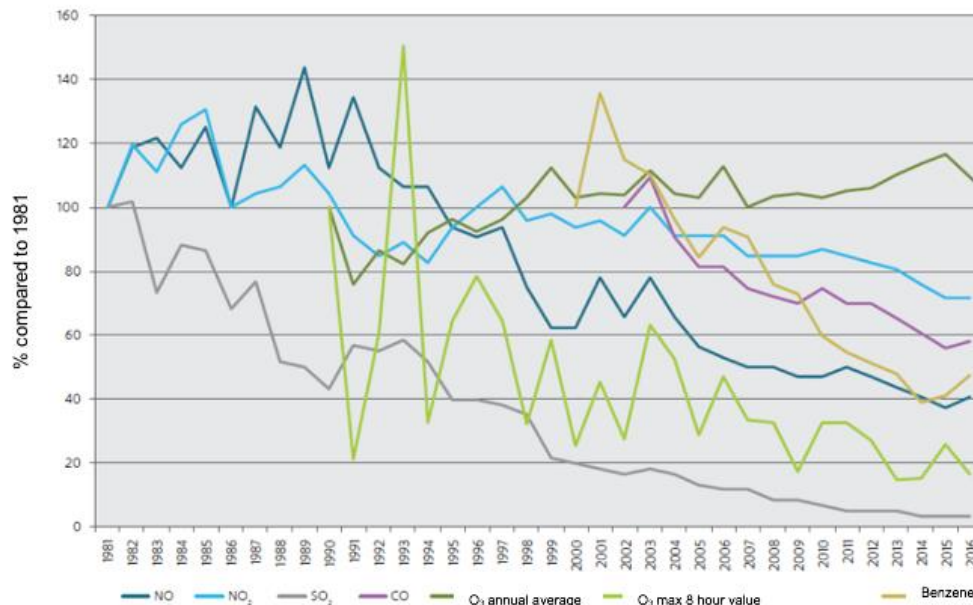


Figure 2: Reductions of the gaseous air pollutants in Flanders compared to the concentrations in 1981 (VMM, 2020b).

However, there are still exceedances of the guidelines imposed by Europe and the WHO for some substances. The main challenges of Flanders are to further reduce the concentrations of NO_x, PM and NH₃. With the Air policy plan 2030, Flanders wants to tackle these challenges (VMM, 2020b). The plan must lead to the achievement of all the goals for Flanders in the short term, by 2030 and by 2050. The short-term goals are not exceeding the European air quality standards and/or target values anywhere in Flanders and meeting the emission ceilings for 2020 defined in the NEC Directive. In 2030, Flanders must reach the emission ceilings of the NEC directive for 2030. The aim is to halve the health impact from air pollution, as estimated by the WHO, compared with 2005. The area of ecosystems where the carrying capacity for eutrophication or acidification is exceeded must also be reduced by a third compared with 2005. By 2050, air pollution from anthropogenic sources, such as industry, agriculture and traffic, must be drastically reduced in order that the air quality in Flanders complies with the guidelines defined by the WHO (Departement Omgeving Vlaanderen, 2019). Specific guidelines are set up for the different sectors that contribute to the pollution of air, i.e. the transport sector, the industry sectors, the agricultural sector, the households and tertiary sectors. With the present measures, Flanders believes it will achieve its goals in the future.

3. Important gaseous air pollutants

The aim of this thesis is to investigate the impact on air quality during the lockdown. Therefore, knowledge about the most important pollutants that determine air quality is necessary. First, the primary gaseous pollutants VOC's (volatile organic compounds), NO_x (nitrogen oxides), SO₂ (sulphur dioxide) and NH₃ (ammonia) will be discussed in this chapter. The sources of these pollutants and the evolution of the concentrations in Flanders over the years will be described. Further, the possible harmful effects related with elevated concentrations of these pollutants will be identified. Additionally, the primary pollutants VOC's and NO_x are related to the formation of the secondary pollutant O₃ in the troposphere (Krupa & Manning, 1988). This topic will be covered in the second part of this chapter. Particulate matter and heavy metals are also important air quality indicators but are out of the scope of this thesis.

3.1. Primary pollutants

Primary pollutants are emitted directly by a source and enter the atmosphere. Afterwards, they can be dispersed and diluted. This way, the negative effects caused by the pollutants can be diminished for the surrounding environment and people near the sources. Reactive pollutants can be transformed rapidly in the atmosphere near the source and more stable pollutants can be transported over large distances (Sitaras & Siskos, 2008). The primary pollutants can be subject to various reactions in the atmosphere and serve as precursors for secondary pollutants.

3.1.1. VOC's

Volatile organic compounds include a range of substances with a high vapor pressure which allows them to evaporate and diffuse quickly into the atmosphere. A substance is considered to be a VOC if its vapor pressure is higher than 0.01 kPa at atmospheric conditions. Based on the definition they are volatile and mostly present in the gas phase (Atkinson, 1998; Van Langenhove & Walgraeve, 2019). Frequently, methane is considered separately since it is less potent in the formation of ozone. Nevertheless, it is an important compound because of its role as greenhouse gas rather than its role as an air pollutant. Hence, the term non-methane volatile organic compounds (NMVOC's) when discussing air pollutants (Vlaamse Milieumaatschappij, 2020b). NMVOC's are partially released in the atmosphere with the combustion of fossil fuels in motor vehicles. However, in 2018, only 7% of the VOC emissions were related with traffic due to stringent emission standards for vehicles. Other emission sectors in Flanders are agriculture (the housing of cattle, pigs and poultry and their manure storage), industrial processes (coating, solvent use,...), households (use of fossil fuels for heating, paints, glues and other products) and the energy sector (petroleum refineries as main source). Each responsible for respectively 26%, 24%, 16% and 4% of the NMVOC emissions in 2018 (Vlaamse Milieumaatschappij, 2020a; VMM, 2020b; Vlaamse Milieumaatschappij, 2020d). Other anthropogenic sources are fuel storage at service stations, fuel transport, landfills and other waste facilities. The presence of NMVOC's in paints, glues and other products for private or professional use leads to indoor air pollution (Atkinson, 1998; Barletta et al., 2005; Thurston, 2017). NMVOC's are also released by biogenic sources such as vegetation, soils and oceans. These sources were responsible for 20% of the emissions in 2018.

This group of air pollutants is important since they include various harmful, sometimes carcinogenic, substances. VOC's include carbonyl compounds such as formaldehyde (HCHO) and acetaldehyde (CH₃CHO), aromatic compounds as BTEX (benzene, toluene, ethylbenzene and xylene isomers) and chlorinated VOC's as tetrachloroethene (C₂Cl₄) and vinyl chloride. In addition, VOC's can form secondary organic aerosols which lead to secondary particulate matter that is responsible for severe adverse health effects on human beings (Sharma & Agarwal, 2018). Since 2010, Belgium has been meeting the proposed NEC-emission ceilings for NMVOC's. The emissions were reduced with 44% in 2018 as compared to 2000. Efforts in the energy, industry and traffic sectors caused the decline in NMVOC's concentrations. These efforts include, process optimization and more efficient use of energy with new developed clean technologies. Additionally, stricter policy measures were introduced regarding NMVOC emissions, the use of solvents (including prohibition of certain solvents) and the protection of storage tanks. Clean-up techniques, such as waste gas treatment and the use of catalysts in cars, also helped to decrease the emissions of NMVOC's (Vlaamse Milieumaatschappij, 2020b).

3.1.2. NO_x

Nitrogen oxides (NO_x) cover the substances nitrogen oxide (NO) and nitrogen dioxide (NO₂). The two are paired together in one category, i.e. NO_x, as most atmospheric NO₂ is derived from NO emissions (Harrison, 2005). These compounds are emitted during high temperature combustions of fossil fuels in stationary sources, e.g. power plants, and mobile sources, e.g. motor vehicles (EEA, 2013). The transport sector was responsible for 61% of the NO_x emissions in Flanders in 2018, 17% was related with industry, 6% came from the energy sector, 8% from agriculture and horticulture with the use of manure and 8% resulted from other sources (VMM, 2020b). Natural sources of NO and NO₂ are bacterial activities in soils, forest fires and lightning (Atkinson, 1998). Pronobis (2020) illustrates with Figure 3 how nitrogen present in solid and liquid fuels is converted into nitrogen oxides during combustion at high temperatures, i.e. the formation of fuel NO_x. The fuel nitrogen decomposes in the combustion flame to form intermediate nitrogen compounds such as HCN, CN, CNO, NH₃ and NH. In presence of oxygen compounds, the nitrogen compounds are oxidized to NO, see path A in Figure 3. The more oxygen that is available during the combustion the more NO that will be produced. Reduction from NO to N₂ can take place in the combustion chamber, see path B in Figure 3.

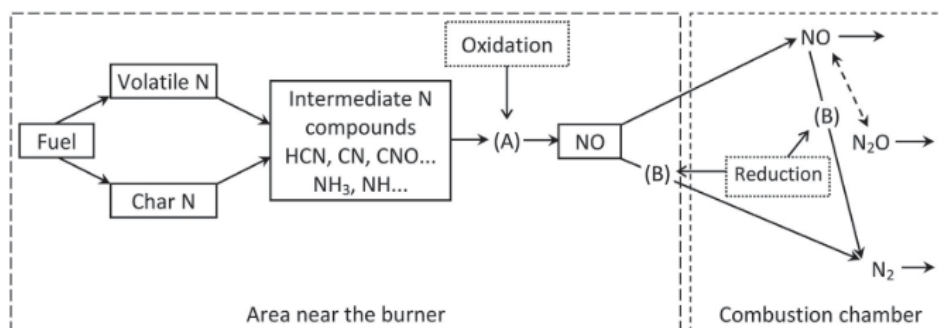
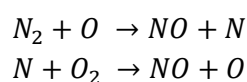
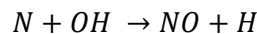


Figure 3: Conversion of fuel nitrogen into nitrogen oxides (Pronobis, 2020).

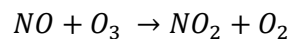
Even more important is the production of thermal NO_x during combustion with the reaction of gaseous nitrogen and oxygen:



In reducing conditions in the combustion chamber, the following reaction also gives NO:



Hydrocarbons present in the fuel can react with N₂ creating intermediate N compounds such as the ones in Figure 3. These compounds can then again be oxidized to form NO. The nitrogen oxides present in the exhaust gasses consists mainly out of NO. NO has a short atmospheric lifetime and has little negative effects. Yet, after oxidation by ozone in the atmosphere, NO₂ is formed:



NO₂ is hence a primary and a secondary pollutant. This toxic, reddish-brown gas with a sharp odor has a longer atmospheric lifetime and creates a risk for human health and ecosystems (Daly & Zannetti, 2007; Vlaamse Milieumaatschappij, 2020b; Vlaamse Milieumaatschappij, 2020c). NO₂ can form the acid HNO₃ in droplets in the atmosphere. When washed out with rain, HNO₃ can end up on land and vegetation and in waters. Thereby damaging these receptors due to acidification. HNO₃ in the atmosphere can further react with NH₃, producing NH₄NO₃ which contributes to the formation of secondary particulate matter (WHO, 1997). Nitrogen oxides can also be transformed to N₂O, which is a strong greenhouse gas. However, the key issue is the contribution of NO_x in the tropospheric ozone formation, which will be discussed in Section 3.2.1.

The NO_x emissions in 2018 in Flanders were 47% less than the emissions in 2000. This reduction is achieved by various measures in the transport and energy sector such as the use of three-way catalytic converters in gasoline cars and the application of exhaust gas recirculation and selective catalytic reduction in trucks. Diesel engines still emit too much NO_x gases as the total transport sector is still responsible for 61% of all NO_x emissions in 2018, with 32% from road traffic. Therefore this sector will need even further measures (VMM, 2020b).

3.1.3. SO₂

Sulphur dioxide is most commonly emitted into the air by the combustion of high-sulphur (fossil) fuels, typically found in shipping, industry and power generation. The content of sulfur in vehicle fuels has declined sharply resulting in road traffic representing only a small proportion of the SO₂ emissions. A minor portion of the SO₂ in ambient air originates from the smelting of ores and from natural sources as volcanoes (Kampa & Castanas, 2008). Gaseous SO₂ in the troposphere has the capacity to acidify ecosystems via dry deposition. After oxidation to particulate sulphate (SO₄²⁻) in aerosols in the atmosphere, the pollutant can be washed out with rain in the form of H₂SO₄ and thereby acidify water and soil, this process is called wet deposition. This acid rain is also responsible for the destruction of buildings and corrosion of metals (Vlaamse Milieumaatschappij, 2020b). Breathing in highly SO₂ concentrated air can damage the lungs and this air can cause irritation of the eyes. In addition, in the presence of ammonia, salts can be formed, leading to inorganic aerosols. (EEA, 2013). Therefore, SO₂ is a precursor of secondary PM_{2.5}. In Flanders, the emission values for SO₂ imposed by the EU are respected everywhere in 2019. However, the values imposed by the WHO are still exceeded in some places. The VMM (2020) reports that SO₂ concentrations in 2018 were decreased by 77% in Flanders compared with the concentrations in 2000 and that the levels have stagnated in recent years.

The greatest reduction was found in the industrial and transport sectors. The sulphur content of fuels has been greatly reduced over the years and a shift from coal and oil to gas combustion and green energy (such as wind and solar energy) took place in power plants and households (Rijksoverheid, 2019). Further measures were taken as several techniques exist to remove SO₂ from exhaust gases. Fortunately, the critical level for SO₂ to ensure the protection of vegetation was also respected in 2019 in Flanders (Vlaamse Milieumaatschappij, 2020a).

3.1.4. NH₃

Ammonia emissions mainly originate from agricultural activities. These emissions come from the livestock, manure storage and spreading and the use of synthetic nitrogen fertilizers (Asman et al., 1998). 95% of the NH₃ emissions in 2018 in Flanders came from agriculture and horticulture (VMM, 2020b). Other, less important, anthropogenic sources are biomass burning, industrial processes and fossil fuel combustion. Natural sources include the manure of wild animals, the ocean and natural soils (Schifer et al., 2014). NH₃ has a relatively short atmospheric lifetime as it is active in the neutralization reactions of the acids H₂SO₄, HNO₃ and HCl to form respectively (NH₄)₂SO₄ or NH₄HSO₄, NH₄NO₃ and NH₄Cl aerosols (Pinder et al., 2007; Scudlark et al., 2005). The reaction between NH₃ and H₂SO₄ or NH₄HSO₄ is favored over the other reactions (CENR, 2000). Due to the formation of these various aerosols, NH₃ can be considered as an important precursor for secondary particulate matter and therefore has an impact on human health when emitted in the atmosphere (Behera & Sharma, 2010). The reduced nitrogen compounds NH_x (NH₃ and NH₄⁺) also have a great impact on the environment as they are acidifying and eutrophying pollutants when they end up on land, water and vegetation via wet and dry deposition. Acidification occurs when the formed acids in the atmosphere end up in the environment and lower the pH. Eutrophication occurs when an excessive amount of nutrients ends up in the environment. This causes changes in biodiversity and invasions of new species in terrestrial ecosystems and algal blooms and hypoxia, i.e. low oxygen levels present in tissues, in aquatic ecosystems (Pinder et al., 2008). In 2020, the impact of acidification and eutrophication on the environment were estimated by the EEA (2020) using critical loads, i.e. the load of pollutants that the ecosystem can absorb without causing negative effects. They conclude that these critical loads are still exceeded in most parts of Europe. In Flanders, the total deposition of NH_x was reduced by 32% in 2019 compared with the depositions in 2000. However, the critical levels for the protection of vegetation were still exceeded in 2019, requiring more efforts from the agriculture and horticulture sector to reduce their NH₃ emissions (Vlaamse Milieumaatschappij, 2020a).

3.2. Secondary pollutants

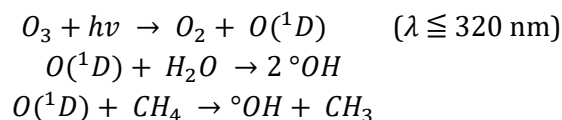
Secondary pollutants are not emitted directly by a source but they are formed in the atmosphere out of primary pollutants, i.e. precursors. The products may undergo various physical, chemical or photochemical reactions in the atmosphere. The secondary pollutants can be present far away from emission sources of precursor pollutants due to dispersion processes (WHO, 1997). This section will focus on the formation of the secondary pollutant ozone in the troposphere, i.e. the first 10 km of the atmosphere where temperature decreases with altitude, except for when temperature inversion exists (Krupa & Manning, 1988).

3.2.1. Ozone

Ozone is an important pollutant as it forms a photochemical smog layer in the troposphere as opposed to the stratosphere where ozone forms a protective layer against UV light. The smog can affect human health by irritation of the eyes, damaging the lungs, creating headaches and even induce asthma (VMM, 2020b). Ozone can also damage materials like rubber and textiles (Lee et al., 1996). Additionally, tropospheric ozone adversely affects vegetation, forests and agricultural crops. When O₃ penetrates the leaves, it dissolves in the aqueous layer and can be transformed into H₂O₂ which can be further converted into reactive oxygen species, e.g. superoxide and hydroxyl radicals (Rai et al., 2011). These radicals may give rise to several damaging reactions leading to lower growth rates, yield, quality and modified sensitivity to biotic and abiotic stresses (Krupa & Manning, 1988; Fuhrer et al., 1997). On top of that, O₃ is also a greenhouse gas contributing to global warming.

A number of substances can serve as O₃ precursors, namely NO_x, CO and VOC's. De Leeuw (2002) estimated the tropospheric ozone forming potentials (TOFP) for each precursor to reflect the total amount of O₃ that can be produced with the breakdown of the specific substance. The TOFP values are used as weighing factors when determining the combined contribution in ozone formation. NMVOC is used as reference and therefore the TOFP of NMVOC is equal to 1. It should be noted that NMVOC's commonly occur in a mixture. The TOFP strongly depends on the composition of this mixture as each NMVOC has a different chemical structure determining its reactivity and thus the potential to create O₃. Since the composition of this mixture often is not known, a lumped TOFP value is used. CO has a relatively low tropospheric ozone forming potential (0.11) compared to NO_x (1.22) and VOC's (1 for NMVOC's and 0.014 for methane (CH₄)).

Tropospheric O₃ formation results through various reactions. In clean air, i.e. in absence of NO_x, the process starts with the formation of OH-radicals out of the pre-existing O₃ in the troposphere. The source of the pre-existing O₃ is mainly the stratosphere (Finlayson-Pitts & Pitts, 1993). Photolysis of O₃, in the presence of sunlight (*hν*) with a wavelength (*λ*) less than 320 nm, creates excited oxygen O(¹D) (Atkinson, 1998). O(¹D) then reacts with water vapor or CH₄ to form hydroxyl radicals (Van Langenhove & Walgraeve, 2019) (Lelieveld & Dentener, 2000).



The OH radicals play an important role in the atmosphere as they can oxidize the present organic compounds. Since they are formed in the presence of sunlight, they're most important in defining the atmospheric chemistry during the day. The radicals initiate the oxidation of CO and CH₄ creating peroxide radicals ([°]HO₂ and [°]CH₃O₂). The latter form H₂O₂ and CH₃O₂H which can be washed out of the clean atmosphere with rain. These reactions are presented in Figure 4 (Van Langenhove & Walgraeve, 2019).

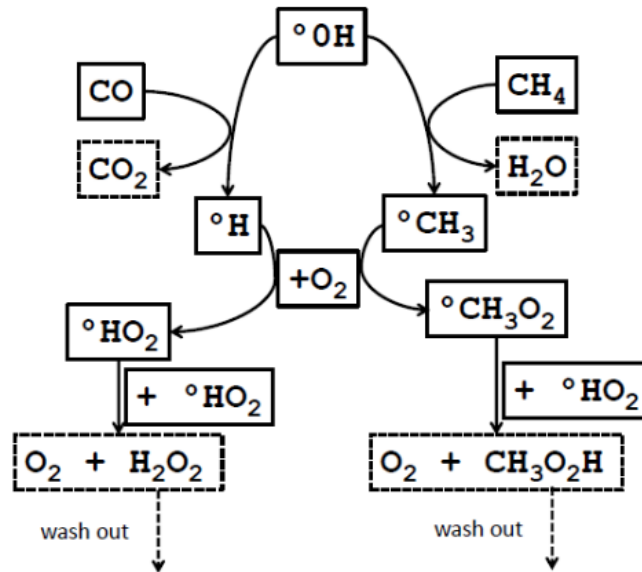
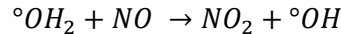
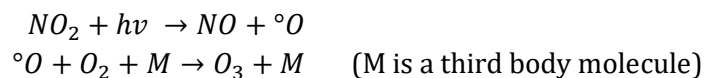


Figure 4: Reaction scheme for the oxidation of CO and methane in a clean, unpolluted atmosphere (Van Langenhove & Walgraeve, 2019).

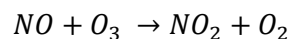
If NO_x compounds are present in the atmosphere, thus creating a polluted atmosphere, the peroxide radicals will react with NO to form NO_2 and the OH radicals are regenerated, this creates a chain reaction. The OH radicals will initiate new oxidation reactions, creating new peroxide radicals and these can then again form new NO_2 .



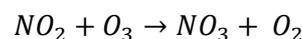
The large increase in NO_2 is very important, since it decomposes in the presence of sunlight to form ozone (Krupa & Manning, 1988; Kansal, 2009).



As mentioned earlier, ozone can react with NO to form NO_2 and O_2 . With this reaction ozone destruction is carried out. In the presence of a high amount of NO , for example near emission sources, this ozone titration can form an ozone sink (EEA, 2008).



The tropospheric ozone concentrations are thus dependent of the ozone formation and destruction and thus of the ratio $[\text{NO}_2]/[\text{NO}]$. The higher this ratio, i.e. the more NO_2 present in the troposphere, the more tropospheric ozone is present. During the night, when there is no sunlight, in reaction with nitrogen dioxide, ozone can be decomposed to oxygen and nitrate radical (Van Langenhove & Walgraeve, 2019).



The nitrate radical is a source for HNO₃ after formation to N₂O₅. In presence of sunlight, the NO₃ radical is rapidly decomposed to NO₂ again. A scheme of the ozone formation and degradation is presented in Figure 5 (Atkinson, 1998).

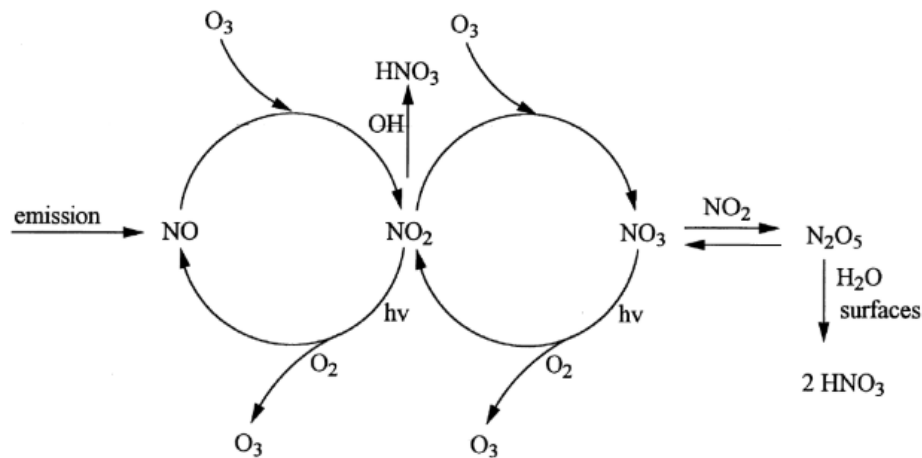
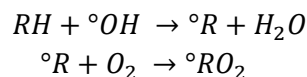
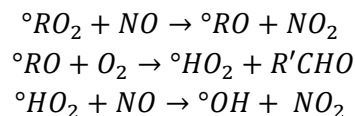


Figure 5: Ozone formation and degradation in the troposphere in the absence of VOC's (Atkinson, 1998).

The [NO₂]/[NO] ratio is influenced by the presence of VOC's. VOC's can be oxidized in the troposphere by the present OH radicals to form new radicals.



These radicals can then react with the present NO creating NO₂. This way, the [NO₂]/[NO] ratio is influenced and the ozone degradation is dominated by the ozone formation.



Not only O₃ precursors determine the O₃ concentrations but also the solar radiation that drives the photochemical reactions. The VMM (2019) observed this evidently in the measurements of ozone concentrations in the summer of 2019, when heat waves hit Flanders that period. As is visible in Figure 6, the concentrations in 2019 peaked far above the WHO and EU standards. It is also clear in this graph that the mean O₃ concentrations from 1990-2018 are higher during summer, exceeding the WHO standards but meet the EU standards. During the summer months, more sunlight is available to decompose NO₂ to O₃. Therefore, in these months the problem of photochemical smog is more prevalent. Furthermore, The VMM (2020) concludes that background O₃ concentrations have increased over the years but that peak concentrations have been reduced. Due to measures in Flanders, the O₃ precursors emissions have dropped and this explains the reduction in the peak concentrations. However, globally these emissions are still too high so that ozone formation still proceeds. The O₃ originating from places with high precursor emissions can be transported to Flanders increasing the background O₃ concentrations.

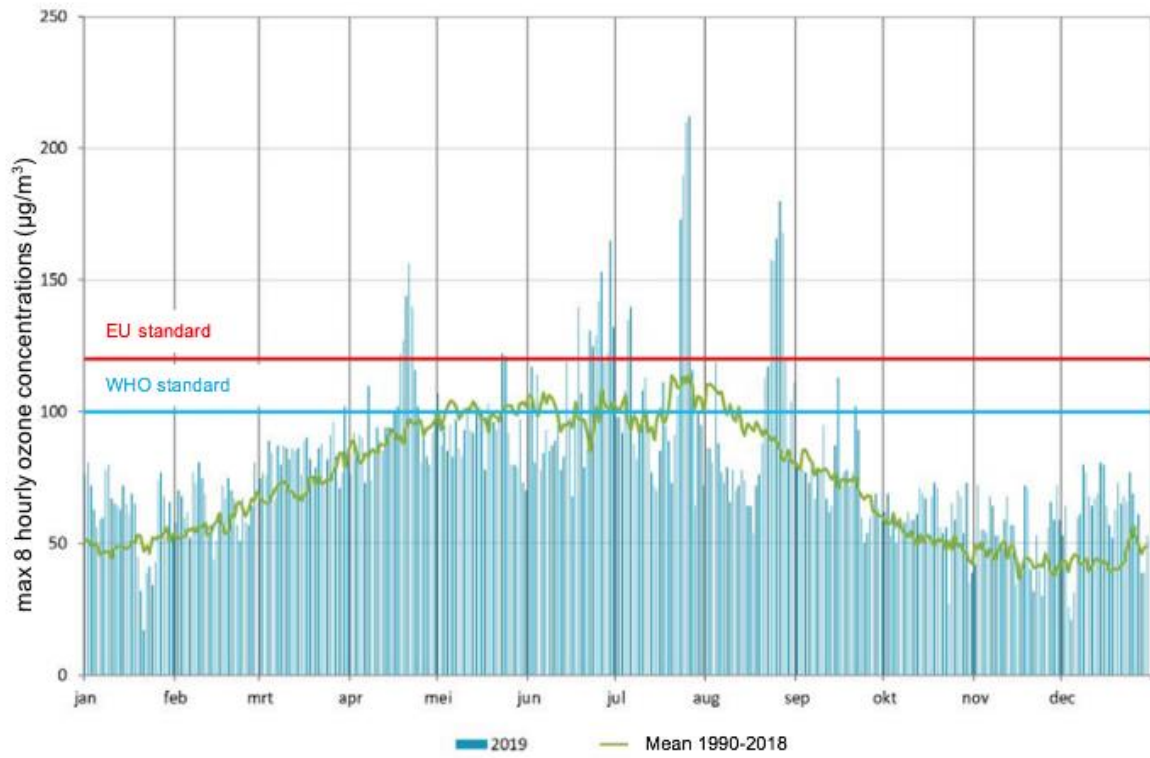


Figure 6: Comparison of daily maximum ozone 8-hour means measured in 2019 with long-term average over the period 1990-2018 ($\mu\text{g}/\text{m}^3$) (The VMM, 2020).

4. Monitoring networks for air pollutants

Monitoring air quality is essential in order to verify models, detect the effect(s) on air quality from certain measures such as the ones related with the corona pandemic and assess the efficiency and sufficiency of further abatement (United Nations, 2018). The information obtained by monitoring can be used in environment policies to check whether the guidelines set by the WHO and EU are respected and if the goals are/will be achieved. As stated in Section 2.1, Belgium has to provide an emission inventory to the European Commission and the EEA every year, but also to the UN to prove the agreement with the NEC directive, the LRTAP strategy and the SDG's. The last reports were submitted on 15 and 31 march 2020 in accordance with the international commitments. The reports consist of inventory emissions per pollutant and per sector in kton. This chapter covers the monitoring networks for the air pollutants in Flanders and the analytic methods that are used for each pollutant.

4.1. Monitoring networks in Flanders

In Flanders, the agency *Vlaamse Milieumaatschappij (VMM)* is tasked with the monitoring of air pollutants. The agency belongs to the policy area "Environment" of the Flemish government and their task is to promote a good living environment in Flanders (VMM, 2017b). The agency carries out various measurements throughout Belgium in order to determine the current water, air and climate conditions and they publish reports with their results every year to inform the public.

At any time, it is possible to check the current air quality in Flanders via the website of the VMM (2021) or via www.irceline.be. Through maps of Flanders, the air quality is represented using different colors that represent different classes, ranging from horrible to excellent. The maps are generated by means of a computer model that interpolates the most recent, non-validated measured values of the VMM's telemetric measuring stations, i.e. stations that are remotely controlled, across Flanders. The classes are assigned to an air quality index. In Belgium, the BeLAQI-index is used, which is given in Figure 7 (irCELine, 2019).

Index	Classification	PM ₁₀ daily mean (µg/m ³)	PM _{2.5} daily mean (µg/m ³)	O ₃ max 1-hourly mean per day (µg/m ³)	NO ₂ max 1-hourly mean per day (µg/m ³)
1	Excellent	0 - 10	0 - 5	0 - 25	0 - 20
2	Very good	11 - 20	6 - 10	26 - 50	21 - 50
3	Good	21 - 30	11 - 15	51 - 70	51 - 70
4	Fairly good	31 - 40	16 - 25	71 - 120	71 - 120
5	Moderate	41 - 50	26 - 35	121 - 160	121 - 150
6	Poor	51 - 60	36 - 40	161 - 180	151 - 180
7	Very poor	61 - 70	41 - 50	181 - 240	181 - 200
8	Bad	71 - 80	51 - 60	241 - 280	201 - 250
9	Very bad	81 - 100	61 - 70	281 - 320	251 - 300
10	Horrible	>100	>70	>320	>300

Figure 7: BeLAQI index scale, health impact classification and associated concentration scales for PM₁₀ daily mean, PM_{2.5} daily mean and O₃ and NO₂ daily maximal 1-hour mean (irCELine, 2019).

The index uses the last measured concentrations of the pollutants PM₁₀, PM_{2.5}, O₃ and NO₂. The pollutant that gives rise to the highest index, determines the total index. The concentrations used for the indices are linked with a 'relative risk' to human health, sourced from the HRAPIE project (Health risks of air pollution in Europe) from the WHO (2013). The relative risks indicate what the increase is in health impact per 10 µg/m³ increase in pollutant concentrations. This was calculated by using doses-response relations. The index shows the short term impact of the current air quality on human health.

To obtain the concentrations of the air pollutants present in the atmosphere, 110 measuring stations are spread across Belgium, including Flanders, Wallonia and Brussels (IrCELine, 2021). The stations are located so that industrial, suburban, urban, rural and traffic-oriented situations are all incorporated. Not all of them belong to the VMM but in agreement with the different owners of the stations, the VMM is also permitted to use these data (VMM, 2013a). Automatic and semiautomatic measurements are performed for the different substances in different measuring stations. Automatic measurements are real-time measurement, i.e. the results are displayed on the measuring device. With semi-automatic measurements, samples are taken during a specific period and are automatically analyzed in a lab. Some of these stations also measure weather variables such as temperature, wind direction, etc.

4.2. Analytical methods

Various analytical methods exist to determine the concentrations of air pollutants in the ambient air. In this section a brief discussion is given of the analytic methods used by the VMM to measure the gaseous pollutants ozone, nitrogen oxides and the volatile organic compounds in Flanders.

4.2.1. O₃

The ozone monitoring network consists of 20 telemetric stations across Flanders, all of them owned by the VMM. The measuring device that is used for the detection of O₃ is an UV absorption analyzer, i.e. API (Advanced Pollution Instrumentation) model T400 (VMM, 2016), see Figure 8. This device utilizes UV spectroscopy to determine the concentrations of O₃ according to the quantity of light absorbed. A 254 nm UV light signal passes through the sample cell where it can be absorbed in proportion to the present ozone concentrations (Teledyne Technologies Incorporated, 2021). This technique is suitable for measuring concentrations in ambient air as it has a low detection limit, namely 0.6 ppb. The measurements are performed automatically every hour and are subject to an uncertainty of 15 %. Data are recorded automatically, in real time and are also remotely available.



Figure 8: The model T400 UV absorption O₃ analyzer (Teledyne Technologies Incorporated, 2021).

4.2.2. NO_x

In 2016, the NO_x monitoring network consisted of 70 measuring stations across Flanders of which 45 belong to the VMM and the others are in cooperation agreement with other entities. Both passive samplers and automatic monitors are used to measure NO, NO₂ and NO_x concentrations. Passive samplers from IVL (2015) are used to capture NO₂ compounds (VMM, 2011). They work on the principle of molecular diffusion of gases. The sampling continues four weeks and afterwards the samples are analyzed in a laboratory by means of ion chromatography (VMM, 2013a; VMM, 2016; Vlaamse Milieumaatschappij, n.d.). This semi-automatic detection method gives four-weekly average concentrations with an uncertainty of 10 %.

The automatic measuring stations make use of the TS (Thermo Scientific) model 42i monitor, which is a chemiluminescence NO-NO₂-NO_x analyzer, see Figure 9 (Thermo Fisher Scientific Inc., n.d.). This analytic method is based on the principle that NO, in the reaction with ozone, produces a characteristic luminescence with an intensity linearly proportional to the NO concentration (Thermo Fisher Scientific Inc., 2007). Therefore, in order to analyze NO₂ it must be first transformed to NO. The air is split in two streams when it enters the monitor. The first stream is used to analyze the NO concentrations, the second stream is used to determine the NO_x concentrations. In order to obtain the NO₂ concentration, the NO concentration is subtracted from the NO_x concentrations. This method gives real-time measurements every half-hour and the data are immediately available.



Figure 9: Model 42i Chemiluminescence NO-NO₂-NO_x Analyzer (Thermo Fisher Scientific Inc., n.d.).

4.2.3. VOC's

The VOC monitoring network consists of 17 measuring stations across Flanders. Automatic monitors are used in 9 of these stations to measure BTEX compounds. In one of these stations also 1,2-dichloroethane is measured. Three types of monitors are utilized that make use of gas chromatography (GC) with either a flame ionization detector (FID) or a photoionization detector (PID). Figure 10 shows the monitor with FID, the model 3A AirmoBTX 1000 and AirmoBTX GC 866 from Chromatotec group (2016) are used by the VMM (Chromatotec group, 2009; VMM, 2019). These are both designed to detect and measure BTEX concentrations and the last is also used for 1,2-dichloroethane. The analytes are sampled on an absorbent trap and afterwards released with thermo-desorption and injected on the column for the separation with GC. The carrier gas is H₂. The 3A AirmoBTX 1000 model has a detection limit of 50 ppt. The GC955 Synspec benzene/BTEX analyzer is the third automatic monitor used by the VMM to detect and measure BTEX and uses PID, see Figure 11 (Synspec, 2019). The volatile components are trapped on a sorbent consisting of TENAX GR, i.e. a porous material with 23% graphitized carbon (Buchem B.V., 2015).

The compounds are then thermally desorbed from the material and the sample is separated with the use of GC, the used carrier gas is nitrogen. The analysis of the separated compounds is done with PID. The detection limit for benzene with this equipment is 0.03 ppb. The measurements with the previously mentioned automatic monitors provide half-hourly concentrations for the given substances.

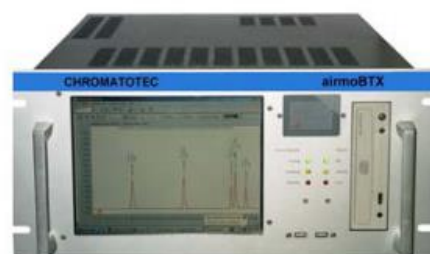


Figure 10: AirmoBTX (Chromatotec group, 2009).

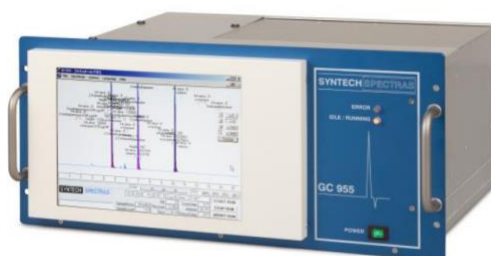


Figure 11: The GC955 Synspec benzene/BTEX analyzer (Synspec, 2019).

Radiello adsorption tubes are used as passive samplers in 8 stations. In 7 stations passive Radiello samplers with Carbograph 4 are used to measure 24 different VOC's such as alkanes, alkenes and aromatic hydrocarbons. Since 2019, aldehydes and ketones are measured in the remaining station, however, only 3 compounds had concentrations above the detection limit, namely the sum of acetone and acrolein, acetaldehyde and formaldehyde. Passive Radiello samplers with DNPH were used in this station. In this station, also 32 VOC's are actively sampled on an adsorption tube with Carbotrap 300 for 24 hours every 4 days, using a pump. The passive sampling continues for two weeks. Afterwards, the samples are automatically analyzed in a laboratory using different techniques.

ATD-GC (Automated Thermal Desorption Gas Chromatography) is used to detect and quantify the 24 different VOC's from the passive samples and the 32 different VOC's from the active samples. The samples containing aldehydes and ketones are analyzed using UPLC-UV (Ultra Performance Liquid Chromatography UV-absorption)(VMM, 2017a). Analyzing VOC's is more labor-intensive than analyzing ozone and NO_x and often greater uncertainty is found on the results (VMM, 2016).

5. Determining the impact of anthropogenic events on air quality

The corona pandemic, that resulted in a lockdown in several places around the world, provides a unique opportunity for scientists who conduct research on air quality. Like this study, various researchers studied the impact of the corona measures on the air quality. It is also interesting to compare these studies with studies that investigate the impact of other anthropogenic events on air quality. This chapter gives an overview of the methodologies that are used in literature to study the impact of anthropogenic effect on air quality (with a main focus on the corona pandemic) as well as an overview of their main conclusions. Additionally, a more thorough review is provided on the use of machine learning approaches for quantifying the anthropogenic effect on air quality, more specifically the use of random forest models. As this will be the type of method that will be used in this work.

5.1. Before-and-after evaluation

The most straightforward method that can be used to determine the impact of an anthropogenic event on air quality is a before-and-after evaluation. This technique uses data prior to the start of the event to compare it with data after the start of the event in order to detect any possible impact. This was done in many studies regarding the air quality after the start of the COVID-19 lockdown. This can be done in a quantitative way or in a qualitative way.

5.1.1. Quantitative evaluation

A quantitative before-and-after evaluation was performed in the study of Broomandi et al. (2020). The authors compared the averaged concentrations of various air pollutants in Tehran (Iran) for the period of 21 March to 21 April 2020 with the concentrations of the same period in 2019. The results, expressed as percentage increase or decrease, of their study are given in Table 4. A decrease was observed for all the pollutants except for ozone which showed an increase of 3%. The increase in O₃ concentrations is explained by the reduction of NO_x emissions during the lockdown. Less NO is present in the atmosphere to break down the O₃ but a sufficient amount of NO₂ is still present to form O₃ in the presence of sunlight. The [NO₂]/[NO] ratio increases, leading to higher ozone levels. The EEA (2020) compared NO₂ concentrations during the week of 16-22 March 2020 with the same week in 2019 using data from 3000 monitoring stations across European countries. A drop in the NO₂ levels with 40%, 56% and 40% was observed in respectively Barcelona, Milan and Lisbon. A quantitative evaluation was also carried out in South Korea by Vuong et al. (2020), in India by Yadav et al. (2020), in China by Chen et al. (2020), in Brazil by Nakada & Urban (2020), in the U.S. by Berman & Ebisu (2020) and in many other countries. Almost all these studies lead to the same conclusions: a decrease in concentrations of the air pollutants during the lockdown except for an increase in the ozone concentrations.

Table 4: The change in concentrations expressed in % for the air pollutants during the lockdown in Iran (Broomandi et al., 2020).

O ₃ (ppb)	CO (ppm)	NO ₂ (ppb)	SO ₂ (ppb)	PM ₁₀ (µg/m ³)	PM _{2.5} (µg/m ³)
+ 3%	-13%	-13%	-12.5%	-11.3%	+10.5%

Kerimray et al. (2020) investigated the change in air quality in Kazakhstan also by doing a before-and-after evaluation. The authors decided to compare the concentrations of the air pollutants during the lockdown, i.e. 19 March -14 April 2020, with the concentrations of the period just before the start of the lockdown, i.e. 2 March – 18 March 2020. The outcome of their study is presented in Table 5. Again a significant decrease is observed in the NO₂ and CO concentrations and an increase in the O₃ concentrations. The increase of SO₂ levels was explained by the emissions coming from coal combustion. Hence, the reduction in emissions coming from traffic didn't have much influence on these concentrations. The same way of investigating the impact of the lockdown on the concentrations of air pollutants was done in China by Wang et al. (2020). The results of their study are consistent with the other studies: a decrease in PM_{2.5}, PM₁₀, CO and NO₂ concentrations and the O₃ concentrations increased.

Table 5: The change in concentrations expressed in % for the air pollutants during the lockdown in Kazakhstan (Kerimray et al., 2020).

NO ₂ (µg/m ³)	SO ₂ (µg/m ³)	CO (µg/m ³)	O ₃ (µg/m ³)
-35%	+7%	-49%	+15%

Brimblecombe & Lai (2021) investigated the change in diurnal patterns of NO₂ concentrations by comparing data of two weeks before the start of the lockdown with data of the first two weeks of the lockdown. They did this for various sites in Beijing. The bimodal pattern of NO₂ was still seen during lockdown but less pronounced than before the lockdown due to the reduction in NO emissions.

Zhou et al. (2010) examined the impact of transportation control measures on emission reductions during the 2008 Olympic Games in Beijing, (China). To do so, they divided the city in grid cells and for each grid cell the transport emissions were calculated based on the type of the vehicles that passed the specific roads and their speed. This way, grid-based emission inventories are obtained and together with data from monitoring stations, the situation before the event can be compared with the situation during the event. These transportation control measures are similar to those taken to prevent the spread of the coronavirus but not as drastic. Zhou et al. (2010) report that VOC, CO, NO_x and PM₁₀ emissions coming from traffic were reduced with respectively 55.5%, 56.8%, 45.7% and 51.6% during the Olympic games (July 28- August 22 2008) compared to the period before the event (June 22-July 5 2008). Lee et al. (2005) performed the same type of study to investigate if there was an impact on urban air quality due to the restriction of the operation of passenger vehicles during Asian Game events in Busan (Korea). The authors compared the criteria air pollutant concentrations, measured in 13 monitoring stations, from before the event (13–28 September 2002) with concentrations during the event (29 September–14 October 2002). Remarkably, they experienced that all air pollutant levels increased during the event. The reason for this was the change in meteorology. This study already demonstrates that doing a before-and-after evaluation is not always accurate to determine the impact of certain anthropogenic events on air quality since other factors, such as the weather, also have an influence. To conclude, a quantitative evaluation gives a good first insight in changes in air pollutant levels during the lockdown but a clear conclusion on the impact on air quality cannot be made.

5.1.2. Qualitative evaluation

A qualitative before-and-after evaluation can be performed by calculating a dimensionless Air Quality Index (AQI). This AQI is then linked to a specific category class, making it possible to qualitatively assess the air quality and the related health impacts. The results for the period of the lockdown can be compared with the period before the start of the lockdown. A considerable disadvantage is that there is no universally acknowledged AQI. The calculation of it differs between countries. As mentioned in Chapter 4, the BeLAQI-index is used in Belgium. Since the calculation of this index is rather abstract, the study of Xu et al. (2020) will be used as an example of a qualitative before-and-after evaluation. Xu et al. (2020) investigated the impact of the COVID-19 event on the air quality near central China. They use the United States Environmental Protection Agency (US EPA) AQI. To calculate the daily AQI, sub-indices (sub-AQI) are first calculated for the six air pollutants based on daily concentrations of PM_{2.5}, PM₁₀, SO₂, CO, NO₂ and the daily average 8-hour maximum concentrations of ozone as shown in Equation (1). With sub-AQI_p : the air quality sub index for air pollutant p, C_p: the concentration of the air pollutant p, C_{low}: the concentration breakpoint that is ≤ C_p, C_{high}: the concentration breakpoint that is ≥ C_p, I_{low}: the index breakpoint corresponding to C_{low}, I_{high}: the index breakpoint corresponding to C_{high}. The breakpoints and the corresponding indices are predefined by the U.S. EPA (2018). The final daily AQI equals the maximum sub-AQI, see Equation (2).

$$subAQI_p = \frac{I_{high} - I_{low}}{C_{high} - C_{low}} (C_p - C_{low}) + I_{low} \quad (1)$$

$$AQI = \max(subAQI_1, subAQI_2, \dots, subAQI_n) \quad (2)$$

After obtaining the value for the AQI, it can be classified into six possible classes linked with a color and related to specific health effects, this is shown in Table 6 (AirNow, 2016).

Table 6: US EPA AQI (AirNow, 2016).

Color	Levels of concern	Values of AQI	Description of Air Quality
Green	Good	0-50	Air quality is satisfactory, and air pollution poses little or no risk.
Yellow	Moderate	51-100	Air quality is acceptable. However, there may be a risk for some people, particularly those who are unusually sensitive to air pollution.
Orange	Unhealthy for sensitive groups	101-150	Members of sensitive groups may experience health effects. The general public is less likely to be affected.
Red	Unhealthy	151-200	Some members of the general public may experience health effects; members of sensitive groups may experience more serious health effects.
Purple	Very unhealthy	201-300	Health alert: The risk of health effects is increased for everyone.
Maroon	Hazardous	301 -500	Health warning of emergency conditions: everyone is more likely to be affected.

The study tries to evaluate the change in air quality by comparing the distribution of the six AQI classes in January, February and March averaged over 2017-2019 with the distribution in the same months in 2020. This was done for the cities Anqing, Hefei, and Suzhou. The lockdown was introduced at the beginning of February 2020 in these cities. The combined results for these three cities is shown in Figure 12. The proportion of the green class has increased for each month from 5.7%, 8.7% and 7.2% to respectively 11.8%, 41.8% and 22.6%. This implies that the proportion of the time when the air quality poses little or no risk to human health has increased in these months. In February and March the share of the red class has even reached zero. Based on these results, a qualitative evaluation can be made leading to the conclusion that air quality has improved during the months of lockdown in central China.

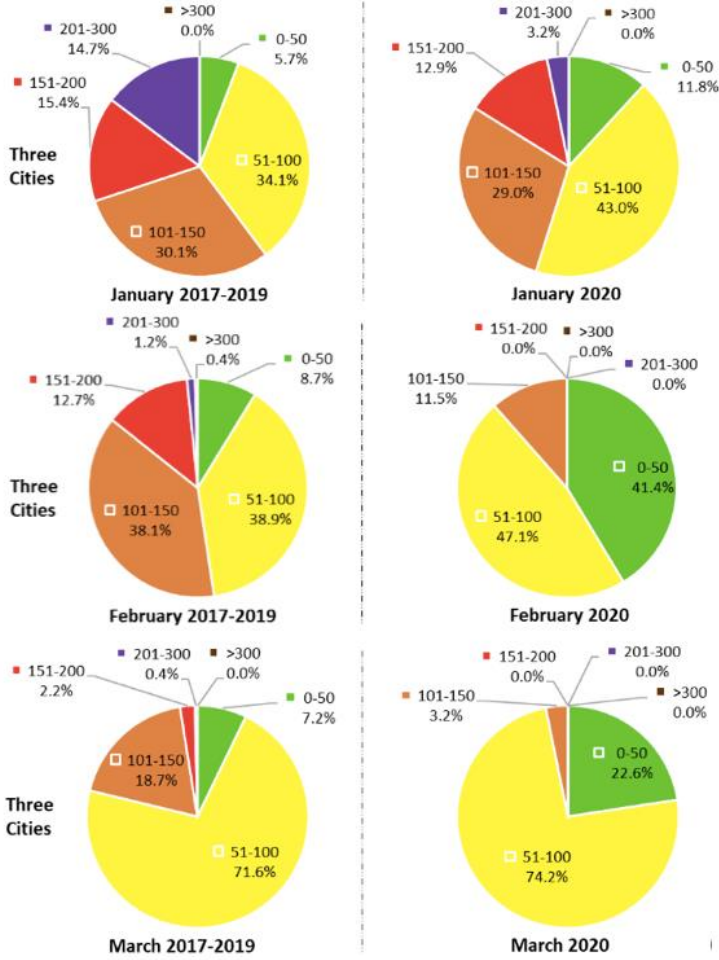


Figure 12: Left: The distribution of the six AQI classes for Anqing, Hefei, and Suzhou in January, February and March averaged over 2017–2019, Right: The distribution of the six AQI classes for Anqing, Hefei, and Suzhou in January, February and March in 2020 (Xu et al. , 2020).

Although before-and-after evaluations give a good indication of the impact of the corona measures on the air quality, their results should be interpreted critically. Most of the studies already outline the weather conditions for the specific study period and area and compare them to the situation of previous years to give an impression of the influence of the meteorology. But the confounding effects of meteorology on the fluctuations in concentrations of air pollutants need to be removed to really isolate the effect of the corona measures. In order to do so, other methods are more effective and will be discussed in the next section.

5.2. Model-based approaches to account for weather influences

Instead of performing a before-and-after evaluation, a model-based approach could be used to investigate the impact of the lockdown on air quality. The influence of the corona measures on the air quality is confounded by the influence of other factors. The main factor that influences the concentrations of air pollutants in the atmosphere is weather. Model-based approaches can be used to estimate the influence of weather on air quality. Subsequently, the created model can be used to filter the effects of the weather conditions by predicting the concentrations for the different air pollutants based on the weather conditions. The predictions can then be compared with the measured concentrations to identify a potential impact resulting from anthropogenic or other events, excluding weather phenomena. This section will first describe the influence of the weather conditions on air pollutant concentrations in the atmosphere, in order to motivate why it is important to take this into account. Afterwards, it will be discussed how this influence can be isolated in air quality research through the use of two different model-based techniques, i.e. machine learning and deterministic models.

5.2.1. Influence of weather conditions

The pollutant concentrations present in the atmosphere are influenced by the location and type of emission source but also by the meteorological conditions. When focusing on the primary emissions coming from traffic, bad dispersion is especially observed in urban areas and in the presence of street canyons. In street canyons high buildings capture the large amount of pollutants coming from the vehicles and wind cannot carry it away. Particularly during traffic peak hours, primary pollutant concentrations can reach high levels. Favorable weather conditions can, however, lower the accumulated concentrations. Liao et al. (2018) define favorable weather conditions as : “high wind speed, high precipitation and a weak temperature inversion.”. Therefore, these meteorological variables are crucial to include when creating a model to predict the concentrations of air pollutants in the atmosphere.

Wind is responsible for dispersion and dilution of the pollutants in the atmosphere. The polluting gases and particulates can also be removed from the atmosphere by dry or wet deposition, but depends on the characteristics of the substances. Dry deposition is a continuous process while wet deposition occurs with precipitation (Leelossy et al., 2014). High amounts of rain are thus responsible for the wash out of pollutants from the atmosphere. It should be noted that the amount of wet deposition during heavy rainfalls influences the amount of dry deposition afterwards. Since the concentrations of the pollutants are lowered in the atmosphere, less pollution can be dragged out by dry deposition (VMM, 2013b). The presence of temperature inversion is also important. Temperature inversion is the mechanism whereby the temperature gradient, which normally runs from high to low in the troposphere, is reversed. This way, a warm layer retains the substances and prevents them from being dispersed (Trinh et al., 2019). The WHO (1997) explains the concept as follows: “As a mass of air rises it cools but as long as its temperature remains greater than that of the surrounding air it will retain buoyancy and continue to rise. Conversely, if the actual temperature falls more slowly than that of the mass of air, or even increases, the cooling air will rapidly become heavier than the surrounding air and it will fail to rise. Consequently, a temperature inversion occurs when the air temperature rises with height above the ground.”.

The earth's surface does also participate in the dispersion of pollutants by means of various processes like frictional drag, evaporation and transpiration, heat transfer and terrain induced flow modification (Stull, 1988). The part of the troposphere that is influenced by these processes is called the boundary layer. The thicker this layer, the more the pollutants are subject to dispersion due to turbulence in this layer and can move to the layer above, i.e. the free atmosphere. Figure 13 shows the changes in the boundary layer during the day (Leelossy et al., 2014). The boundary layer height (BLH) is influenced by the meteorological conditions and the time of the day (Bronsema, 2011). Often at night the earth's surface cools down because of the heat release to the atmosphere. This creates temperature inversion and therefore a stable boundary layer. In this stable layer less turbulence is present and pollutant concentrations can accumulate. The amount of clouds is an important parameter in the cooling of the earth surface. When there are many clouds at night, the heat coming from the earth's surface is trapped. When there is a clear sky, i.e. little clouds, the heat can escape to higher layers in the atmosphere and the earth's surface cools down more rapid. During the day, however, the earth's surface heats up due to solar radiation and this process is positively influenced by a clear sky. The generated vertical heat flow leads to more turbulence. Together with winds, this leads to air flows in the boundary layer and therefore creating a larger mixed layer (Bronsema, 2011). In high pressure regions, the BLH is generally smaller than in low pressure regions. High pressure regions are characterized by calm weather conditions and little clouds. In high pressure regions air moves downwards because the air flows out of the core of the region, this is called divergence. In low pressure regions, hot air rises upwards to higher altitudes in the troposphere. The air is replaced by winds moving towards the low pressure region, this is called convergence (NoodweerBenelux, 2021). A detailed description of the processes present in the boundary layer is given in the work of Stull (1988). Effective dispersion occurs thus when the atmosphere is unstable, i.e. a high level of turbulence and mixing, and the BLH is sufficiently large.

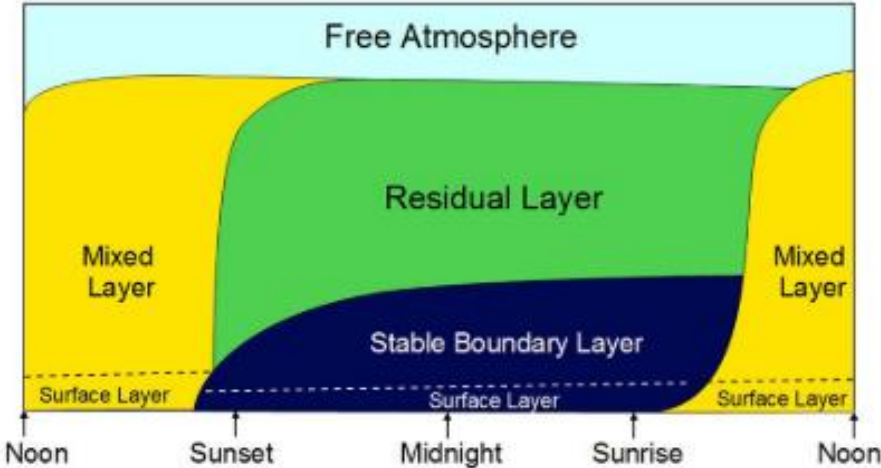


Figure 13: Changes in the boundary layer during the day (Leelossy et al., 2014).

5.2.2. Machine learning: Random Forest

Tom Mitchell (1997), a machine learning pioneer, defines Machine Learning as follows: “Machine Learning is the study of computer algorithms that improve automatically through experience.”. More specific, in machine learning algorithms are used to find relations in large datasets. It is possible to analyze both linear and non-linear relationships between predictors and outcome variables (Varian, 2014). A predictive model (often a regressor or classifier) can be established during a so-called training phase. The final product of such a training phase is a regressor or classifier that is capable of predicting an outcome of interest. The training dataset, used for training the model, consists of the outcome variable (in this study the air pollutant concentration) and the predictors (in this study the weather variables used to predict the air pollutant concentration) (Cole et al., 2020). Additionally, a test dataset is necessary to evaluate the model performance. It is thus possible to find a function that maps the weather conditions on the atmospheric air pollution and this can be used to predict the air pollution for a given weather condition. Predictions can be made with new data of the predictors, i.e. out-of-sample predictions with out-of-sample data. A problem that frequently occurs with machine learning is that the model describes the relationships in the training data so precisely that it starts to overfit new data, i.e. the model memorizes the training data rather than extracting relevant patterns from it. As a result, predictions on unseen data will be inaccurate. A trade-off must be made between a complex model that fits the data well and a simple model that generalizes well the new data.

Since it is aimed to predict the continuous outcome variable “air pollutant concentration”, a regression problem arises. Solving a regression problem can be done by using tree-based models, namely with a regression decision trees. Regression trees can be seen as an extension of linear regression. A big advantage is that the trees can be visualized and are therefore easier to interpret. An example of a simple decision tree is given in Figure 14 (Gross, 2020). With this method the dataset is divided in subsets by using splitting rules starting from the top of the tree, point A in Figure 14, i.e. the root of the tree (James et al., 2013). The tree is constructed via recursive binary splitting, i.e. the dataset is split into two branches at each internal node of the tree (A, B and C in Figure 14) until the terminal nodes or the “leaves” (D, E, F and G in Figure 14) are reached. With recursive binary splitting the best split is used at every node for that particulate step. This is done by finding the split that minimizes the RSS (residual sum of squares), i.e. a measure that indicates the difference between the predictions and the training observations. This way, the predictor space is split in simple regions. The predictions for the observations are captured in the terminal nodes of the tree. For a more detailed explanation of this concept, see the work of James et al. (2013) and Breiman (1984).

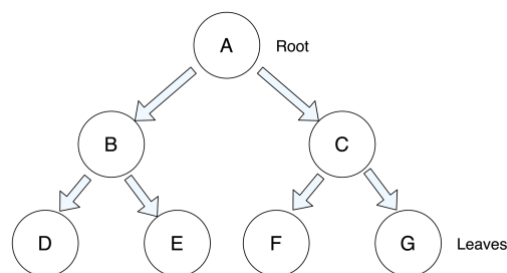


Figure 14: Decision tree (Gross, 2020).

A tree model can become very large if little errors are allowed since a lot of splits are used, creating many branches and many leaves (Varian, 2014). This makes the tree complex and hard to interpret. Using complex trees also increases the chance of overfitting. In order to prevent overfitting, randomness can be added to the dataset with the use of bagging or boosting. Bagging or bootstrap aggregation is a technique that allows to reduce the variance of a model. A “bootstrap” sample is taken randomly from the given dataset, this is repeated several times. Multiple bootstrap replicates (B is used to refer to the number of replicates) of the training dataset are used to build a set of trees, where each tree is fit on a separate replicate. The predictions made with the B constructed trees are then averaged. Breiman (2001) introduced the random forest algorithm that expands the principle of bagging to even further reduce the variance of the model. A scheme of the random forest method is presented in Figure 15 (Chakure, 2019). A large set of individual decision trees (Tree 1, Tree 2,...) is randomly created from bootstrapped training samples out of the dataset to form the random forest. When creating each tree, a different set of m predictors is selected out of the p existing predictors each time a split arises at an internal node. Often m is chosen to be equal to the square of p . When m and p are equal, this method is equivalent to what is often called bagging. Out of the m predictors, one is randomly chosen upon which the split criteria will be based. This way of constructing the trees prevents that one strong predictor is always preferred at the top split. Therefore, the random forest consists out of a set of trees that are decorrelated to some extent. The final algorithm is obtained by averaging the trees. The variance is strongly reduced as compared to a single tree and the predictions will be more accurate.

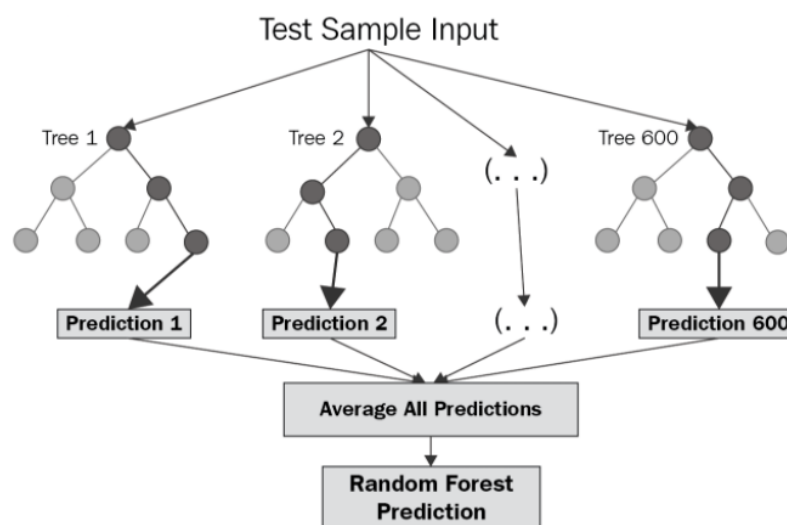


Figure 15: A random forest model (Chakure, 2019).

A benefit of this method is that it is possible to determine which predictor has the greatest influence on the predictions. By observing how much the RSS (residual sum of squares) is reduced by using a specific predictor at splits. The higher the amount of reduction, the more important the predictor. A random forest model can thus serve as a robust tool to predict concentrations of air pollutants during the COVID-19 event based on weather variables. Compared to deterministic models (see further in Section 5.2.3), no data are needed of the emissions during the period of the lockdown, data on the weather variables are sufficient.

The VMM (2020a) used a random forest model approach to determine the impact of the corona measures on the air quality in Flanders. They used the “RMWeather” package, for the statistical software program “R”, that contains tools to conduct meteorological normalization on air quality data (Grange, 2020). The random forest model was trained using daily air pollutant concentrations and a set of weather variables. The training dataset consist of values starting from 01/01/2015 to 29/02/2020, that is the period before the start of the lockdown. The ‘RMWeather” package randomly selects 80% of the provided training dataset to use as actual training set, the other 20% is used to test the performance of the model. A model was created for each air pollutant (NO_x , NO_2 , O_3 , $\text{PM}_{2.5}$, PM_{10} and black carbon) for 13 different measuring locations, i.e. 78 different model. The models were used to make predictions for the period of 01/03/2020 to 10/05/2020. The results for NO_2 at the station situated in Brussels is given in Figure 16. The dotted line indicates the start of the lockdown. It is clear that from this point a difference occurs between the measurements and the predictions made with the random forest model. The observed NO_2 concentrations are lower than predicted in the lockdown. It is also remarkable how well the model predicts the concentrations before the start of the lockdown.

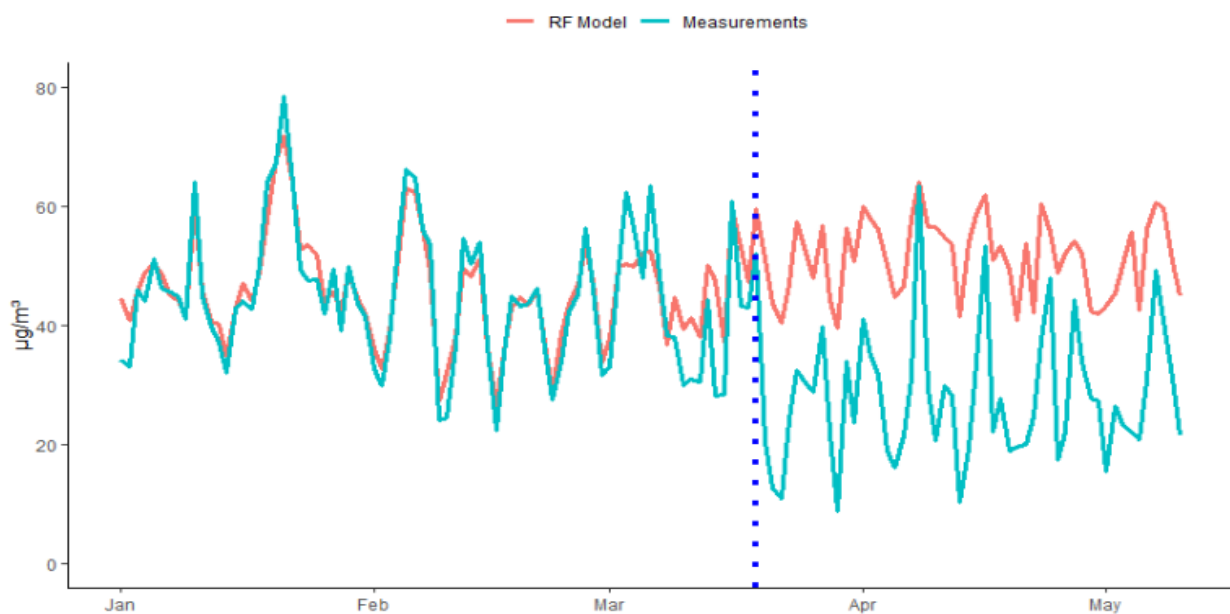


Figure 16: NO_2 daily average concentrations in Brussels (The VMM, 2020a).

The VMM summarizes their results as follows:

- 1) The impact of the corona measures is largest on the traffic-related pollutants, i.e. NO_x , NO_2 and black carbon, and in the locations with the highest amount of traffic. The predictions with the model for these pollutants were higher than the observed concentrations.
- 2) No impact was observed on the PM concentrations during the lockdown. This was partially attributable to the unfavorable weather conditions in this period and the low performance score of the model for PM.
- 3) The measured O_3 concentrations were higher than predicted with the model.

These results are already very meaningful for the situation in Flanders and this study will try to build further on them by working with hourly values instead of daily values. By training the specific models for each pollutant at each station with hourly values, these models can be used to predict hourly concentrations during the lockdown. The predicted hourly concentrations can then be compared with the measured hourly concentrations to investigate more in detail if there is any impact due to the corona measures. Additionally, the hourly measured concentrations can be used to construct daily patterns for each pollutant. An average daily pattern for each pollutant for the first month of the lockdown can be compared with an average daily pattern for that same period in previous years to compare the daily profiles before and after the corona event. The average daily patterns for the first month of the lockdown can also be compared with the constructed average daily pattern based on predicted hourly values. This way, it is hoped to add value to the existing results of the VMM.

5.2.3. Deterministic models

Air pollution concentrations can also be determined by using mathematical equations based on the chemical and physical processes present in the atmosphere that influence air quality. Chemical Transport Models (CTM) are an example of a deterministic approach and can be used to evaluate the impact of the corona measures on the air quality (Mallet & Sportisse, 2008). In order to construct such a model, knowledge is necessary on the different processes and a lot of assumptions need to be made as it is impossible to translate the atmospheric composition completely into equations. After the CTM model is constructed, the air pollutant concentrations can be simulated based on input data that consists out of emission data of the pollutants, meteorological and geographical data (VMM, 2020a). The main difference with the random forest models is that CTM are first-principle models that are constructed based on knowledge compared to the data driven random forest models. The model performance can be evaluated by comparing the simulation results with the measured concentrations (Ballesteros-González et al., 2020). Therefore, data of the air pollutant concentrations needs to be available. When the model performs successfully, it can be used to assess the impact of the lockdown on air quality. The CTM needs to run two scenario's. Once for a Business As Usual (BAU) scenario and once for the lockdown scenario. The meteorological and geographical input data are constant parameters during the two runs, this way the effect of meteorology is isolated. The BAU scenario assumes emissions as if there was no change in traffic due to the COVID-19 event and the second scenario assumes lower emissions due to the reduction in traffic. Making these assumptions is not so evident. The results of the two runs can be compared and the difference can be attributed to the impact of the corona measures. The Global Modeling and Assimilation Office (GMAO) of NASA (National Aeronautics and Space Administration) developed the Goddard Earth Observing System, Version 5 (GEOS-5) model that has a CTM configuration that can be used to simulate air pollutant concentrations. Pott et al. (2021) used the GEOS CTM to determine changes in air pollution during the lockdown in the U.K. The study of S. Wang et al. (2021) is an example of a deterministic approach to investigate the impact of the COVID-19 lockdown on the air quality in the south of China. They used the Community Multi-scale Air Quality (CMAQ) model with different emission scenario's.

6. Data collection and pre-processing

A valid dataset was obtained through data collection and pre-processing. Valid data for this study are data that has been properly collected, derived from a legitimate source, and that includes concentrations of air parameters as well as weather conditions over a sufficiently long period of time. Section 6.1 describes in detail how and from where the data were collected and which data were available for this research. Section 6.2 explains how the data were converted into a finished training dataset and data for which predictions will be made.

6.1. Data collection

In cooperation with the VMM, data were collected from various measuring stations across Flanders and Brussels. Four locations with measuring stations were selected for this study, each location representing a different traffic situation. The first location is Veurne, which represents a background situation with limited traffic. The next location is a public park in Ghent, “Het Baudelopark”, which represents an urban-background situation with relatively little traffic. The third location is in the center of Brussels at the intersection “Kunst-Wet” and represents an urban situation with a lot of traffic. The last location is again in Brussels but outside the center, i.e. Sint-Jans-Molenbeek, also representing an urban-traffic situation. At each location, air pollutants are monitored. The meteorological variables were monitored in the stations of Veurne, Ghent and Sint-Jans-Molenbeek. Traffic data was also available for the station in the center of Brussels. A detailed specification of the various locations follows later in this section.

The three air pollutants of particular importance for this study are NO, NO₂ and O₃. The concentrations of these substances are measured and registered every hour by the VMM (2020a). In addition, weather variables are being measured and registered by the VMM. An overview of the four locations with the corresponding data that were available is presented in Table 7 and Figure 17. Figure 18 shows a photograph of each location to give a more clear view of the type of location. These images were obtained from Google Maps (Google, 2019).

Table 7: The measuring locations with the available data.

<i>Location</i>	<i>Type</i>	<i>Meteo data</i>	<i>O₃ data</i>	<i>NO_x data</i>	<i>Traffic data</i>
Veurne	Background	✓	✓	✓	✗
Ghent, Baudelopark	Urban-background	✓	✓	✓	✗
Brussels, Kunst-Wet	Urban-traffic	✗	✗	✓	✓
Sint-Jans-Molenbeek	Urban-traffic	✓	✓	✓	✗

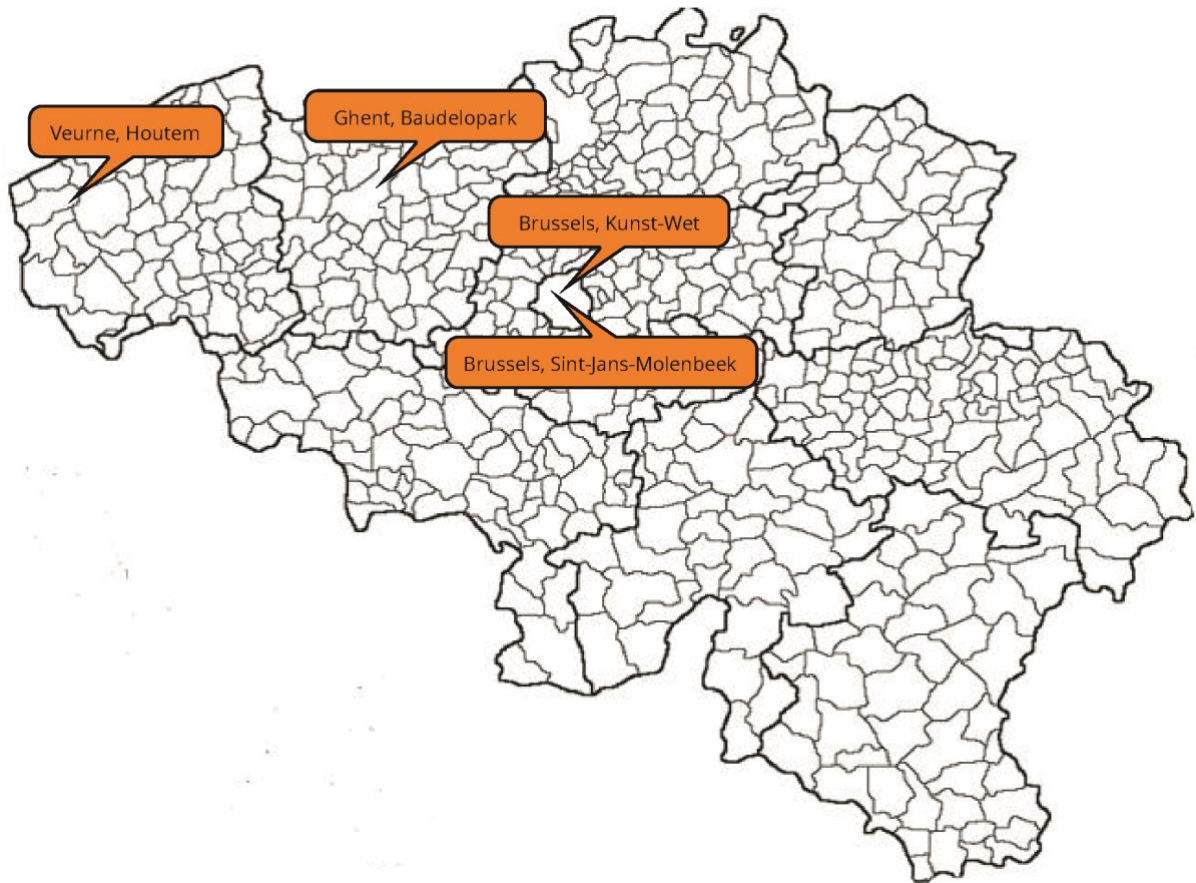


Figure 17: Map of Belgium showing the different locations used for data collection.



Figure 18: The four different locations, top left: background location Veurne, top right: urban-background location Ghent, bottom left: urban-traffic location Kunst-Wet, bottom right: urban traffic location Sint-Jans-Molenbeek (Google, 2019).

6.1.1. Background location: Veurne

The city of Veurne is located in West-Flanders close to the border with France and has 12.096 inhabitants (Informatie Vlaanderen, 2020b). The station, measuring the levels of pollutants, is located in Houtem, a distant village part of Veurne, approximately 10 km outside the city center of Veurne and 9 km away from the Belgian coast. The station is situated between agricultural fields, along a small road with little traffic (Google Maps, n.d.; IrCELine, n.d.). It is important that a background location with little traffic is included in this study as a reference. A reference is essential to confirm that any decrease or increase in traffic related pollutants is in fact due to the reduction in traffic caused by people staying at home during the lockdown and not by other factors such as meteorological influences. The weather variables and the levels of nitrogen oxides and ozone are measured in the same station.

6.1.2. Urban-background location: Ghent, Baudelopark

The park is centrally located in Ghent beside the river the "*Leie*". Ghent is a city with 263.614 inhabitants (Informatie Vlaanderen, 2020a). On top of this, there are many students who study in this city and live there during the week. UGent, for which this thesis is being carried out, is located in Ghent and has over 48.000 students (Universiteit Gent, 2020). Since 1st January 2020, a low-emission zone has been introduced in Ghent to create a healthier atmosphere for its citizens (Stad Gent, 2020). Cars that do not meet the required emission standards are no longer allowed to enter the city ring road. In this way, the city also wants to encourage people to take public transport when they want to visit the city center, which is beneficial for the air quality and the peace and quiet in the city. The measuring station is located in this low-emission zone. This station measures all weather variables as well as the pollutants NO, NO₂ and O₃.

6.1.3. Urban-traffic location: Brussels, Kunst-Wet

Brussels is the capital of Belgium and Europe. The city has about 1.1 million residents. Of these, 30% are of foreign origin, making it a richly multicultural city (Brussels Hoofdstedelijk Gewest, 2018). Brussels is divided into 19 municipalities. The Kunst-Wet site belongs to the municipality of Brussels-City. The site refers to the metro station located at the intersection of the streets "*Kunstlaan*" and "*Wetstraat*" (Beliris, 2016). It is one of the busiest places in Brussels because of the passengers of the metro who enter and leave the underground station and because of the numerous vehicles that cross this place via the ring of Brussels (i-CITY, n.d.). The capital is located in a low emission zone but the ring road does not belong to that zone. So even the most polluting cars pass through this intersection. Therefore, this location is chosen to represent an urban-traffic situation. An important feature of this location is that it is situated in a street canyon. The VMM (2013) define a street canyon as "a narrow street surrounded by high-rise buildings in which air pollution is less likely to disperse". The VMM has a measuring station on this site that measures only NO and NO₂, data for O₃ was lacking. The meteorological data was provided by the measuring station located in Sint-Jans-Molenbeek, another municipality of Brussels. A considerable benefit is that Brussel Mobiliteit (2021) provides traffic data for the Kunst-Wet site. Therefore, it is possible to link the traffic data with the data of the air pollutants.

6.1.4. Urban-traffic location: Brussels, Sint-Jans-Molenbeek

As previously specified, Sint-Jans-Molenbeek is a municipality of the capital Brussels. This study aims to investigate the relationship between O_3 and the NO_x also for an urban-traffic situation. However, the O_3 concentrations are not measured in the station of Kunst-Wet. Therefore, the station in Sint-Jans-Molenbeek was additionally chosen to represent an urban-traffic situation. This is feasible as this station too is located at a place with a lot of traffic, namely next to the N8 national road. The measuring station of the VMM both measures all pollutants (NO , NO_2 and O_3) and meteorological variables and is thereby very suitable for this research. Although, at this location there is no street canyon present so the situation is not completely identical to the one in Kunst-Wet.

6.2. Data pre-processing

As mentioned before, the data of the air pollutants and the weather variables were provided by the VMM. Since it was opted to work with hourly values in this study, the raw data that were obtained needed further processing for some of the variables. This section will be a detailed discussion of how the data were filtered and processed, which calculations were involved and what decisions were made regarding the elimination of non-valid data.

6.2.1. Meteorological data

Meteorological data were achieved from the measuring stations in Veurne, Ghent and Sint-Jans-Molenbeek. Temperature, relative humidity, wind speed and wind direction are the variables that are directly measured in the stations of the VMM. Values for the medium cloud cover (MCC) and the boundary layer height (BLH) are predicted using a specific model. Altogether, data were offered for six variables which describe the weather conditions in Flanders. Table 8 presents an overview of the final weather variables that will be used in this study. The next two sections will elaborate on how these weather variables were obtained.

Table 8: Weather variables with the corresponding units.

Variable	Temperature			Windspeed			Wind Direction	BLH	MCC
	Mean	Min	Max	Mean	Min	Max			
Unit	°C			m/s			°	m	-

6.2.1.1. Temperature, Relative humidity, Wind speed and Wind direction

The following variables, with the corresponding units, are measured every half hour in the measuring stations of the VMM:

- Temperature in 0.1 Celsius degrees (°C)
- Relative humidity in %
- Wind speed in 0.01 m/s
- Wind direction in degrees (°), where 0° represents the north, 90° the east, 180° the south and 270° the west.

Meteorological data were made available for this study for each variable starting from 1 January 2015 up to 15 November 2020. These data were already validated by the VMM. To obtain hourly values, the half-hourly values were simply averaged. This was easily feasible for the temperature, relative humidity and wind speed. For convenience, the units for temperature and wind speed were adjusted from 0,1 °C and 0,01 m/s to respectively °C and m/s. However, for the wind direction the values could not simply be averaged as a few constraints had to be respected. For example, if the average of 345° and 15° is to be calculated, the average is not 180° (representing the direction “south”) but 0° (representing the direction “north”) as is visible in Figure 19 (Sasquatch Station, 2017). Hence, if the difference between the two values, from which the average is to be derived, is greater than 180°, 180° must be subtracted from the average. It must also be understood that when this operation is performed and the result is less than zero, 360 degrees must be added. Keeping this in mind, hourly values were also obtained for the wind direction. Additionally the maximum and minimum value per hour were calculated for the temperature and wind speed.

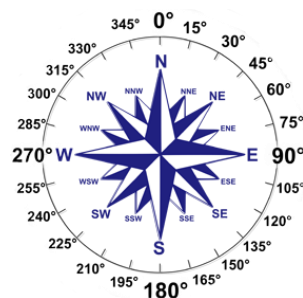


Figure 19: Wind directions (Sasquatch Station, 2017).

6.2.1.2. The Medium cloud cover and Boundary layer height

The medium cloud cover and the boundary layer height were estimated on a six hour basis with a deterministic, meteorological model by the ECMWF (European Centre for Medium-Range Weather Forecasts). The data of these predictions are not public but the VMM has permission to access them and it's allowed to use them in the context of this thesis. The MCC and the BLH are important parameters that provide significant benefits in terms of training the model as they affect the atmospheric concentrations of pollutants. As mentioned in Section 5.2.1, air pollutant concentrations are influenced by the height of the atmospheric boundary layer. Holtslag et al. (2013) define the atmospheric boundary layer as “the lower part of the atmosphere that is in continuous interaction with Earth’s surface owing to friction and heating or cooling”. The lower the height of this layer, the more compact the volume in which air pollution can be dispersed and consequently the higher the concentrations of the air pollutants. The variable “BLH” is expressed in meters. Subsequently, the medium-level cloud cover is the amount of clouds present at a medium height in the atmosphere, ranging from 1800m to 3600m above the earth's surface (ECMWF, 2021). This variable indicates the degree of cloud cover by using a score from 0 to 1. Where 0 indicates no cloud cover, i.e. a clear sky, and 1 indicates completely dense cloud cover at medium altitude.

The MCC and the BLH values are thus available for every six hours, i.e. at the following times: 0h, 6h, 12h and 24h, this starting from 1 January 2015 up to 20 November 2020. To determine the hourly averages for these variables, a linear interpolation was made between the successive six-hourly values. The hourly values from 1 January 2015 up to 15 November 2020 were retained for this study.

6.2.2. Air pollutant concentrations data

Validated data of the air pollutants were available per hour starting from 1 January 2015 up to 9 October 2020 for the four measuring stations: Veurne, Ghent, Brussels (Kunst-Wet) and Sint-Jans-Molenbeek. Non-validated data were used to complete this up to 15 November 2020. Conversion to hourly values was no longer necessary in this case. The concentrations of the pollutants are all expressed in $\mu\text{g}/\text{m}^3$. No further calculations were necessary for the data of the air pollutants.

6.2.3. Traffic data

The VMM provided the traffic data they obtained from Brussel Mobiliteit (2021). These data were only available for the location Brussels (Kunst-Wet), per hour starting from 01/01/2020. These data contain the number of cars passing the counting station for the two present lanes. No further conversions or calculations were applied.

6.2.4. Final dataset

Finally for each location, the air pollutant and meteorological data were put together in RStudio forming a data frame with hourly values starting from 1 January 2015 to 15 November 2020. For the variables MCC and BLH there were respectively 10 and 9 days for which there were no values available. Therefore, data for these days were eliminated for all the variables. The RMWeather package was used in this study for setting up the random forest model. This package also provides some functions to prepare the data. With these functions, variables are added to the dataset that add value in creating the model. The first variable that is added is the Unix date, i.e. a number representing each date in time. The second is the Julian day, i.e. a number that indicates which of the day in the year it is, going thus from 1 to 365 (or 366). The third variable is the weekday, i.e. a number representing which day in the week it is, going from 1 to 7. Finally, the last variable is the hour, i.e. a number representing which hour in the day it is, going from 1 to 24. These variables are valuable as it gives the opportunity to investigate the influence of the day in the year, the day in the week and the hour in the day on the concentrations of the pollutants.

It was opted to construct the training set with data from 1 January 2015 to 31 December 2019. If the model should be trained with data until exactly before the lockdown it is difficult to see whether the difference between the model predictions and the measured values are due to the corona measures or due to poor model performance. If predictions are also made a short period before the corona measures were introduced, the model errors can be detected and thereby taken into account when making statements about predictions during the lockdown.

Table 9 gives the first values of the final dataset used for constructing the model for the pollutant NO for the station in Veurne. The same type of final dataset was constructed for the other pollutants and for the other locations. Unfortunately, for the location Kunst-Wet the final training dataset consist out of data starting from 07/12/2016 until 31/12/2019 as the previous values were missing. The missing values were indicated in the dataset as negative values equal to -9999. The cause of these missing values is not known, however it may be because of malfunctioning of the measuring equipment. It is important that these missing values, indicated with -9999, are removed from the trainings dataset in order to create a logic model.

Therefore all the negative values for the pollutant for which the model is trained, are eliminated out of the specific training dataset together with the data of the variables that are related with these values. For each pollutant at every location, a specific model is created with the final training dataset. The obtained models can then be used to make predictions for the period 01/01/2020 to 15/11/2020 based on data of the weather variables.

Table 9: First values of the final dataset for NO for the station in Veurne.

<i>Date</i>	<i>NO</i>	<i>T_{mean}</i>	<i>T_{min}</i>	<i>T_{max}</i>	<i>WS_{mean}</i>	<i>WS_{min}</i>	<i>WS_{max}</i>	<i>RH</i>
2015-01-01 01:00:00	1.0	1.05	1	1.1	6.225	5.72	6.73	94
<i>WD</i>	<i>BLH</i>	<i>MCC</i>	<i>Unix date</i>	<i>Julian day</i>	<i>Weekday</i>	<i>Hour</i>		
192.50	448.558	0	1420070400	1	4	1		

In Chapter 7, the results will be discussed and used to answer the following research questions:

- How do the pollutant concentrations change during the lockdown?
- Are the possible changes linked with the corona measures, more specifically with the reduction in traffic?
- Are the possible changes in the air pollutant concentrations different in the different locations representing a specific type of traffic situation?
- Are there any changes in the daily patterns of the air pollutants due to the corona measures?
- Is the possible change of the daily patterns different for a week day compared to a weekend day?

7. Results and discussion

In this chapter the results of this study will be presented and discussed. In the first section a before-and-after evaluation will be described for each location to give a first indication of the influence of the corona measures on the pollutant concentrations. In the second section, model validation and interpretation will be covered for each pollutant at each location in order to evaluate the model performance before looking at the results conducted with the random forest models. Additionally, the variables will be identified that are most important in predicting the concentration of the different pollutants and the relation between the variable and the pollutant concentration will be examined. The third section covers the results based on the model simulations for each pollutant. The predictions of the pollutant concentrations will be compared with the measured concentrations in order to investigate the possible impact of the corona measures. This study aims to go beyond the study carried out by the VMM by investigating the impact of the lockdown on the daily patterns of the pollutants. This is feasible since the models are constructed with hourly values. The results for the location Sint-Jans-Molenbeek will be analyzed more in detail. Finally, in order to confirm that the corona measures caused a reduction in traffic, the data on traffic for the location Kunst-Wet (Brussels) will be used.

7.1. Before-and-after evaluation

For each location, some statistics were calculated for both the dependent variables (the air pollutants) and the independent variables (the meteorological variables). More specifically, the mean values, the 95th percentile and the 5th percentile were calculated for the year 2017, 2018 and 2019 and for the period of six months before and after the start of the lockdown. The mean values of the air pollutants six months before the start lockdown can be compared with the mean values for the six months after the start of the lockdown in order to see any change in concentrations. The mean values for the years 2017, 2018 and 2019 are interesting because they give a representation of the pollutant concentrations and weather conditions in Flanders during standard years, i.e. without a pandemic event. The 95th percentile indicates the value for which the variable is 95% of the times below, meaning only 5% of the data for that variable is higher than this value. The 5th percentile indicates the value for which the variable is 95% of the times higher, meaning that only 5% of the data of that variable is below this value. The results are presented in Table 10, Table 11, Table 12 and Table 13 for respectively Veurne, Ghent, Sint-Jans-Molenbeek and Kunst-Wet.

In the measuring station in Veurne, the concentrations of O₃, NO and NO₂ increased with respectively 15%, 18% and 4% in the six months after the start of the lockdown compared to the prior six months. In Ghent, the O₃ concentration increased with 54%, while the NO and NO₂ concentrations decreased with respectively 58% and 28%. The same trend is observed in the urban-traffic locations with a decrease of the NO and NO₂ concentrations with respectively 43% and 18% in Sint-Jans-Molenbeek and respectively 57% and 25% in Brussels, Kunst-Wet. The O₃ concentrations increased in Sint-Jans-Molenbeek with 53%. As mentioned before, various factors influence the concentrations of the air pollutants in the atmosphere, including weather conditions. Therefore, it is important to also consider them when comparing concentrations of two different periods.

At the background location little traffic is present in normal conditions and it's not located close to industry. Therefore, the increase of the NO_x -concentrations during the lockdown are most likely due to changes in weather conditions. When looking at the weather conditions, in every station the same trends are visible: the values for the relative humidity, windspeed, medium cloud cover and boundary layer height are lower in the period during the lockdown compared to the six months before 18 march 2020 and the temperature is higher. When less wet deposition is present due to lower precipitation and less diluting occurs due to lower wind speeds, NO and NO_2 compounds can accumulate in the air. In addition, a lower BLH means a smaller volume in which these pollutants are subject to turbulence also leading to less favorable conditions for air pollution. Less clouds during the night are not beneficial for air pollution as this stimulates the formation of temperature inversions. However, less clouds during the day leads to more solar radiation which is the driver for many processes that stimulate turbulence in the atmosphere. The rise in O_3 concentrations in the background location during the lockdown can be explained by the increase in solar radiation, which drives the ozone formation reactions.

Even though the weather conditions are less favorable for pollution dispersion and dilution, reductions in NO_x concentrations are found at the other measuring locations and the increase in O_3 is higher than in the background location. These results are in line with the results in the study of the VMM and the other studies mentioned in Chapter 5. It may thus be tentatively concluded that these changes are due to other factors than weather, namely due to the lockdown. However, it should be noted that in this before-and-after evaluation a period of six months after the lockdown was chosen. Thereby comparing periods with different seasons and thus different weather conditions. Additionally, the strict COVID-19 lockdown didn't actually last for six months as gradually more corona measures were halted towards the summer. Therefore, it is more interesting to evaluate the first month of the lockdown and compare it with the same period in other years. Evaluating a period of six months after the lockdown can be used to investigate persisting effects of the lockdown on the air quality.

The observed higher O_3 levels during the lockdown at the stations in Ghent, Sint-Jans-Molenbeek and Kunst-Wet are related with the lower NO levels. Since less NO is present in the atmosphere due to lower emissions, the ozone titration is halted. This negative relation between NO and O_3 was visualized in Figure 20. In this figure, the yearly average concentrations for the two pollutants are plotted for each measuring station, excluding Kunst-Wet as O_3 isn't measured at that location. It is clear that the lower the NO concentrations, the higher the O_3 concentrations are. It is also visible that the lowest NO concentrations are measured in the background location Veurne and the highest in the urban-traffic location. This is expected since NO-emissions are strongly related with traffic. Consequently, the background location has the highest O_3 concentrations and the urban-traffic location the lowest. The same relation between NO and O_3 was found in the report of the VMM in 2013 on the photochemical air pollution (Vancraeynest, 2013).

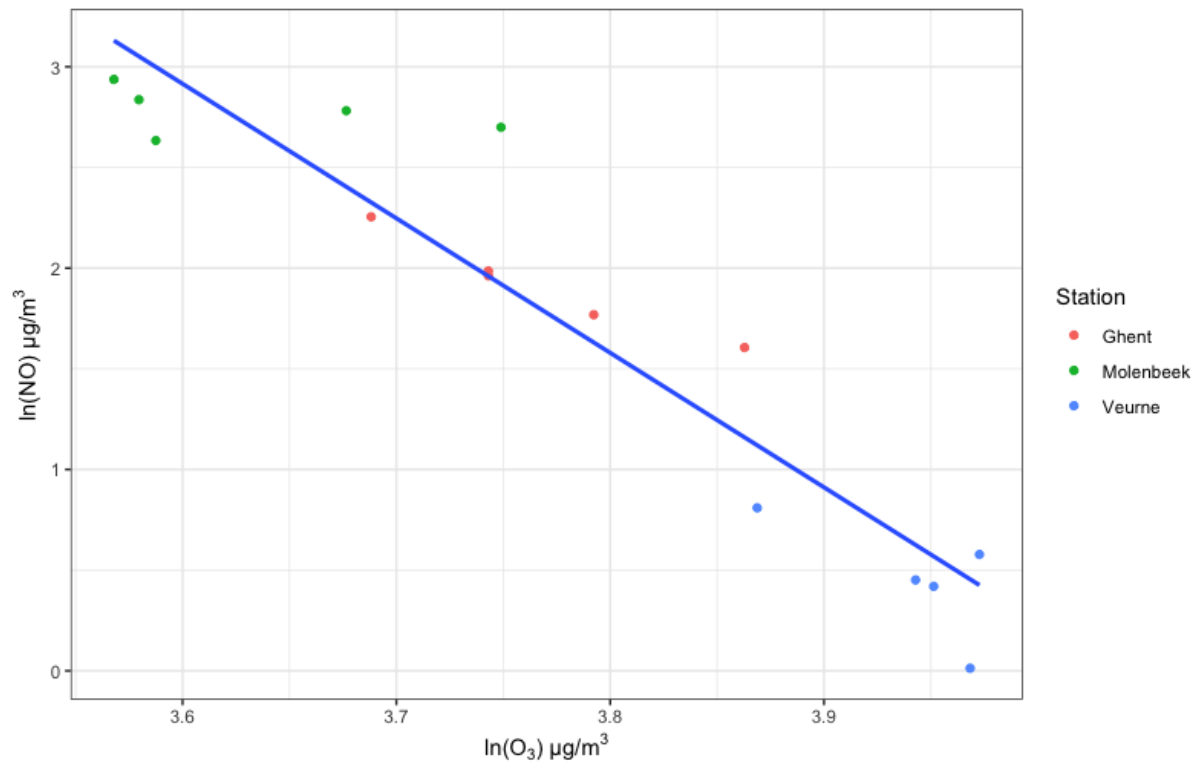


Figure 20: Relation between the yearly NO and O₃ concentrations.

Table 10: Statistics for the background location Veurne.

Input Variable	2017		2018		2019		6 months before the start of the lockdown		6 months after the start of the lockdown	
O₃ ($\mu\text{g}/\text{m}^3$)	<i>mean</i>	52.5	<i>mean</i>	52.7	<i>mean</i>	52.9	<i>mean</i>	49.4	<i>mean</i>	57.2
	<i>P95</i>	92.5	<i>P95</i>	96.5	<i>P95</i>	89.5	<i>P95</i>	78.0	<i>P95</i>	100
	<i>P5</i>	8.50	<i>P5</i>	7.50	<i>P5</i>	11.5	<i>P5</i>	9.10	<i>P5</i>	16.0
NO ($\mu\text{g}/\text{m}^3$)	<i>mean</i>	1.69	<i>mean</i>	1.55	<i>mean</i>	1.05	<i>mean</i>	0.76	<i>mean</i>	0.90
	<i>P95</i>	7.50	<i>P95</i>	7.00	<i>P95</i>	5.00	<i>P95</i>	3.50	<i>P95</i>	3.50
	<i>P5</i>	0.00	<i>P5</i>	0.00	<i>P5</i>	0.00	<i>P5</i>	0.00	<i>P5</i>	0.00
NO₂ ($\mu\text{g}/\text{m}^3$)	<i>mean</i>	11.6	<i>mean</i>	11.2	<i>mean</i>	10.2	<i>mean</i>	9.02	<i>mean</i>	9.37
	<i>P95</i>	33.5	<i>P95</i>	30.5	<i>P95</i>	29.0	<i>P95</i>	27.5	<i>P95</i>	26.0
	<i>P5</i>	1.50	<i>P5</i>	1.50	<i>P5</i>	1.50	<i>P5</i>	1.50	<i>P5</i>	1.50
Relative Humidity (%)	<i>mean</i>	84	<i>mean</i>	83	<i>mean</i>	84	<i>mean</i>	90	<i>mean</i>	74
	<i>P95</i>	100	<i>P95</i>	100	<i>P95</i>	99	<i>P95</i>	100	<i>P95</i>	97
	<i>P5</i>	57	<i>P5</i>	53	<i>P5</i>	56	<i>P5</i>	72	<i>P5</i>	45
Temperature ($^{\circ}\text{C}$)	<i>mean</i>	11.4	<i>mean</i>	11.3	<i>mean</i>	11.49	<i>mean</i>	8.68	<i>mean</i>	14.5
	<i>P95</i>	21.1	<i>P95</i>	22.0	<i>P95</i>	21.3	<i>P95</i>	16.1	<i>P95</i>	23.2
	<i>P5</i>	1.20	<i>P5</i>	0.55	<i>P5</i>	2.30	<i>P5</i>	2.00	<i>P5</i>	5.80
Wind Speed (m/s)	<i>mean</i>	5.47	<i>mean</i>	5.26	<i>mean</i>	5.34	<i>mean</i>	6.42	<i>mean</i>	5.13
	<i>P95</i>	10.7	<i>P95</i>	10.4	<i>P95</i>	10.8	<i>P95</i>	12.8	<i>P95</i>	10.6
	<i>P5</i>	1.87	<i>P5</i>	1.67	<i>P5</i>	1.73	<i>P5</i>	2.10	<i>P5</i>	1.46
Wind Direction ($^{\circ}$)	<i>mean</i>	204	<i>mean</i>	172	<i>mean</i>	189	<i>mean</i>	198	<i>mean</i>	173
	<i>P95</i>	332	<i>P95</i>	336	<i>P95</i>	333	<i>P95</i>	312	<i>P95</i>	335
	<i>P5</i>	32	<i>P5</i>	16	<i>P5</i>	23	<i>P5</i>	63	<i>P5</i>	22
MCC (-)	<i>mean</i>	0.33	<i>mean</i>	0.27	<i>mean</i>	0.33	<i>mean</i>	0.40	<i>mean</i>	0.26
	<i>P95</i>	0.96	<i>P95</i>	0.98	<i>P95</i>	0.97	<i>P95</i>	0.98	<i>P95</i>	0.94
	<i>P5</i>	0	<i>P5</i>	0	<i>P5</i>	0	<i>P5</i>	0	<i>P5</i>	0
BLH (m)	<i>mean</i>	766.5	<i>mean</i>	688.1	<i>mean</i>	766.4	<i>mean</i>	940.3	<i>mean</i>	736.9
	<i>P95</i>	1621	<i>P95</i>	1491	<i>P95</i>	1675	<i>P95</i>	1817	<i>P95</i>	1633
	<i>P5</i>	152.5	<i>P5</i>	117.7	<i>P5</i>	133.6	<i>P5</i>	191	<i>P5</i>	109.8

Table 11: Statistics for the urban-background location Ghent, Baudelopark.

Input Variable	2017		2018		2019		6 months before the start of the lockdown		6 months after the start of the lockdown	
O₃ (µg/m ³)	<i>mean</i>	42.3	<i>mean</i>	44.2	<i>mean</i>	47.7	<i>mean</i>	37.5	<i>mean</i>	57.6
	<i>P95</i>	88.0	<i>P95</i>	97.5	<i>P95</i>	92.5	<i>P95</i>	69.5	<i>P95</i>	112
	<i>P5</i>	1.50	<i>P5</i>	1.50	<i>P5</i>	2.50	<i>P5</i>	1.00	<i>P5</i>	14.8
NO (µg/m ³)	<i>mean</i>	7.69	<i>mean</i>	6.07	<i>mean</i>	5.26	<i>mean</i>	6.48	<i>mean</i>	2.73
	<i>P95</i>	34.0	<i>P95</i>	28.0	<i>P95</i>	22.5	<i>P95</i>	27.0	<i>P95</i>	11.0
	<i>P5</i>	0.00	<i>P5</i>	0.00	<i>P5</i>	0.00	<i>P5</i>	0.00	<i>P5</i>	0.00
NO₂ (µg/m ³)	<i>mean</i>	27.4	<i>mean</i>	25.7	<i>mean</i>	23.6	<i>mean</i>	24.7	<i>mean</i>	17.7
	<i>P95</i>	60.1	<i>P95</i>	55.5	<i>P95</i>	56.5	<i>P95</i>	55.0	<i>P95</i>	44.5
	<i>P5</i>	7.00	<i>P5</i>	7.00	<i>P5</i>	6.00	<i>P5</i>	6.50	<i>P5</i>	4.50
Relative Humidity (%)	<i>mean</i>	79	<i>mean</i>	76	<i>mean</i>	78	<i>mean</i>	86	<i>mean</i>	69
	<i>P95</i>	99	<i>P95</i>	98	<i>P95</i>	98	<i>P95</i>	99	<i>P95</i>	97
	<i>P5</i>	47	<i>P5</i>	42	<i>P5</i>	45	<i>P5</i>	66	<i>P5</i>	34
Temperature (°C)	<i>mean</i>	12.1	<i>mean</i>	12.5	<i>mean</i>	12.4	<i>mean</i>	8.93	<i>mean</i>	15.7
	<i>P95</i>	22.9	<i>P95</i>	24.6	<i>P95</i>	23.4	<i>P95</i>	16.3	<i>P95</i>	25.2
	<i>P5</i>	0.90	<i>P5</i>	1.15	<i>P5</i>	3.00	<i>P5</i>	2.62	<i>P5</i>	7.15
Wind Speed (m/s)	<i>mean</i>	3.78	<i>mean</i>	3.74	<i>mean</i>	3.81	<i>mean</i>	4.48	<i>mean</i>	3.71
	<i>P95</i>	7.02	<i>P95</i>	6.86	<i>P95</i>	7.15	<i>P95</i>	8.10	<i>P95</i>	7.05
	<i>P5</i>	1.49	<i>P5</i>	1.47	<i>P5</i>	1.54	<i>P5</i>	1.70	<i>P5</i>	1.30
Wind Direction (°)	<i>mean</i>	205	<i>mean</i>	187	<i>mean</i>	194	<i>mean</i>	197	<i>mean</i>	179
	<i>P95</i>	334	<i>P95</i>	346	<i>P95</i>	338	<i>P95</i>	296	<i>P95</i>	341
	<i>P5</i>	47	<i>P5</i>	29	<i>P5</i>	35	<i>P5</i>	67	<i>P5</i>	24
MCC (-)	<i>mean</i>	0.33	<i>mean</i>	0.28	<i>mean</i>	0.33	<i>mean</i>	0.38	<i>mean</i>	0.27
	<i>P95</i>	0.94	<i>P95</i>	0.97	<i>P95</i>	0.96	<i>P95</i>	0.98	<i>P95</i>	0.92
	<i>P5</i>	0	<i>P5</i>	0	<i>P5</i>	0	<i>P5</i>	0	<i>P5</i>	0
BLH (m)	<i>mean</i>	767.6	<i>mean</i>	722.3	<i>mean</i>	783.2	<i>mean</i>	891.1	<i>mean</i>	799.0
	<i>P95</i>	1637	<i>P95</i>	1578	<i>P95</i>	1696	<i>P95</i>	1790	<i>P95</i>	1642
	<i>P5</i>	131.9	<i>P5</i>	114.6	<i>P5</i>	121.0	<i>P5</i>	149.6	<i>P5</i>	111.6

Table 12: Statistics for the urban-traffic location Sint-Jans-Molenbeek, Brussels.

Input Variable	2017		2018		2019		6 months before the start of the lockdown		6 months after the start of the lockdown	
O₃ (µg/m ³)	<i>mean</i>	36.7	<i>mean</i>	39.5	<i>mean</i>	42.8	<i>mean</i>	33.6	<i>mean</i>	51.3
	<i>P95</i>	78.6	<i>P95</i>	93.5	<i>P95</i>	91.5	<i>P95</i>	64.5	<i>P95</i>	103
	<i>P5</i>	2.00	<i>P5</i>	2.00	<i>P5</i>	2.00	<i>P5</i>	2.00	<i>P5</i>	7.00
NO (µg/m ³)	<i>mean</i>	13.8	<i>mean</i>	16.2	<i>mean</i>	14.8	<i>mean</i>	15.2	<i>mean</i>	8.66
	<i>P95</i>	54.3	<i>P95</i>	61.5	<i>P95</i>	55.5	<i>P95</i>	64.0	<i>P95</i>	26
	<i>P5</i>	2.00	<i>P5</i>	3.00	<i>P5</i>	3.00	<i>P5</i>	3.00	<i>P5</i>	3.00
NO₂ (µg/m ³)	<i>mean</i>	33.3	<i>mean</i>	35.1	<i>mean</i>	30.8	<i>mean</i>	27.3	<i>mean</i>	22.5
	<i>P95</i>	70.5	<i>P95</i>	70.0	<i>P95</i>	65.5	<i>P95</i>	56.6	<i>P95</i>	53.5
	<i>P5</i>	7.00	<i>P5</i>	10.0	<i>P5</i>	7.00	<i>P5</i>	5.00	<i>P5</i>	3.50
Relative Humidity (%)	<i>mean</i>	76	<i>mean</i>	69	<i>mean</i>	71	<i>mean</i>	79	<i>mean</i>	63
	<i>P95</i>	100	<i>P95</i>	93	<i>P95</i>	93	<i>P95</i>	94	<i>P95</i>	91
	<i>P5</i>	42	<i>P5</i>	37	<i>P5</i>	39	<i>P5</i>	59	<i>P5</i>	30
Temperature (°C)	<i>mean</i>	13.6	<i>mean</i>	12.7	<i>mean</i>	12.4	<i>mean</i>	8.68	<i>mean</i>	15.9
	<i>P95</i>	26.1	<i>P95</i>	25.4	<i>P95</i>	24.1	<i>P95</i>	16.1	<i>P95</i>	26.0
	<i>P5</i>	0.90	<i>P5</i>	0.85	<i>P5</i>	2.25	<i>P5</i>	2.25	<i>P5</i>	7.00
Wind Speed (m/s)	<i>mean</i>	3.47	<i>mean</i>	3.34	<i>mean</i>	3.55	<i>mean</i>	4.22	<i>mean</i>	3.41
	<i>P95</i>	7.23	<i>P95</i>	6.40	<i>P95</i>	6.93	<i>P95</i>	8.06	<i>P95</i>	6.74
	<i>P5</i>	1.20	<i>P5</i>	1.24	<i>P5</i>	1.26	<i>P5</i>	1.38	<i>P5</i>	1.15
Wind Direction (°)	<i>mean</i>	194	<i>mean</i>	180	<i>mean</i>	190	<i>mean</i>	187	<i>mean</i>	175
	<i>P95</i>	333	<i>P95</i>	338	<i>P95</i>	332	<i>P95</i>	279	<i>P95</i>	339
	<i>P5</i>	23	<i>P5</i>	12	<i>P5</i>	17	<i>P5</i>	38	<i>P5</i>	11
MCC (-)	<i>mean</i>	0.34	<i>mean</i>	0.29	<i>mean</i>	0.33	<i>mean</i>	0.39	<i>mean</i>	0.28
	<i>P95</i>	0.95	<i>P95</i>	0.97	<i>P95</i>	0.97	<i>P95</i>	0.99	<i>P95</i>	0.95
	<i>P5</i>	0	<i>P5</i>	0	<i>P5</i>	0	<i>P5</i>	0	<i>P5</i>	0
BLH (m)	<i>mean</i>	754.7	<i>mean</i>	740.7	<i>mean</i>	783.6	<i>mean</i>	888.1	<i>mean</i>	819.4
	<i>P95</i>	1633	<i>P95</i>	1621	<i>P95</i>	1689	<i>P95</i>	1770	<i>P95</i>	1703
	<i>P5</i>	119.3	<i>P5</i>	115.4	<i>P5</i>	121.0	<i>P5</i>	146.3	<i>P5</i>	121.4

Table 13: Statistics for the urban-traffic location Kunst-Wet, Brussels.

Input Variable	2017		2018		2019		6 months before the start of the lockdown		6 months after the start of the lockdown	
NO ($\mu\text{g}/\text{m}^3$)	<i>mean</i>	38.5	<i>mean</i>	34.7	<i>mean</i>	30.5	<i>mean</i>	30.9	<i>mean</i>	13.2
	<i>P95</i>	109	<i>P95</i>	98.1	<i>P95</i>	92.0	<i>P95</i>	87.2	<i>P95</i>	40.5
	<i>P5</i>	4.00	<i>P5</i>	4.00	<i>P5</i>	3.00	<i>P5</i>	3.00	<i>P5</i>	3.00
NO₂ ($\mu\text{g}/\text{m}^3$)	<i>mean</i>	56.1	<i>mean</i>	56.2	<i>mean</i>	51.5	<i>mean</i>	45.2	<i>mean</i>	33.7
	<i>P95</i>	97.2	<i>P95</i>	96.5	<i>P95</i>	91.0	<i>P95</i>	75.5	<i>P95</i>	64.5
	<i>P5</i>	22.5	<i>P5</i>	23.9	<i>P5</i>	20.5	<i>P5</i>	16.5	<i>P5</i>	11.0
Relative Humidity (%)	<i>mean</i>	76	<i>mean</i>	69	<i>mean</i>	71	<i>mean</i>	79	<i>mean</i>	63
	<i>P95</i>	100	<i>P95</i>	93	<i>P95</i>	93	<i>P95</i>	94	<i>P95</i>	91
	<i>P5</i>	42	<i>P5</i>	37	<i>P5</i>	39	<i>P5</i>	59	<i>P5</i>	30
Temperature (°C)	<i>mean</i>	13.6	<i>mean</i>	12.7	<i>mean</i>	12.4	<i>mean</i>	8.68	<i>mean</i>	15.9
	<i>P95</i>	26.1	<i>P95</i>	25.4	<i>P95</i>	24.1	<i>P95</i>	16.1	<i>P95</i>	26.0
	<i>P5</i>	0.90	<i>P5</i>	0.85	<i>P5</i>	2.25	<i>P5</i>	2.25	<i>P5</i>	7.00
Wind Speed (m/s)	<i>mean</i>	3.47	<i>mean</i>	3.34	<i>mean</i>	3.55	<i>mean</i>	4.22	<i>mean</i>	3.41
	<i>P95</i>	7.23	<i>P95</i>	6.40	<i>P95</i>	6.93	<i>P95</i>	8.06	<i>P95</i>	6.74
	<i>P5</i>	1.20	<i>P5</i>	1.24	<i>P5</i>	1.26	<i>P5</i>	1.38	<i>P5</i>	1.15
Wind Direction (°)	<i>mean</i>	194	<i>mean</i>	180	<i>mean</i>	190	<i>mean</i>	187	<i>mean</i>	175
	<i>P95</i>	333	<i>P95</i>	338	<i>P95</i>	332	<i>P95</i>	279	<i>P95</i>	339
	<i>P5</i>	23	<i>P5</i>	12	<i>P5</i>	17	<i>P5</i>	38	<i>P5</i>	11
MCC (-)	<i>mean</i>	0.34	<i>mean</i>	0.29	<i>mean</i>	0.33	<i>mean</i>	0.39	<i>mean</i>	0.28
	<i>P95</i>	0.95	<i>P95</i>	0.97	<i>P95</i>	0.97	<i>P95</i>	0.99	<i>P95</i>	0.95
	<i>P5</i>	0	<i>P5</i>	0	<i>P5</i>	0	<i>P5</i>	0	<i>P5</i>	0
BLH (m)	<i>mean</i>	754.7	<i>mean</i>	740.7	<i>mean</i>	783.6	<i>mean</i>	888.1	<i>mean</i>	819.4
	<i>P95</i>	1633	<i>P95</i>	1621	<i>P95</i>	1689	<i>P95</i>	1770	<i>P95</i>	1703
	<i>P5</i>	119.3	<i>P5</i>	115.4	<i>P5</i>	121.0	<i>P5</i>	146.3	<i>P5</i>	121.4

7.2. Model validation and interpretation

Model validation is important as it is used to evaluate how well the model performs in predicting the pollutant concentrations based on the weather conditions. As mentioned before, the RMWeather package provides a function that randomly divides 80 % of the constructed training dataset (01/01/2015-31/12/2019) into the effective training set and 20% as a test set. The training set is used to construct each model with and the test set is used to validate the specific model. The model is used to predict the concentrations for the test set for the pollutant for which the model was constructed. Afterwards, the predictions are compared with the actual measured concentrations in the test set. By calculating the R-squared (R^2) and the Root Mean Squared Error (RMSE), the goodness-of-fit for each model is measured. The R^2 is a statistical measure, ranging from 0 to 1 that explains how much of the variance of the output can be attributed to the model (Fernando, 2020). It shows how well the independent variables, i.e. the weather variables, can be used to predict the dependent variable, i.e. the pollutant concentration. The closer to 1, the better the model explains the variance of the output, meaning that the model performance is good. The RMSE is the root of the MSE, which is the Mean Squared Error between the predictions and the observations:

$$MSE = \frac{1}{n} \sum_{i=1}^n (y_i - \hat{f}(x_i))^2$$

With n the amount of observations, y_i the i^{th} observation and $\hat{f}(x_i)$ the prediction for the i^{th} observation (James et al., 2013). The lower the RMSE, the closer the predictions are to the observations. In Figure 21, the model validation is visualized for each pollutant at each location. The observed value of the pollutant is plotted against the predicted value of the pollutant and the R^2 and RMSE are given for each model. The model constructed for NO at each location only explains around 67% of the output variation. It can be observed that the model underestimates high values of the NO concentrations, meaning that the model doesn't accurately predict the higher concentrations by using weather conditions. This can be explained by the fact that NO is strongly related with traffic and that high NO concentrations occur when a lot of traffic is present. Predicting these events of heavy traffic can't be easily done based on weather conditions. Therefore, the variance of the NO concentrations can only be partially explained by the model. The models for NO₂ achieve better R^2 values, with 0.80 for the locations Ghent and Sint-Jans-Molenbeek. Lastly, the models for O₃ perform really good at each location with an R^2 nearly equal to 0.90. This indicates that most of the variance in the ozone concentrations can be explained by the models.

Furthermore, the variables that are most important in predicting each pollutant at each location are identified and presented in Figure 22 and Figure 23. For each variable, the variable importance was calculated with a function available in the RMWeather package. Grange (2020) defines the variable importance as "the permutation importance difference of predictions errors". In fact, these values indicate how much the prediction error of the model increases after the variable is permuted, i.e. the values for this variable are rearranged in the dataset and new predictions are made with this dataset. By permutating the variable, the relation with the outcome variable is changed and therefore the predictions and the related prediction errors (Molnar, 2020). A large value for the variable importance is thus attributed to an important variable since it indicates that changing the variable strongly influences the predictions made with the model.

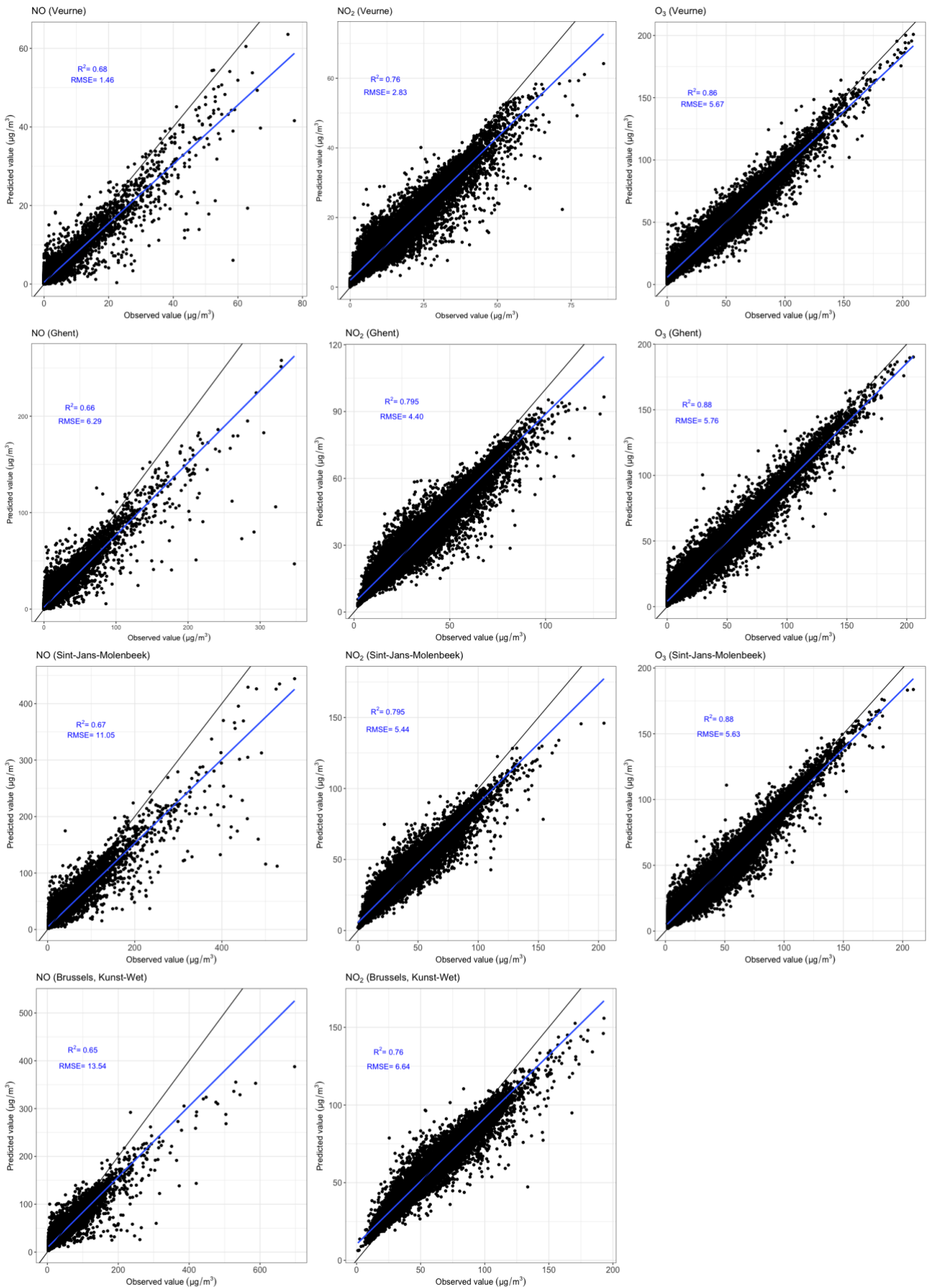


Figure 21: Model validation (01/01/2015 – 31/12/2019) for each pollutant at each measuring location. The black line represents the $y=x$ line and the blue line represents the fitted line to the scatterplot.

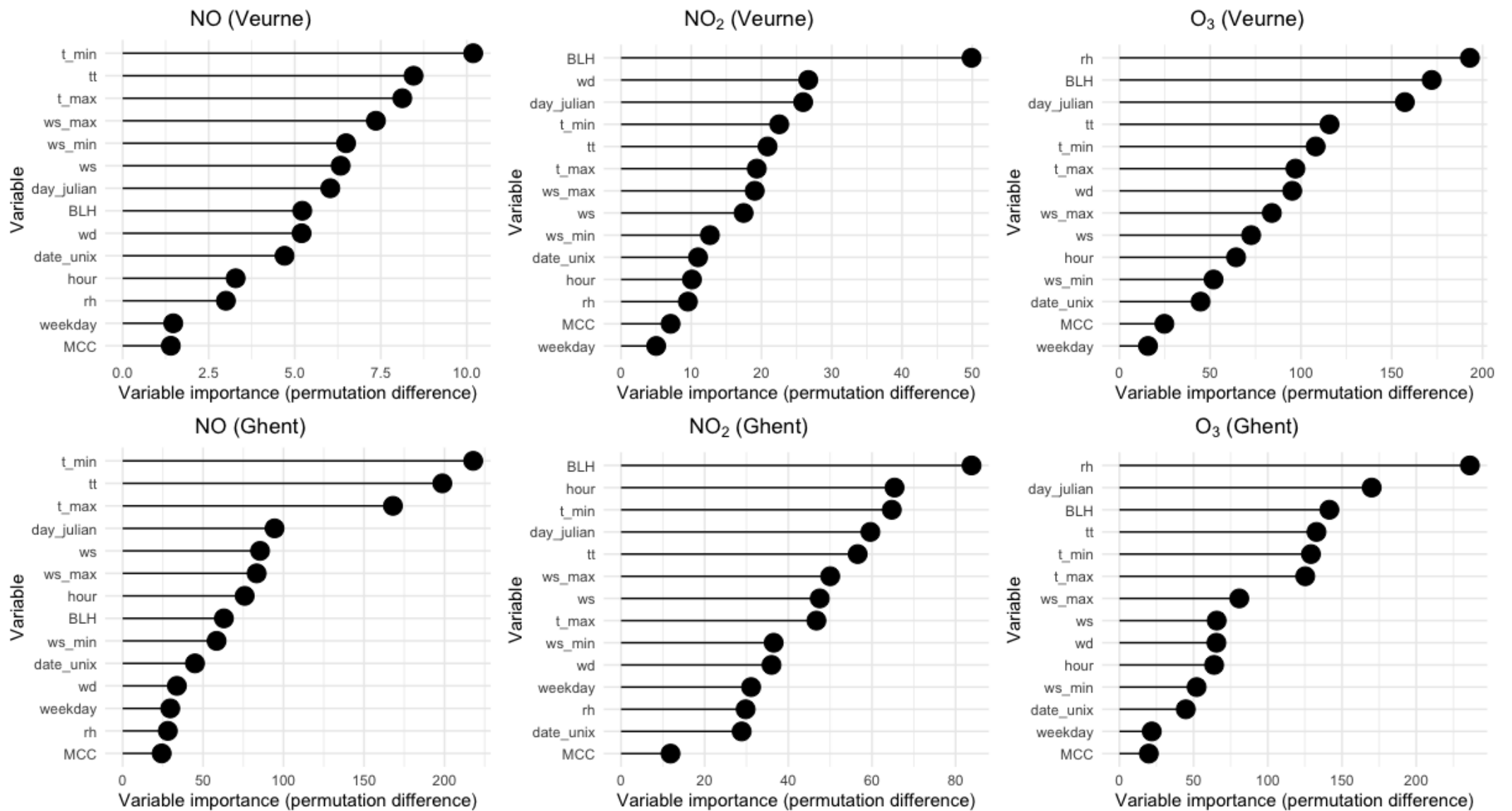


Figure 22: Variable importance for each pollutant. Upper: Measuring station in Veurne. Lower: Measuring station in Ghent.

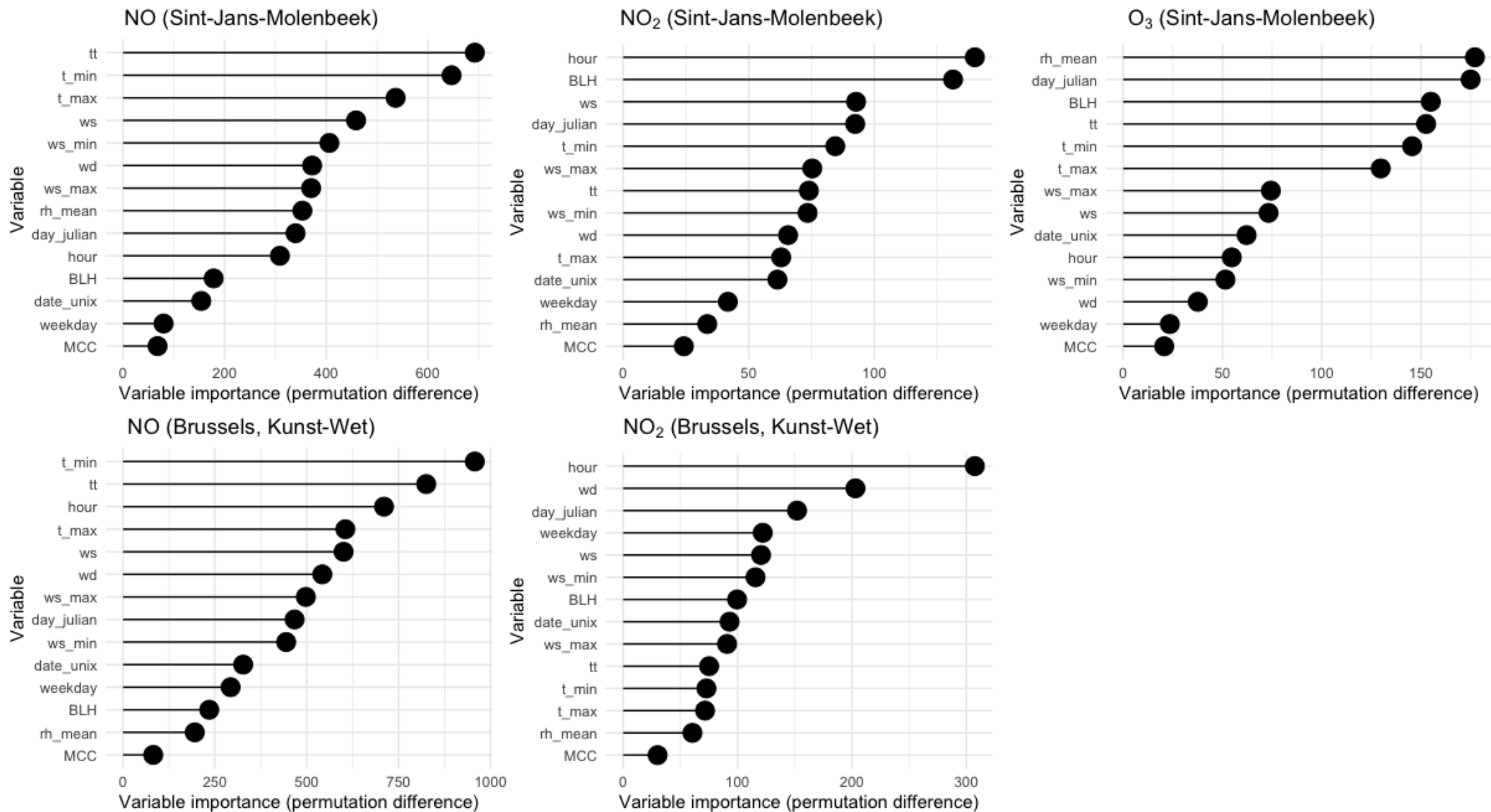


Figure 23: Variable importance for each pollutant. Upper: Measuring station in Sint-Jans-Molenbeek. Lower: Measuring station in Kunst-Wet (Brussels).

The most important variable in predicting the NO concentrations at each location is the temperature, more specifically the minimal temperature. At the station of Kunst-Wet a very high value for the variable importance of the minimal temperature is observed. The influence of the minimal temperature could be linked with presence of temperature inversion which creates a stable atmosphere and therefore traps NO pollution. Furthermore, in Veurne and Sint-Jans-Molenbeek the windspeed is also an important parameter in the NO-models. The windspeed is strongly linked with the amount of dilution of the NO compounds in the atmosphere and therefore influences the present concentrations. In the station of Kunst-Wet, it can be observed that the hour in the day is more important than the windspeed. This is expected since this station is located in a street canyon and therefore less subjected to wind. The importance of the hour in the day is probably linked with the amount of traffic. Traffic peak hours influence the NO concentrations by the increase of NO emissions. The Julian day also reaches the top 5 of most important variables for the station in Ghent. This means that NO concentrations are also related with the day in the year at this location. For the NO₂-models, the BLH stands out for the stations in Veurne, Ghent and Sint-Jans-Molenbeek. It can be remarked that the BLH wasn't even found in the top 5 for Kunst-Wet. The importance of the BLH isn't unexpected since this parameter influences the amount of dispersion of the NO₂ compounds. For the urban-traffic locations, the hour in the day is the most important variable. This again can be linked with the amount of traffic passing by the stations. Furthermore, the Julian day was found in every top 5. In addition, the windspeed and the wind direction have high values for respectively Sint-Jans-Molenbeek and Kunst-Wet. The day in the week can also be considered as important variable for the NO₂-model in Kunst-Wet, again this is probably linked with the amount of traffic. During the work week more traffic is present on the roads than during the weekends. The relative humidity is the most important variable at each location for the O₃-models, subsequently followed by the BLH, the Julian day and the temperature. The relative humidity can be used as indicator of the amount of precipitation. The amount of O₃ present in the air is influenced by rain due to wet deposition. As mentioned before, the BLH is an important feature for dispersion of pollutants in the atmosphere and therefore influences the O₃ concentrations. Furthermore, the importance of the Julian day, i.e. the specific day in the year, can be attributed to the fact that in summer, i.e. warm periods with a lot of sunlight, the ozone levels are higher since ozone formation is driven by sunlight. For the same reason, temperature is an important variable in the O₃ models.

The relation between the most important variables and the pollutant predictions were analyzed more in depth for the urban-traffic location in Sint-Jans-Molenbeek. Predictions were made with the NO-, NO₂- and O₃-model for this location for the period of 01/01/2020 - 15/11/2020, i.e. a new dataset. The NO-predictions were plotted in relation with the temperature and windspeed in Figure 24. The NO₂ predictions were plotted in relation with the BLH and windspeed in Figure 25 and the O₃ predictions with the temperature, RH and BLH in Figure 26. A clear negative correlation was observed between the NO-predictions and the WS. This is expected since high wind speeds causes more dilution of the NO compounds in the air and therefore leads to lower NO-concentrations. The same negative trend is observed with the NO₂ predictions. No obvious trend is found between NO and T but at lower temperatures, higher concentrations are predicted. This could be explained by the fact that temperature inversion is more likely to occur when low temperatures are present at ground level, for example at night, leading to a more stable atmosphere. Furthermore, a negative relation is seen between NO₂ and the BLH. This is also expected since a lower BLH means less volume in which the NO₂ compounds can be diluted. However, no clear relation between O₃ and the BLH can be observed.

A negative relation exists between the O_3 predictions and the RH. At higher levels of RH, less O_3 was predicted. This is explained by the fact that high RH can be related with high amounts of precipitation and therefore more wet deposition. Finally, a positive relation can be observed between O_3 and the temperature. As mentioned before, the ozone formation is driven by the presence of sunlight. At higher temperature it is more likely that a lot of solar radiation is present, therefore creating higher levels of O_3 in the atmosphere.

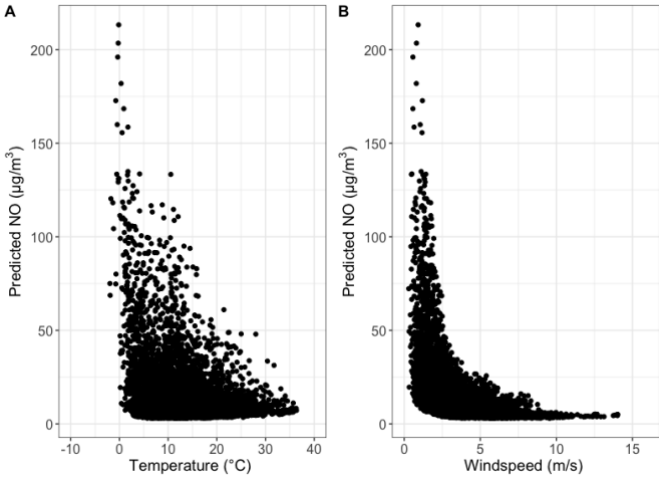


Figure 24: Relation between the NO -predictions and A) the temperature and B) the windspeed.

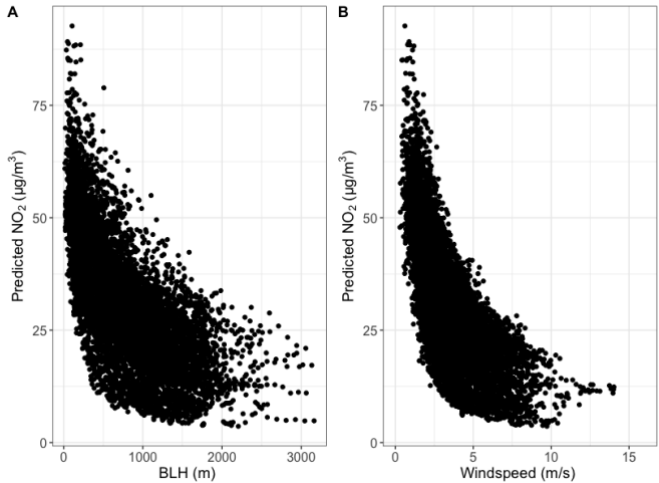


Figure 25: Relation between the NO_2 -predictions and A) the BLH and B) the windspeed.

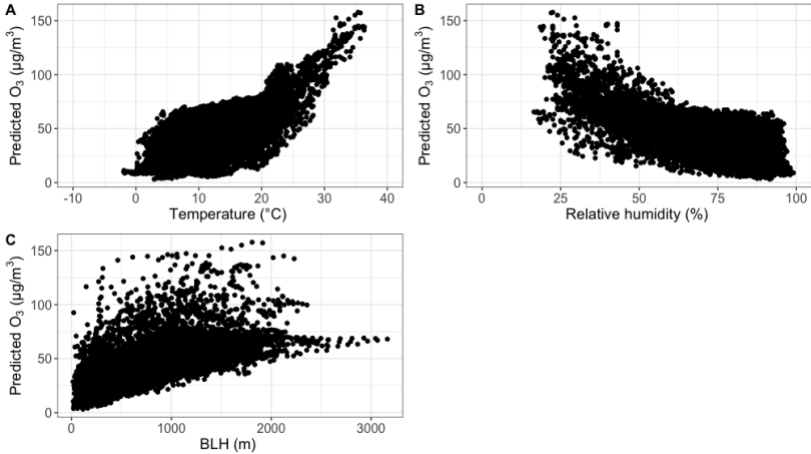


Figure 26: Relation between the O_3 -predictions and A) the temperature, B) the RH and C) the BLH.

7.3. Results based on model simulations

In this section, the predictions made with the random forest model for each pollutant with the new dataset (01/01/2020-15/11/2020) will be compared with the measured concentrations. Since the effect of the weather conditions is isolated with this method, the difference between the predictions and measurements can be attributed to the COVID-19 lockdown. Per location a detailed description of the results will be presented. Additionally, the daily patterns of each pollutant during the first month of the lockdown will be compared with the daily patterns of the same period averaged for the year 2015-2019 to investigate whether there is any change. It is important to note that the analysis of the impact of the lockdown on the daily patterns wasn't performed in the report of the VMM on the impact of the corona measure on air quality in Flanders. Thereby, the aim of this thesis is to establish additional findings to their results. For the stations in Veurne and Sint-Jans-Molenbeek the average daily patterns of Tuesday and a Sunday during the first month of the lockdown will be compared with patterns of the same period in previous years to investigate whether the possible impact of the corona measures is the same for a week day as a weekend day. In addition, the results for the urban-traffic location Sint-Jans-Molenbeek will be analyzed more in depth in Section 7.3.3 by comparing the daily patterns with the patterns constructed with the predictions made with the models for each pollutant.

7.3.1. Background location: Veurne

As there is already little traffic passing by this background location, it is expected that the lockdown will not strongly impact the concentrations of the pollutants related to traffic. In order to investigate this, the measured concentrations and the predictions made with the random forest models are plotted in Figure 27 for NO and in Figure 29 for NO₂. Since these figures are constructed with hourly values, there is a lot of data plotted and this is not easy to interpret. Therefore, the trends in the data are made more clear by fitting a linear regression line, i.e. smoothing the data in Figure 28 and Figure 30. However, by smoothing the data, outliers that are interesting are filtered out. Still, it's chosen to use these figures to compare the predicted values with the measurements. It should be remarked that the scale on the smoothed graphs are smaller in order to have a more detailed look at the difference between the predictions and measurements. The dotted line, indicates the start of the lockdown, i.e. 18th March, in each figure. Figure 28 shows an increase of the measured NO concentrations after the start of the lockdown, but the model also predicts this increase. The VMM (2020a) relates this increase with the change in the weather conditions. The weather was more favorable for air pollution in the period before the start of the lockdown as this period was characterized with heavy rains and gusts of wind. Whereas, the first month of the lockdown was characterized with less wind, less clouds and less rain thus less favorable weather conditions. The model was able to predict this increase in NO concentrations by using data on the weather variables. The NO₂ concentrations predicted with the model match the observed concentrations quite good, except for the period just before the start of the lockdown. There, the predictions are a bit higher. The increase in the measured NO₂ concentrations during the lockdown was also predicted by the model. Finally, Figure 31 and Figure 32 present the results from the O₃-model. The predictions match the observations properly during the lockdown, meaning the model could predict the O₃ concentrations. Yet, starting from august a small difference can be observed between the predictions and measurements.

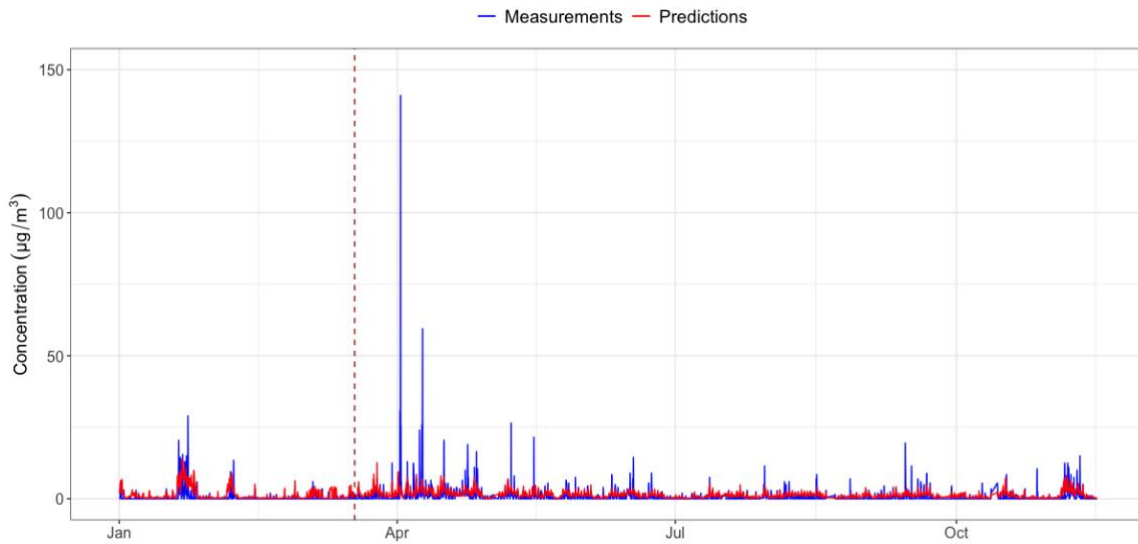


Figure 27: Predicted hourly NO concentrations and measured hourly NO concentrations in 2020 (Veurne).

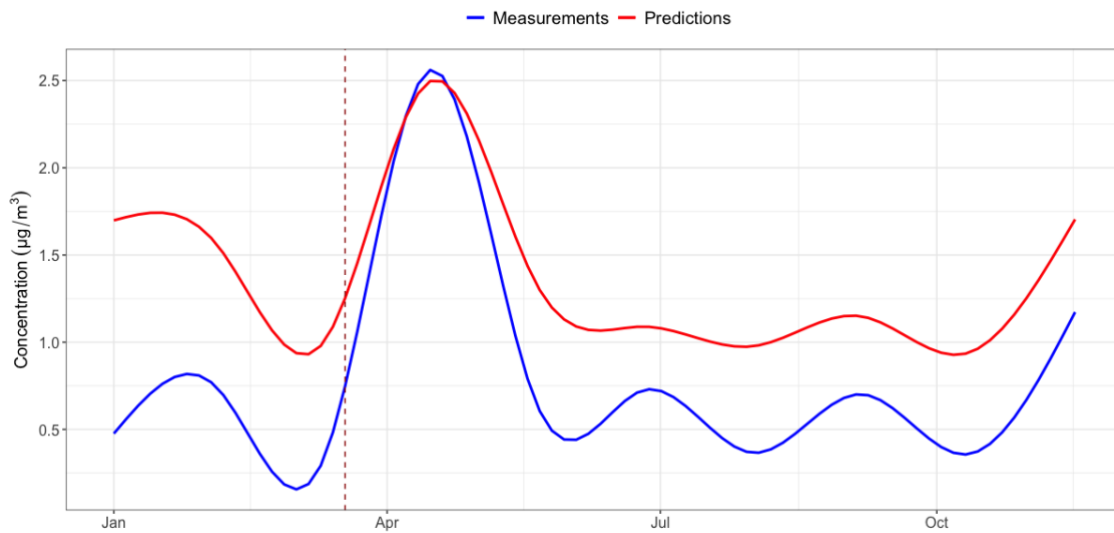


Figure 28: Smoothed predicted hourly NO concentrations and measured hourly NO concentrations in 2020 (Veurne).

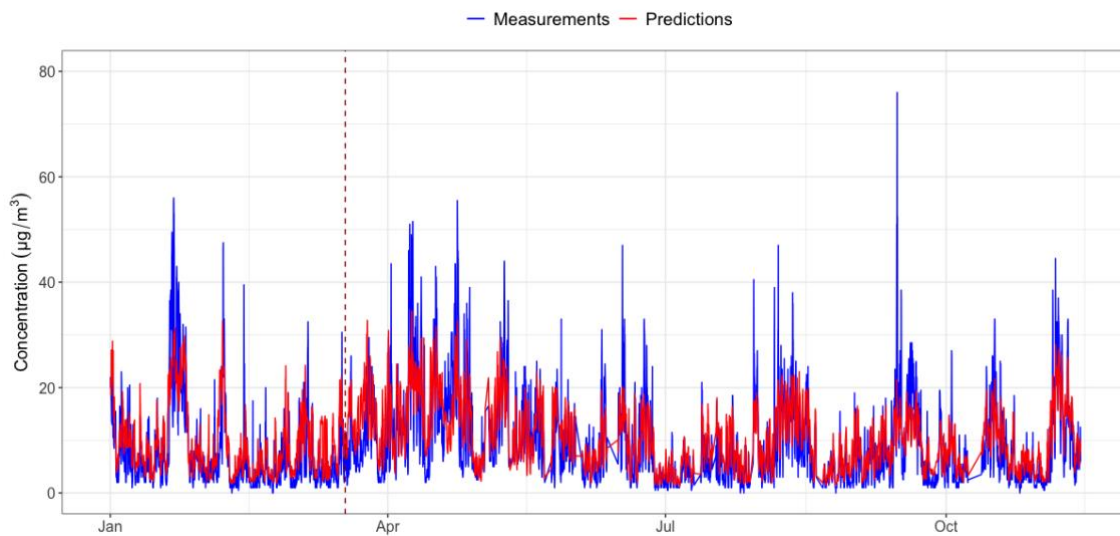


Figure 29: Predicted hourly NO₂ concentrations and measured hourly NO₂ concentrations in 2020 (Veurne).

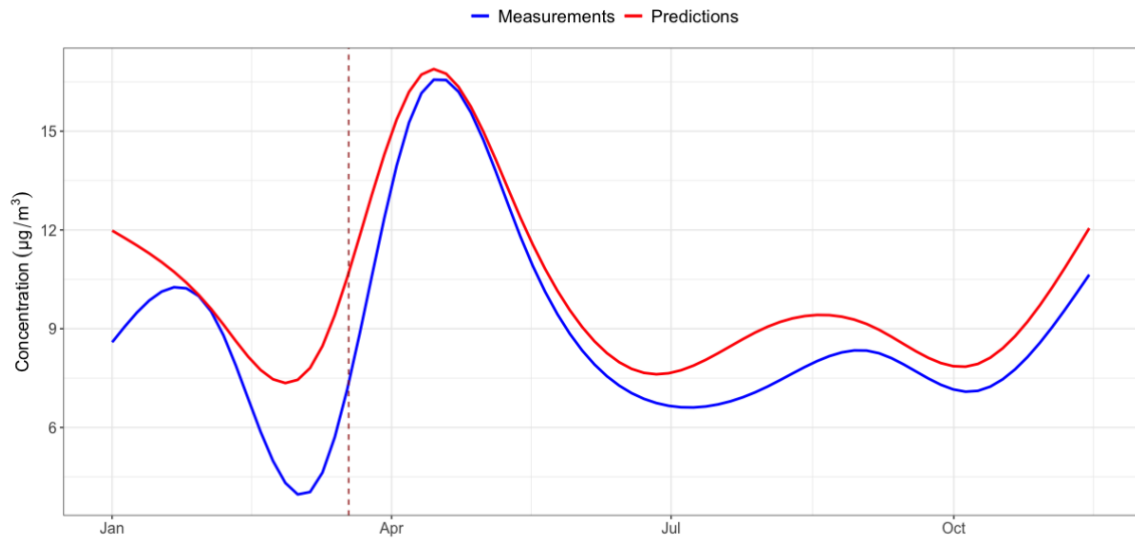


Figure 30: Smoothed predicted hourly NO_2 concentrations and measured hourly NO_2 concentrations in 2020 (Veurne).

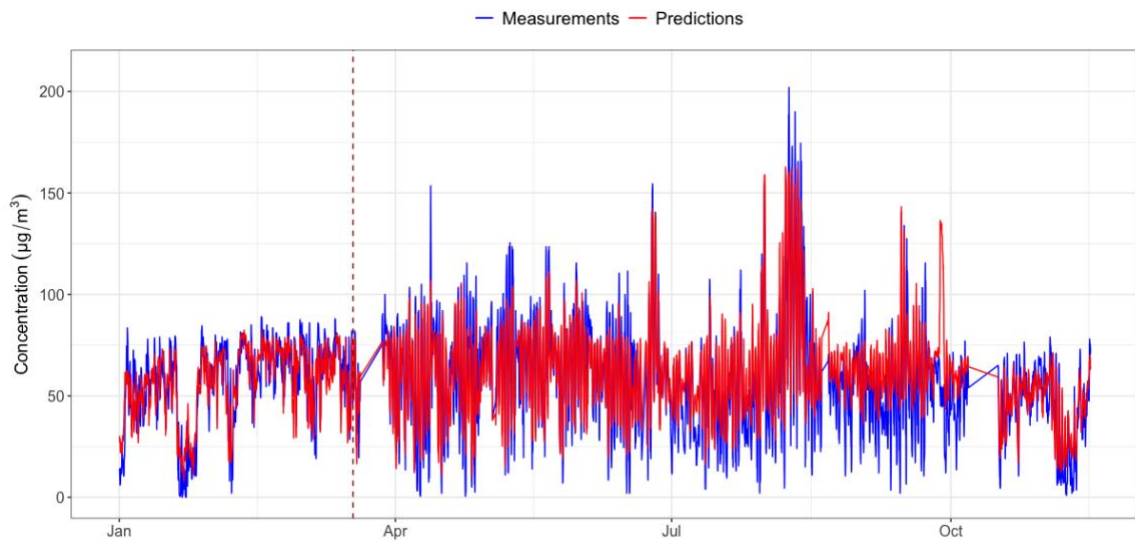


Figure 31: Predicted hourly O_3 concentrations and measured hourly O_3 concentrations in 2020 (Veurne).

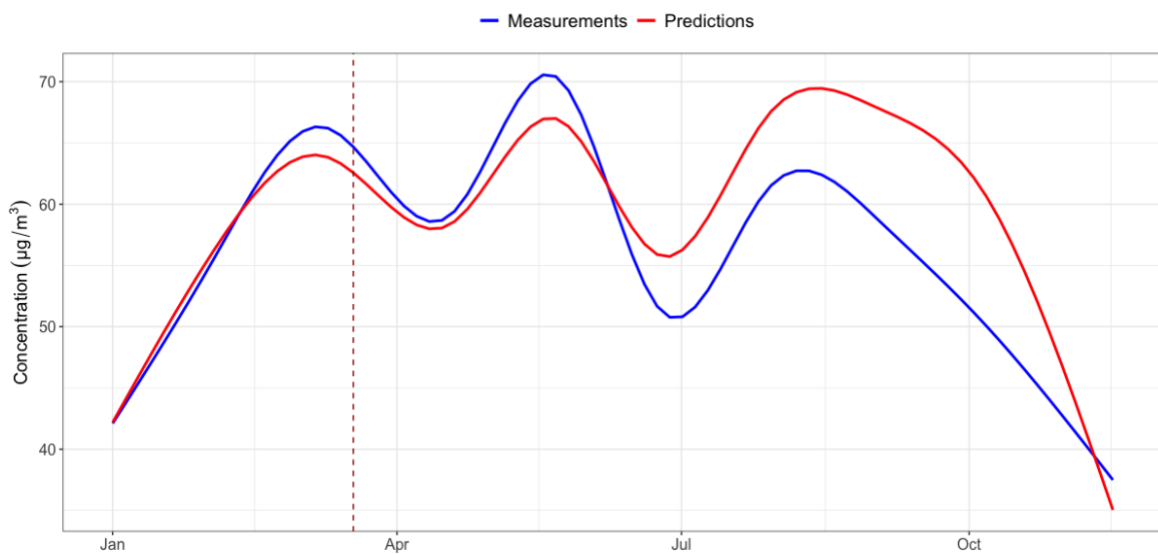


Figure 32: Smoothed predicted hourly O_3 concentrations and measured hourly O_3 concentrations in 2020 (Veurne).

Overall, no clear differences between the measured concentrations and the predictions can be observed during the lockdown. In Figure 29 and Figure 31, it can be seen that there are some gaps in the data for respectively NO_2 and O_3 due to the removal of missing values of the measurements. A remark should be made on the NO-model as the concentrations before the lockdown are overestimated and thus it fails in predicting the concentrations based on the weather conditions. This could indicate an error in the model. To investigate this error, the model performance before and after the start of the lockdown will be compared in Figure 33 and Figure 34. It can be observed that a great deal of the time the observed data before the lockdown is equal to $0 \mu\text{g}/\text{m}^3$ and that the model overestimates the predictions for these data points. The large amount of “zero” values could be due to failure of the measuring device or due to concentrations being lower than the detection limit of the equipment. Another remarkable thing is that the measured values take intervals of $0.5 \mu\text{g}/\text{m}^3$, this was seen at the other locations too. This is probably due to rounding of the data. In Figure 33, it is clear that these lower concentrations with low resolution, i.e. high intervals between the measured values, are overestimated with the model. Figure 34 shows that intermediate concentrations are predicted more accurate but again a large amount of the observations with low concentrations is overestimated. As mentioned before, the NO-models at each location have rather low R^2 values meaning that these models perform less for this substance.

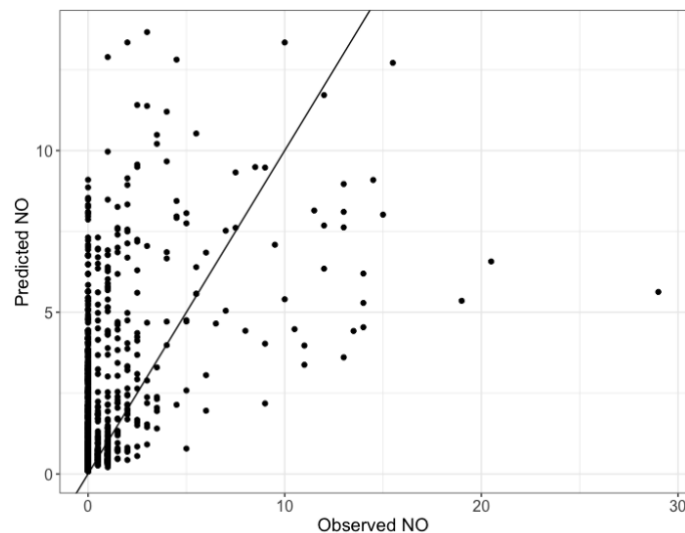


Figure 33: Model performance before the start of the lockdown (01/01/2020-18/03/2020) for NO (Veurne).

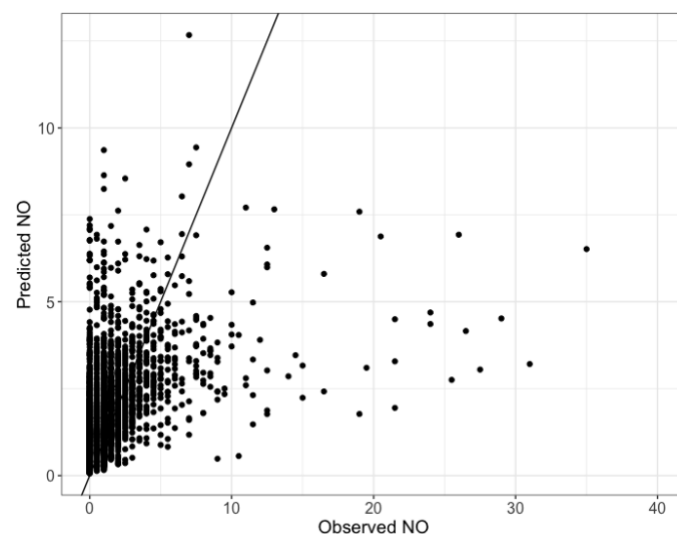


Figure 34: Model performance after the start of the lockdown until 15/11/2020 for NO (Veurne).

Subsequently, the daily profiles were established for each pollutant. The daily patterns were averaged for the first month of the lockdown, i.e. 18/03/2020-18/04/2020. It was opted to compare this profile with the average daily profile for the same period averaged for the years 2015-2019. In Figure 35, it can be seen that the daily patterns for the NO_x compounds didn't change that much during the lockdown. Except for the peaks in NO concentrations at 1 and 2 a.m. during the lockdown with mean concentrations of respectively 11.30 and 12.93 µg/m³. When looking at the data, outliers were found for these hours. Therefore, the error bars were plotted on the daily patterns to have a more accurate overview in Figure 36. The error bars present the interval [+SD, -SD] for each mean hour value, with "SD" the standard deviation. It can be observed that the error bars for the mean NO concentrations at 1 and 2 a.m. are bigger due to the outliers. For the other pollutants, no differences in the length of the error bars are observed for the daily patterns during the lockdown compared with the previous years. The daily profile for NO₂, has the same trend during the lockdown as the years before, namely a decrease in the concentrations starting from 7 a.m., up to a minimum at noon, and an increase towards the evening with a maximum at 8 p.m. This can be described as a bimodal pattern but it is not that clear. The trend of the daily O₃-profiles is the same with a minimum at 6 a.m. and from that point on an increase with a maximum around 2-3 p.m. after which the concentrations drop back. The concentrations during the lockdown reach 84.56 µg/m³ at the peak, while compared with the other years the mean maximum O₃ concentrations is lower during the day with 77.20 µg/m³. The higher peak could be attributed to the higher amount of solar radiation during the first month of the lockdown which drives ozone formations.

In Figure 35 and Figure 36, the daily patterns were calculated by taking the average value per hour for one month, so no distinction was made between a week-day or a weekend day. However, in the weekend much less traffic is present on the road. Therefore, it is interesting to investigate if the impact of the corona measures on the daily profiles is more marked during the weekdays than during the weekends. In Figure 37, the average daily patterns for a Tuesday are compared with the average daily patterns for a Sunday.

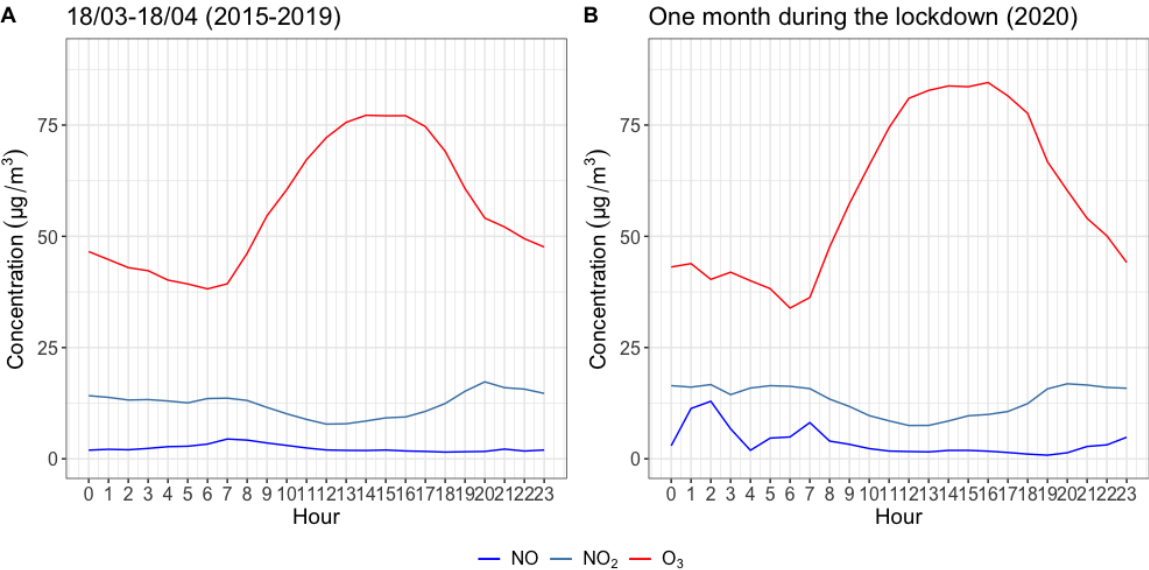


Figure 35: Average daily patterns for the period 18/03-18/04 A) Average of the years 2015-2019 B) Average in 2020 (Veurne).

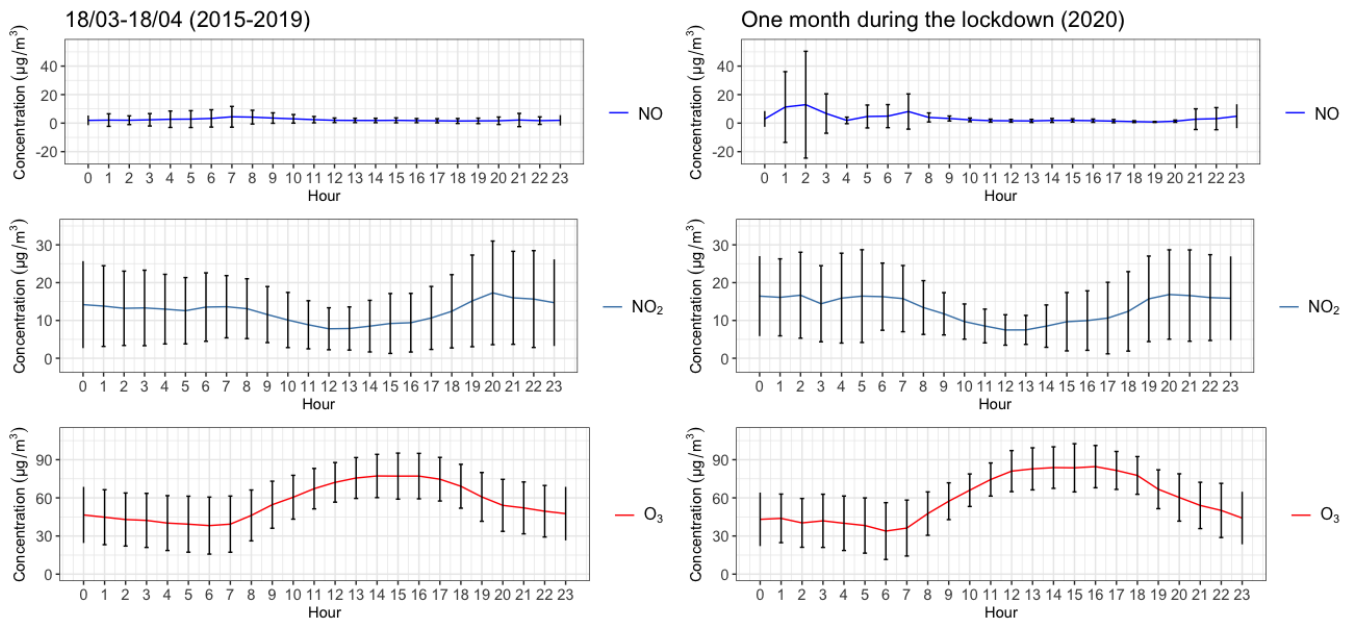


Figure 36: Average daily patterns with error bars, that show the mean concentration \pm SD (Veurne).

When comparing the average Tuesday profile for the period 18/03 – 18/04 in the years 2015-2019 (A in Figure 37) with the average Sunday profile for this period in these years (C in Figure 37), no clear difference can be observed. This means that in normal conditions, the daily profiles for each pollutant are quite the same on a week-day as on a weekend day. The average Tuesday O_3 -profile during the first month of the lockdown differs from the previous years. A sharp decrease can be seen in the concentrations at 6 a.m. in figure B in Figure 37. It should be remarked that the first month of the lockdown only has four Tuesdays. For O_3 only 2 logic values were available at 6 a.m. for these days. Starting from 10 a.m. 20/03/2020 up to 12 p.m. 27/03/2020 values were missing for O_3 . It can be noted that the O_3 -profiles reach higher maximum concentrations during the lockdown both for a Tuesday and a Sunday. No clear changes can be seen in the NO_x -profiles during the lockdown both for a Tuesday and a Sunday.

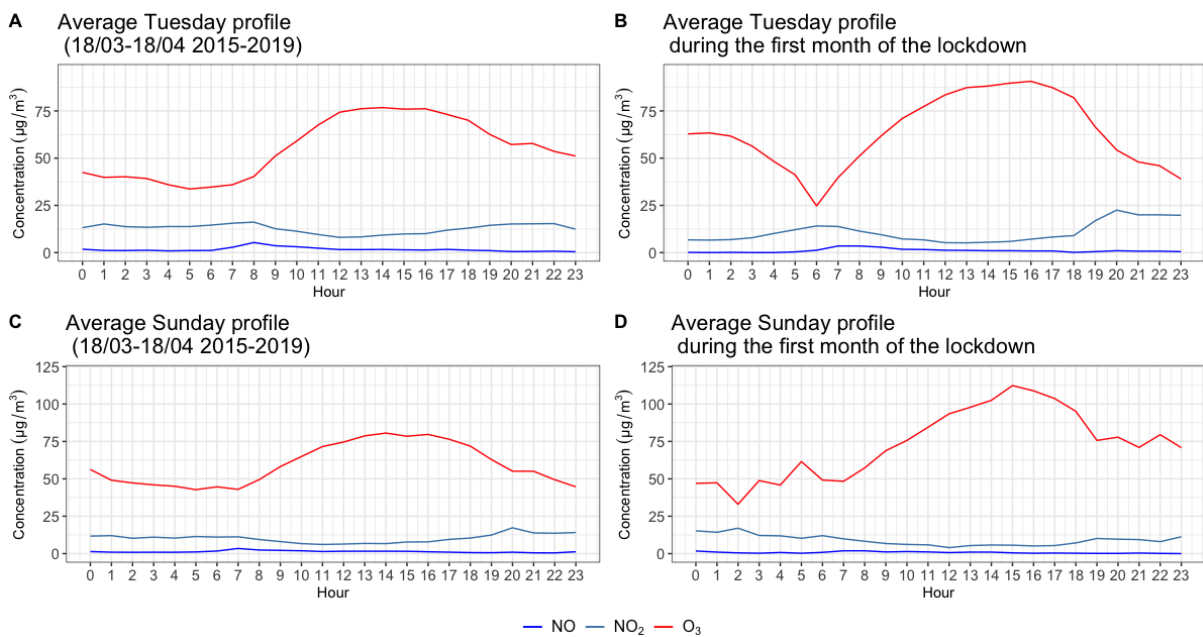


Figure 37: Average daily profiles for a) Tuesday (18/03-18/04 2015-2019), b) Tuesday during the first month of the lockdown, c) Sunday (18/03-18/04 2015-2019) and d) Sunday during the first month of the lockdown (Veurne).

7.3.2. Urban-background location: Ghent, Baudelopark

For the measuring station in Ghent, the hourly concentrations for each pollutant were also estimated with the corresponding model and compared with the measured concentrations. The results were again smoothed to obtain a more detailed understanding. In Figure 38 and Figure 39 it is clear that the predictions for the NO concentrations are overestimated by the model starting from 18 March 2020. As with the background location, the model predicts an increase of the NO levels which could be explained by the change in weather conditions. This increase can be observed in the measurements but it is much less explicit. This could be attributed to the corona measures. Since this location is an urban-traffic situation, more influence of traffic emissions can be expected compared to the background location in Veurne. The corona measures caused for a decline in traffic all around Flanders and this leads to lower NO-emissions coming from vehicles in this period. This could thus be the reason that the measured NO concentrations in this urban-traffic station are lower than predicted with the model. The difference between the measured concentrations and the predictions persists during the summer months but is lower. It can be remarked that again, the model predictions are also overestimated in January.

For NO₂, the difference between the model predictions and observed concentrations is less clear in Figure 40. When looking at Figure 41, the NO₂ model predicts the increase in concentrations during the lockdown, as in the background location, correctly but the values for the predictions are higher than the observed values. The lower concentrations than predicted could thus be attributed to the lockdown as there was less traffic in that period. However, the effect of the lockdown is less pronounced as for NO. A more pronounced difference is observed in the summer period, where the measured concentrations reach very low concentrations. The relatively large prediction errors in the summer months could be attributed to the fact that less traffic was on the road in this period, so less NO emissions are released in the atmosphere. The low NO concentrations in summer are also observed in Figure 39. Lower NO emissions lead to less conversion of NO with O₃ to NO₂ in the air. The lower amount of traffic during summer is attributed to the summer vacation. The model is capable of predicting this decrease in NO₂ concentrations in summer but the measured concentrations are in fact lower. The reason for that could be that due to the corona crisis even less traffic was on the road in summer as more people stayed at home.

Figure 42, shows the hourly values for O₃ in Ghent but again this figure is hard to interpret. The smoothed values in Figure 43 show that the model is very effective in predicting the concentrations the period before the lockdown. With the start of the lockdown, a difference can be seen between the predictions and the measurements. The model predicts that the O₃ levels in that period should be lower than observed. The difference increases with a maximum in May and then decreases until the predictions match the observations again in June. In the summer months the measurements are in turn lower than predicted. Starting from August, the model is again accurate in predicting the concentrations. The higher concentrations during the lockdown than predicted can be explained by the reduction in NO concentrations. As mentioned before, the ozone titration by NO is lowered due to the lower NO emissions and therefore lower NO concentrations in the atmosphere. This leads to accumulation of O₃ concentrations in the air.

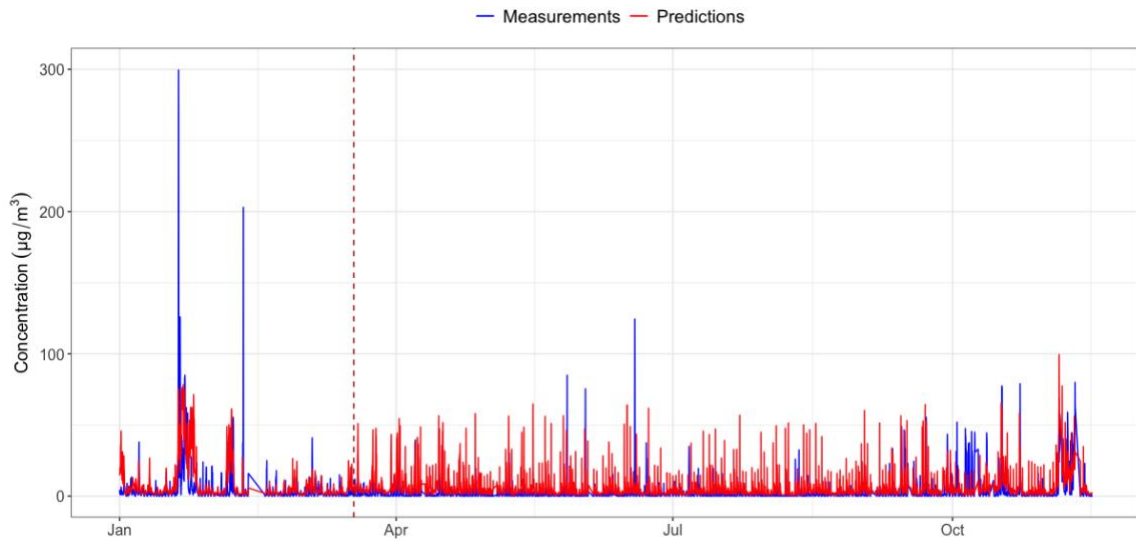


Figure 38: Predicted hourly NO concentrations and measured hourly NO concentrations in 2020 (Ghent).

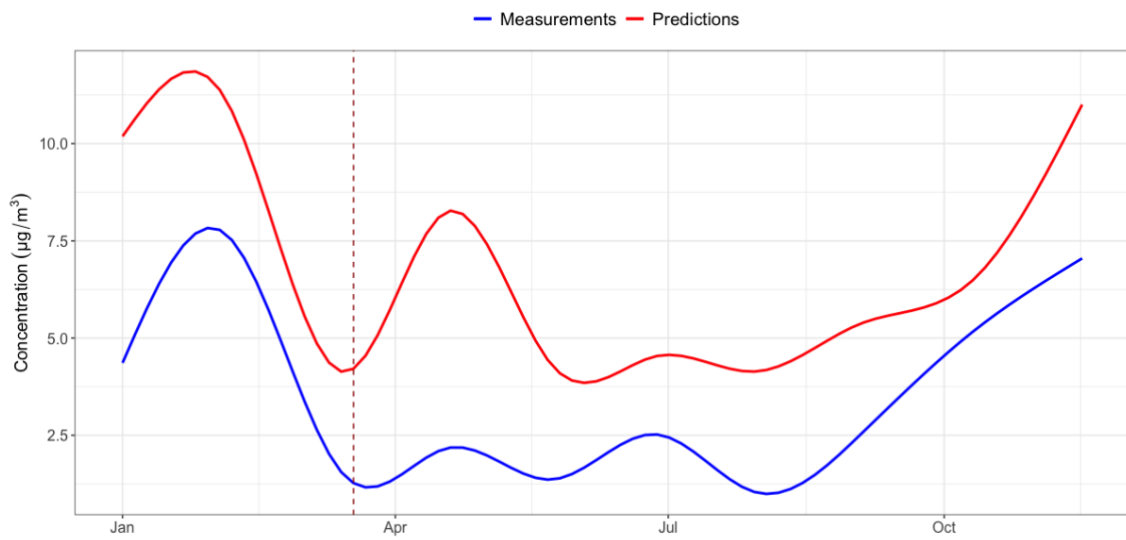


Figure 39: Smoothed predicted hourly NO concentrations and measured hourly NO concentrations in 2020 (Ghent).

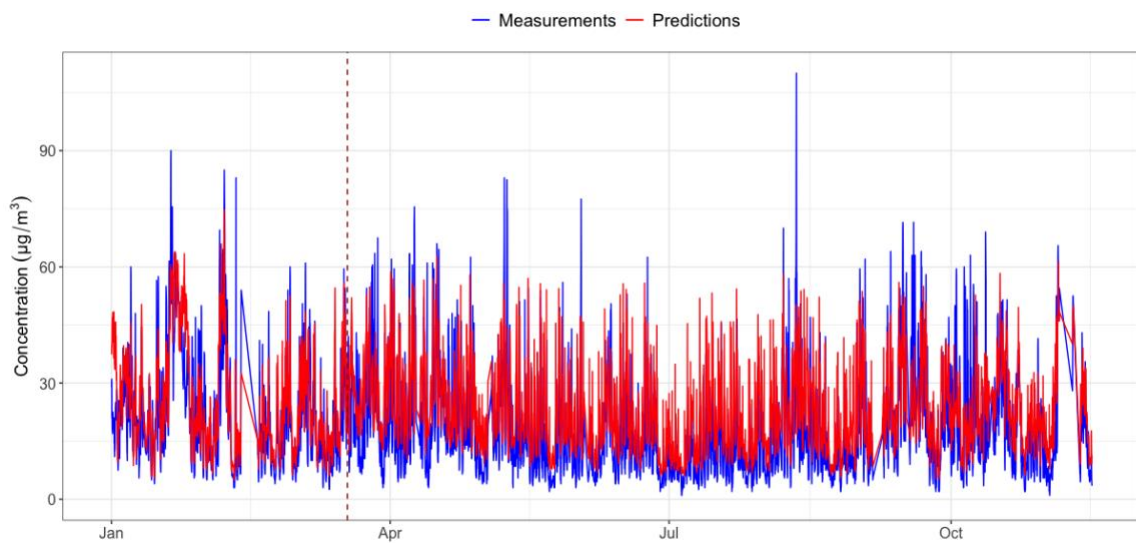


Figure 40: Predicted hourly NO₂ concentrations and measured hourly NO₂ concentrations in 2020 (Ghent).

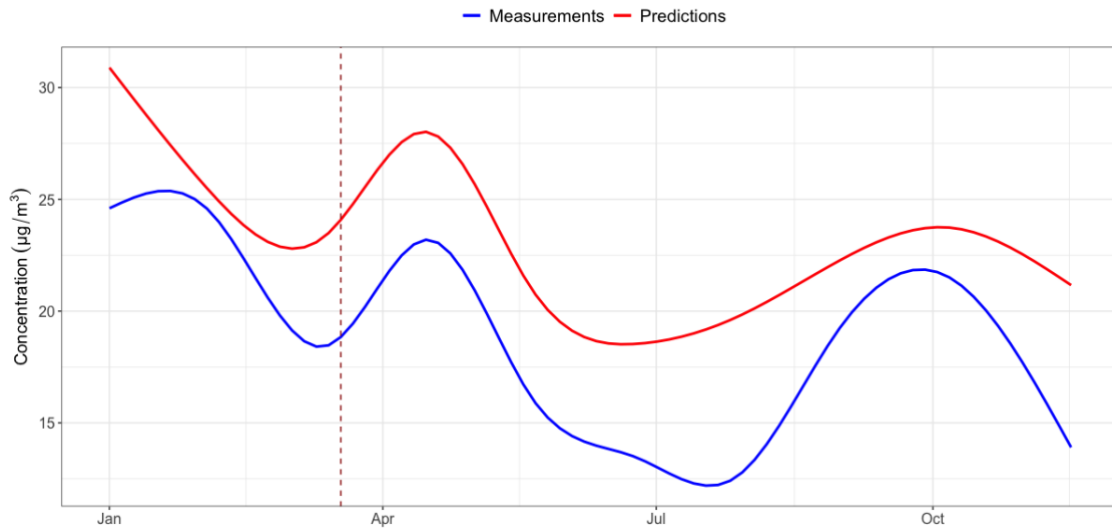


Figure 41: Smoothed predicted hourly NO_2 concentrations and measured hourly NO_2 concentrations in 2020 (Ghent).

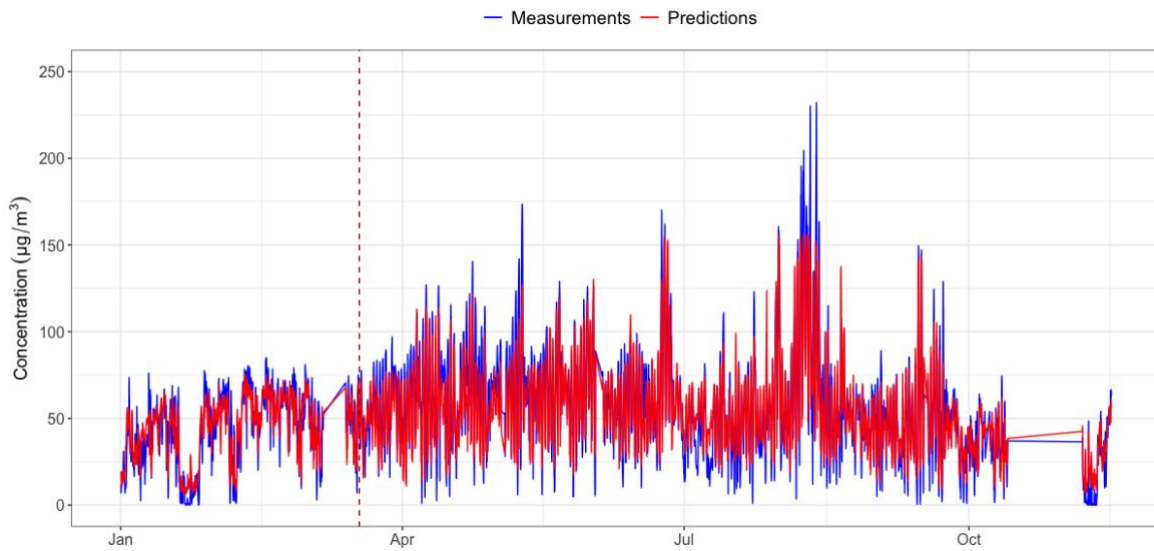


Figure 42: Predicted hourly O_3 concentrations and measured hourly O_3 concentrations in 2020 (Ghent).

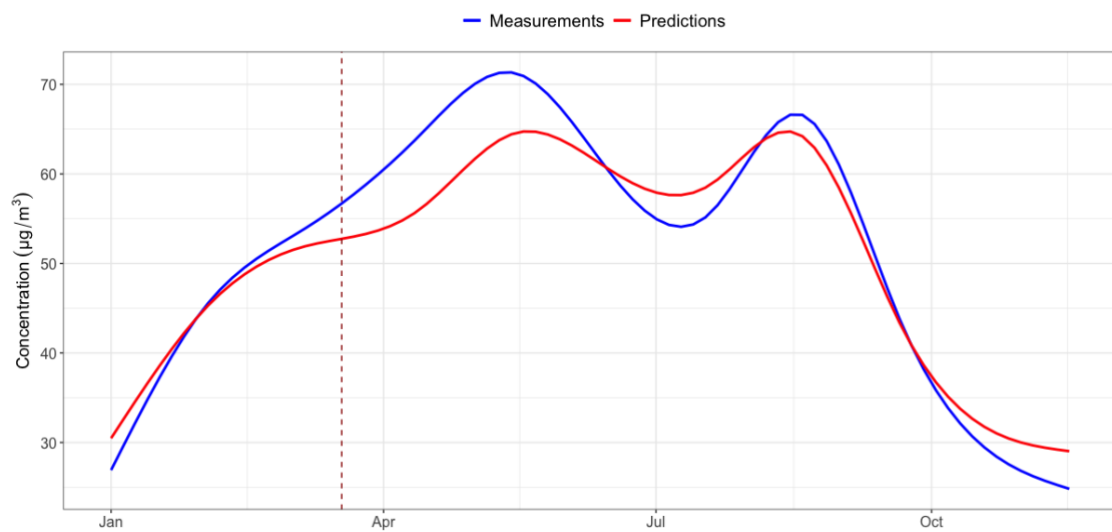


Figure 43: Smoothed predicted hourly O_3 concentrations and measured hourly O_3 concentrations in 2020 (Ghent).

The average daily patterns for the first month of the lockdown are again compared with the average daily patterns of the previous years for the same period. The results for the urban-background location are given in Figure 44. The average NO-profile for the years 2015-2019 shows a clear peak at 7 a.m. with a concentration of 20.32 $\mu\text{g}/\text{m}^3$. The NO-profile during the first month of the lockdown has a more stable pattern throughout the day with a maximum of only 7.71 $\mu\text{g}/\text{m}^3$. The daily profile of the NO₂ concentrations in the previous years follows a bimodal pattern, with the highest peak at 7 a.m. and a second peak between 8 and 9 p.m., which could each be linked with traffic peak hours. This bimodal pattern is still seen during the lockdown but the first peak reaches only 34.48 $\mu\text{g}/\text{m}^3$ opposed to 43.56 $\mu\text{g}/\text{m}^3$ in the previous years and the second peak 30.57 $\mu\text{g}/\text{m}^3$ opposed to 36.21 $\mu\text{g}/\text{m}^3$. The same profile is maintained by O₃ during the lockdown as compared to the other years with a minimum around 6 a.m. and an increase from there until it reaches its maximum concentration at 3 p.m. However, this average maximum is 86.34 $\mu\text{g}/\text{m}^3$ during the lockdown compared to the average maximum of 73.09 $\mu\text{g}/\text{m}^3$ in the previous years. The minimum at 6 a.m. in the O₃ concentrations could be explained by the increase of the NO concentrations in the morning due to higher amount of traffic at that time of the day leading to more NO emissions. The NO reacts with O₃ to form NO₂ and O₂. When the peak hours in the morning are over also more solar radiation reaches the earth driving the ozone formation reaction out of NO₂. This process reaches its maximum in the afternoon as the highest temperature are present at that time. Afterwards, the O₃ concentrations drop again during the traffic peak hours in the evening. It is remarkable that NO concentrations don't show a bimodal pattern as NO₂. It could be expected that with the increase in traffic in the evening during rush hours and therefore the increase in NO emissions, a peak in the NO concentrations would be observed at that time of the day. This can however not be observed in the daily profiles. This phenomenon could be explained by the fact that the reaction from NO with O₃ forming NO₂ goes so fast that the increase in NO emissions can't be measured.

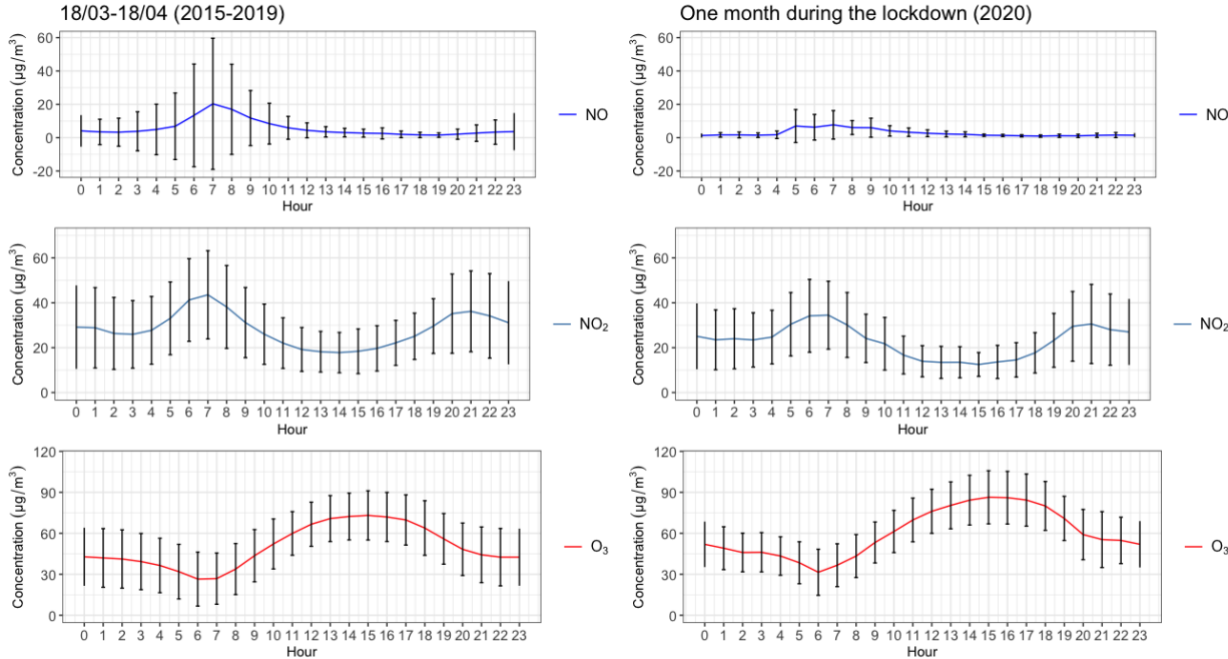


Figure 44: Average daily patterns with error bars, that show the mean concentration +/- SD (Ghent).

7.3.3. Urban-traffic location: Brussels, Sint-Jans-Molenbeek

The results for NO for the urban-traffic location Sint-Jans-Molenbeek are given in Figure 45 and Figure 46. It can be observed in Figure 45 that a difference occurs between the predictions and the measurements with the start of the lockdown, this difference is even more clear in Figure 46. The smoothed concentrations predicted with the model show an increase, as in the background station, to around $18 \mu\text{g}/\text{m}^3$ in May, which is $10 \mu\text{g}/\text{m}^3$ more than the smoothed measured concentrations at that time. Afterwards the model predicts a decrease towards the summer. The increase seen in the smoothed measured concentrations is rather part of the fluctuating concentrations around the same level starting from 18th of March until the summer. As with the station Ghent, this could be explained by the measures during the lockdown. This station experiences a lot of traffic in normal conditions, leading to NO emissions. The amount of traffic decreased during the lockdown and therefore the NO emissions, leading to lower NO concentrations in the atmosphere. Yet again, the model also predicts higher values for the concentrations in January.

The results for NO₂ are given in Figure 47 and Figure 48. Figure 47, shows that the predicted concentrations before the lockdown match the measured concentrations very well. With the start of the lockdown the predictions start to differ with the measurements. The smoothed concentrations in Figure 48 are overestimated reaching a difference of $16 \mu\text{g}/\text{m}^3$ with the smoothed measurements in May. The increase that is predicted with the model is not visible at all in the measured concentrations. In this station, the impact of the corona measures on the amount of traffic clearly translated in lower NO₂ concentrations in the atmosphere. In the summer months, very low concentrations were measured, which do not match the predicted concentrations. However, this can probably be more explained by the fact that during the summer vacation a lot less traffic is on the road than by the corona measures. It can be noted that the difference between the predictions and the measurements during the summer months is less pronounced for NO than for NO₂, this was also observed in the station in Ghent. Still, the results for this urban-traffic station show that the link between the amount of traffic and the NO_x concentrations is evident. Anthropogenic events like the COVID-19 lockdown and the summer vacation, which are responsible for a decrease in the amount of traffic, have an impact on their concentrations in the atmosphere. The models are quite capable of predicting the decrease in NO_x concentrations during the summer months as this is a yearly phenomenon that is present in the data with which the models are trained. The COVID-19 event, however, is exceptional and therefore the prediction errors are larger for that period as the models couldn't predict the reductions related with this event. A clear impact can also be seen in the results for O₃ during the lockdown. The predicted and measured O₃ concentrations are plotted in Figure 49 and the smoothed values in Figure 50. From the first figure it can be observed that the predictions are in line with the measurements and that a difference occurs from 18th March, i.e. the predicted O₃ concentrations are situated lower than the measured O₃ concentrations. This can be confirmed with the smoothed figure. The smoothed predictions reach levels up to $70 \mu\text{g}/\text{m}^3$, whereas the smoothed measurements never go higher than $63 \mu\text{g}/\text{m}^3$. From halfway June the predictions start to match with the observations again. The higher O₃ concentrations during the lockdown can again be explained by the fact that less NO is present in the atmosphere which causes the breakdown of O₃. It can be noted that during the summer vacation the O₃ concentrations also reach high levels but the model predicts this quite good. This indicates that the model expects the high levels of O₃ during the summer but the higher levels during the lockdown are exceptional and can thus be attributed to the corona measures.

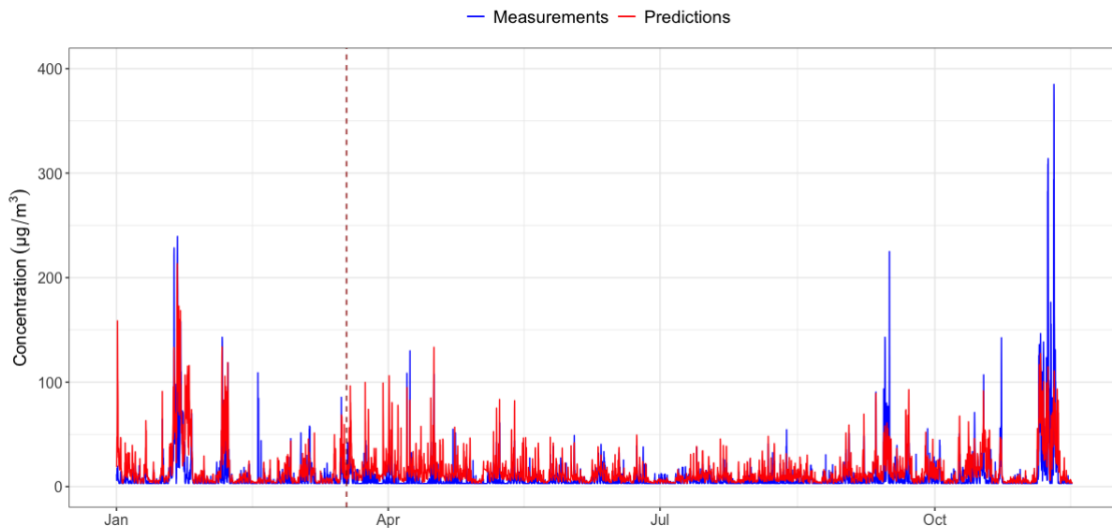


Figure 45: Predicted hourly NO concentrations and measured hourly NO concentrations in 2020 (Sint-Jans-Molenbeek).

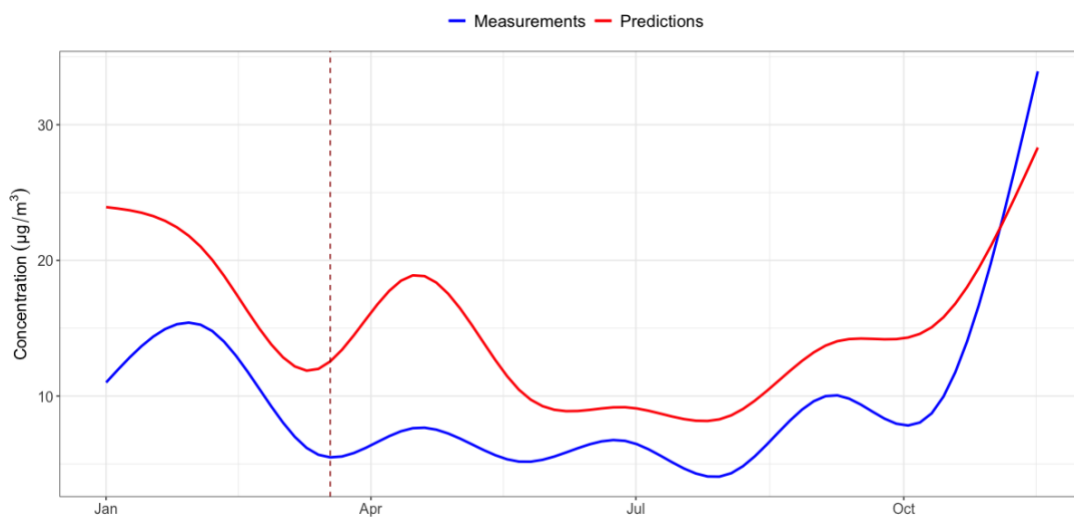


Figure 46: Smoothed predicted hourly NO concentrations and measured hourly NO concentrations in 2020 (Sint-Jans-Molenbeek).

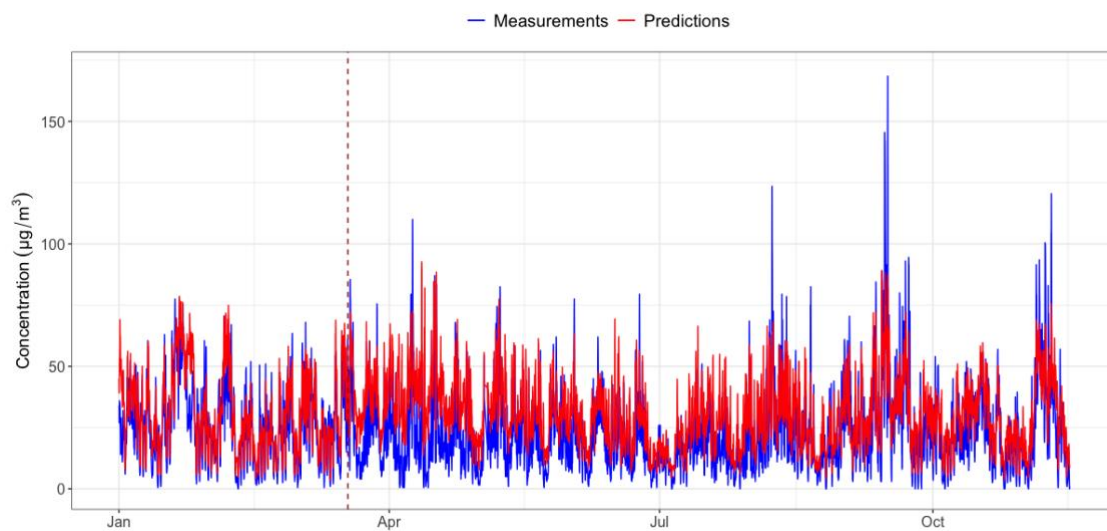


Figure 47: Predicted hourly NO₂ concentrations and measured hourly NO₂ concentrations in 2020 (Sint-Jans-Molenbeek).

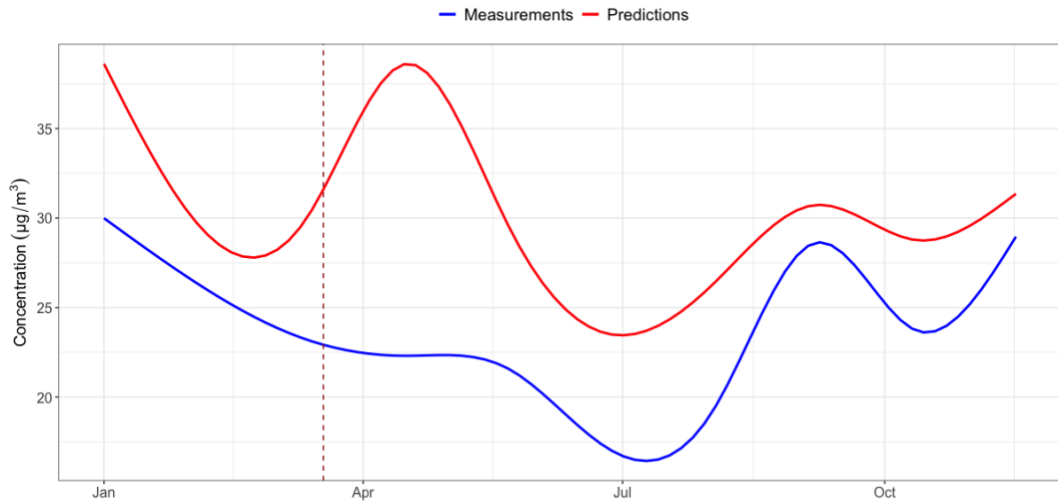


Figure 48: Smoothed predicted hourly NO_2 concentrations and measured hourly NO_2 concentrations in 2020 (Sint-Jans-Molenbeek).

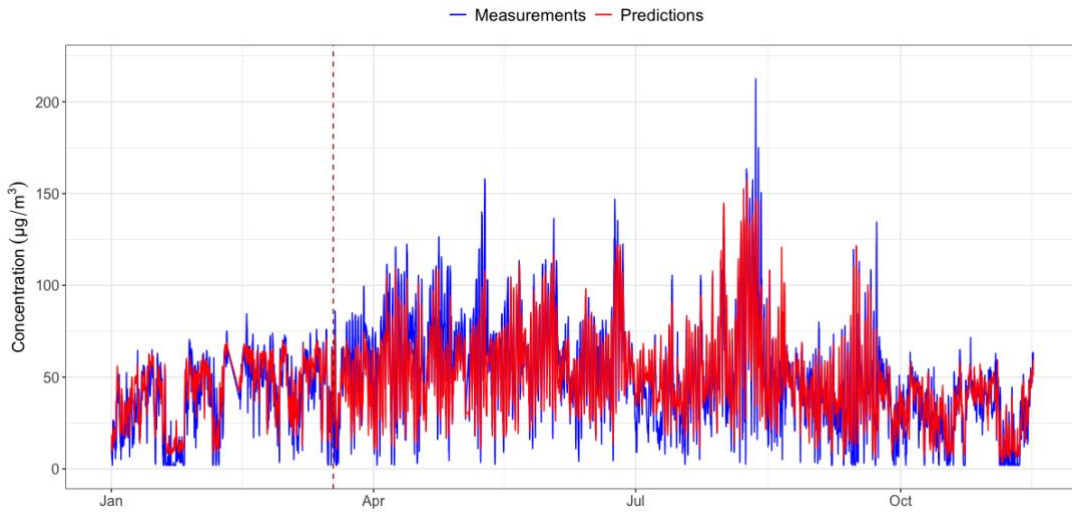


Figure 49: Predicted hourly O_3 concentrations and measured hourly O_3 concentrations in 2020 (Sint-Jans-Molenbeek).

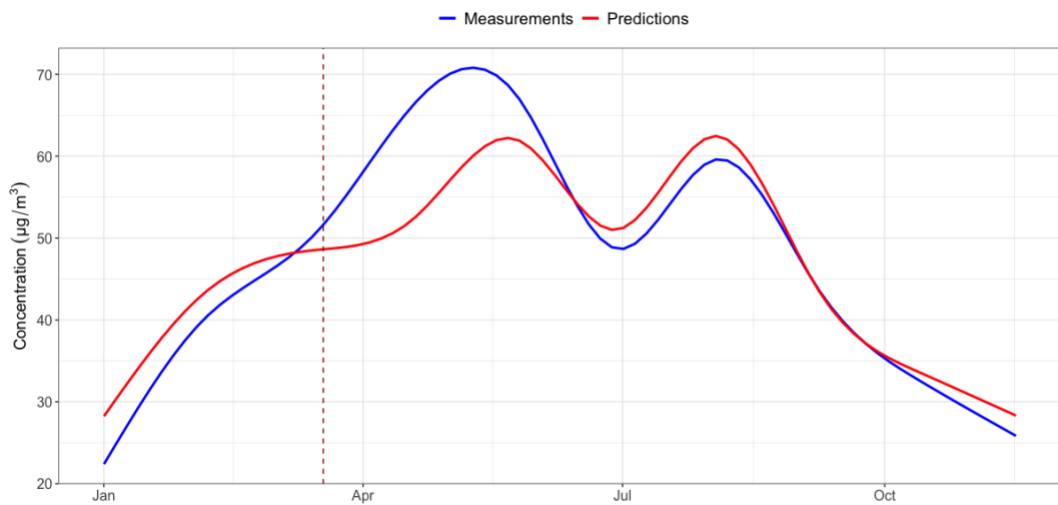


Figure 50: Smoothed predicted hourly O_3 concentrations and measured hourly O_3 concentrations in 2020 (Sint-Jans-Molenbeek).

At this urban-traffic station an obvious difference arises between the measurements and the predicted concentrations with the models. Therefore, it was chosen to calculate this difference, i.e. the prediction errors. The prediction error was calculated by subtracting the measured value from the predicted value. A positive prediction error indicates that the model overestimates the observed values, a negative prediction error indicates an underestimation. A prediction error of zero indicates that the model predicts the concentrations perfectly. The results are given in Figure 51. The left side of the figure shows the prediction errors for the hourly values, the right side shows the smoothed values. Again it should be remarked that the scales on the figures with the smoothed values are different because of this smoothing.

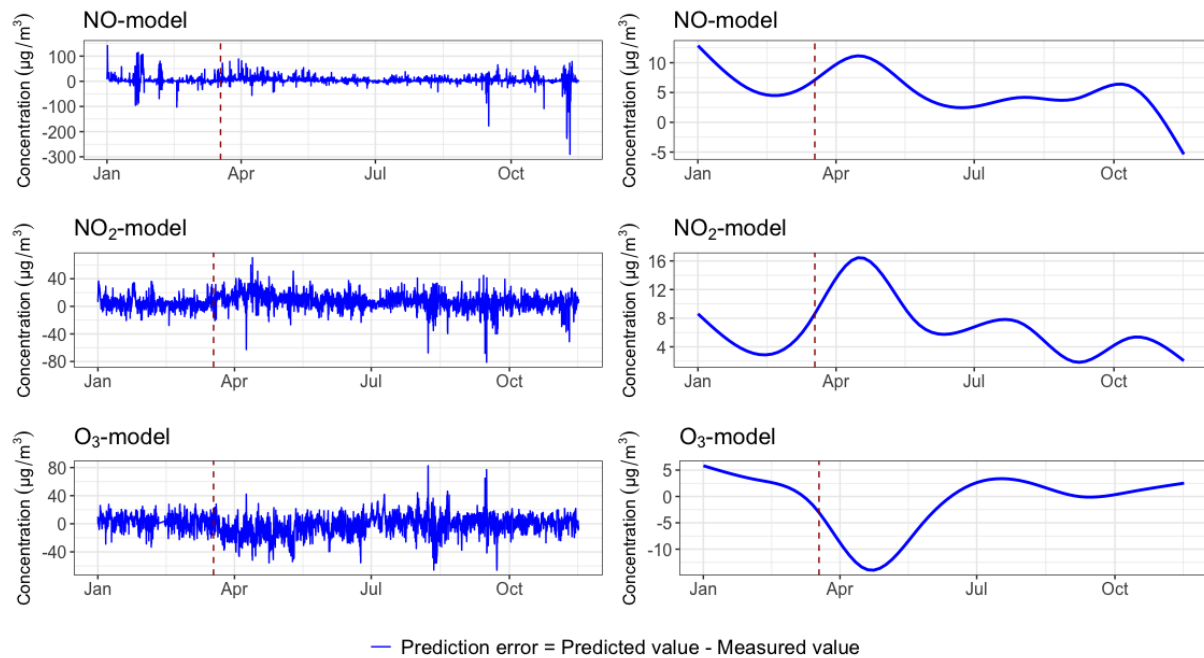


Figure 51: Prediction errors for each pollutant at Sint-Jans-Molenbeek (2020) Right: hourly values. Left: smoothed values.

In Figure 51, it is visible on the smoothed plot for the prediction errors for the NO-model that the difference between the predicted concentration and the measured concentration is around $5 \mu\text{g}/\text{m}^3$ before the start of the lockdown, i.e. in February, this value can be used as the smoothed “reference prediction error” in normal conditions to compare the prediction errors with in lockdown conditions. A positive error can be seen just before the 18th of March and the error increases during the first month of the lockdown. This indicates that the NO-model predictions are higher than the measurements in this period. The large prediction errors seen in January are due to the overestimation of the concentrations in the beginning of this month, this is also seen in Figure 45 and Figure 46. The prediction errors drop drastically in October. On the left side of the figure the prediction error takes values way below zero up to $-300 \mu\text{g}/\text{m}^3$. In Figure 45 it is visible that in November very high concentrations are observed and the model underestimates these concentrations. Since the smoothed function includes these values, the drop is this large.

The smoothed reference prediction error for the NO₂-model fluctuates around a positive value of $4 \mu\text{g}/\text{m}^3$, this means that the model overestimates the NO₂ concentrations in normal conditions with $4 \mu\text{g}/\text{m}^3$. On Figure 51, it is clear that the prediction errors for the NO₂-model increase during the lockdown, indicating that the model predicts higher concentrations than observed in this period.

For the O₃-model, the smoothed prediction error in normal conditions fluctuates around zero. It can be observed that this error drops during the lockdown below zero and increases again until July. The negative values during the lockdown indicate that the measured O₃ concentrations were higher than the predicted concentrations. The results from Figure 51 confirm the earlier statements about the impact of the corona measures on the air pollutant concentrations in this urban-traffic station.

The average daily patterns were also calculated for this station for the first month of the lockdown and for the same period in the years 2015-2019. The results are given in Figure 52 and the results with the error bars in Figure 53. The NO-profile features a pronounced peak at 7 a.m. with an average concentration of 43.28 µg/m³ in the years before the pandemic and drops back to a stable mean concentration of circa 11 µg/m³ throughout the rest of the day. During the lockdown, the NO concentration only peaks with 21.17 µg/m³ and from 11 a.m. the concentration fluctuates between 5 and 8 µg/m³. The smaller morning peak can be attributed to the lower amount of traffic present at the peak hour during the lockdown. The bimodal pattern of the NO₂ concentrations is maintained during the lockdown but it's located lower on the graph and with reduced peaks at 6 a.m. and 8 p.m. Again the second peak isn't seen in the NO-profile which could imply that the conversion of NO to NO₂ and O₃ happens this fast that the monitors aren't able to measure the NO concentrations but that in the morning the NO concentrations remain longer in the atmosphere before they are converted. This could be explained by the fact that the temperature in the morning is lower than in the evening and less O₃ is present. Therefore the conversion happens slower in the morning and more rapid in the evening. Normally, the first and second peak of NO₂ are of the same magnitude with on average a concentration of 51 µg/m³. During the lockdown the second peak (31.82 µg/m³) no longer reaches the same concentration as the first one (39.05 µg/m³). This could imply that the reduction in the amount of traffic during peak hours in the lockdown is larger in the evening. In addition, the average minimum NO₂ concentration is 14.60 µg/m³ opposed to 28.27 µg/m³ before the pandemic.

The O₃-profile shows the same trend during the lockdown as in the previous years, namely a drop in the concentrations at 6 a.m. and an increase towards the afternoon and from around 3 p.m. the concentrations start to decrease again. It can be remarked that the difference between the minimum concentrations and the maximum concentrations is larger during the lockdown, namely 55.41 µg/m³ compared with the difference in the previous years 41.48 µg/m³. During the lockdown the maximum concentration is 84.25 µg/m³ compared with 64.92 µg/m³ during the previous years. As there are less NO compounds present in the atmosphere O₃ is able to accumulate more during the day which leads to a higher peak in the afternoon and higher minimum concentrations compared with "normal" years.

For this urban-traffic location, the difference of the average daily patterns for the pollutants during the lockdown compared with the average profiles of the previous years is very clear. Figure 53, shows that the error bars on the mean hourly values are approximately of the same order before and after the lockdown. So the differences in the daily profile can't be attributed to outliers.

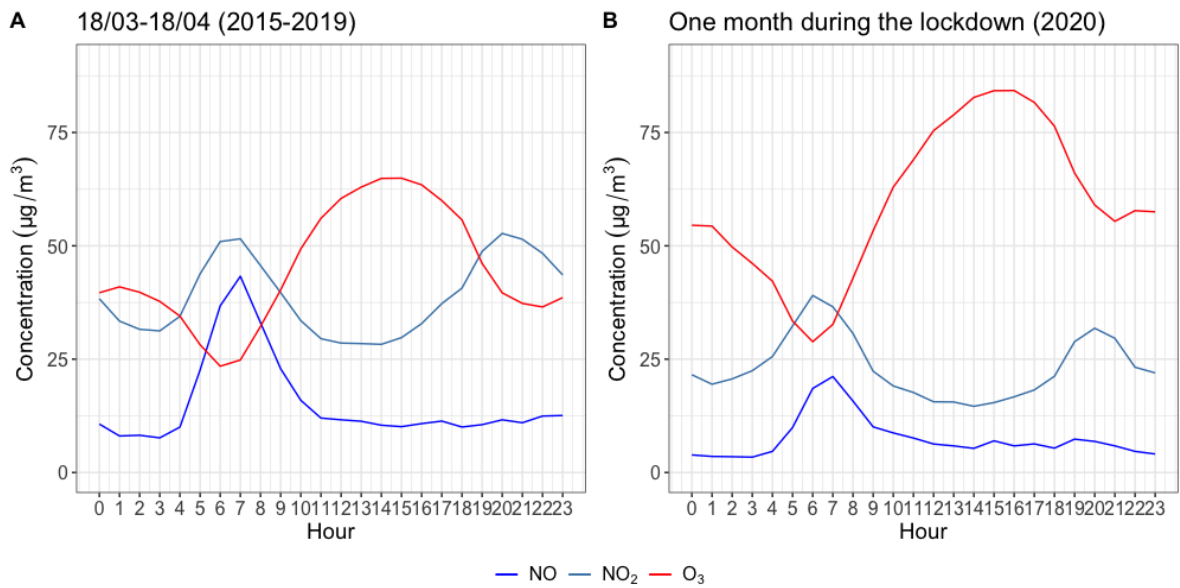


Figure 52: Average daily patterns for the period 18/03-18/04 A) Average of the years 2015-2019 B) Average in 2020 (Sint-Jans-Molenbeek).

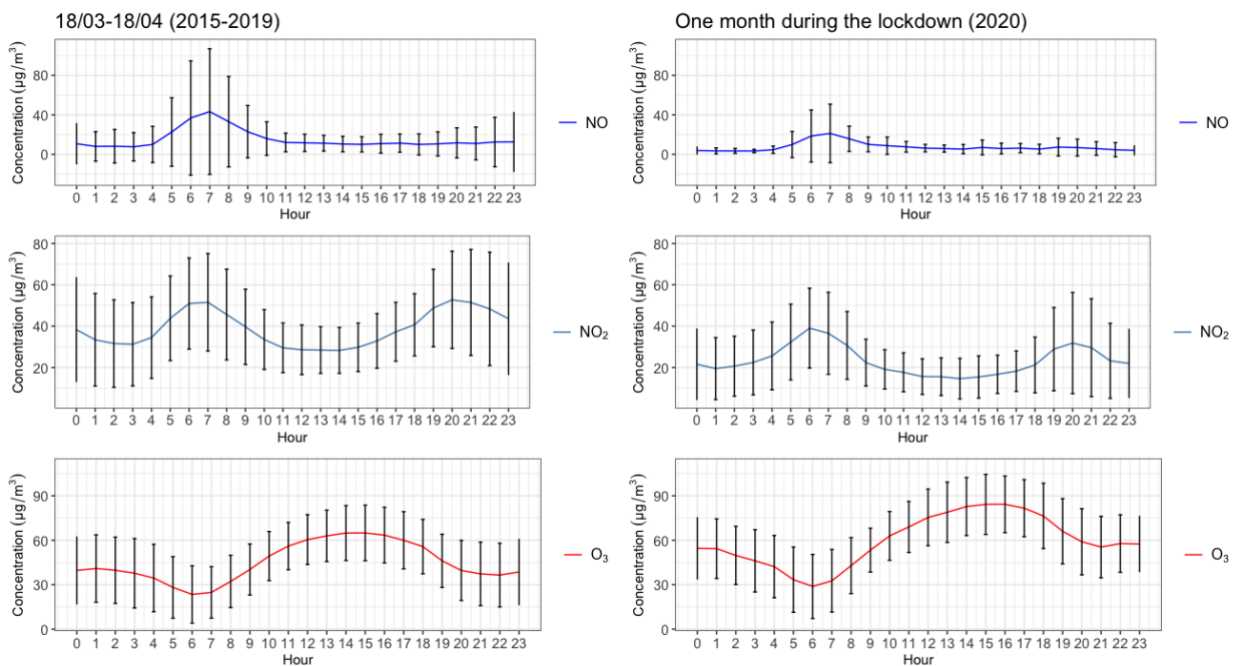


Figure 53: Average daily patterns with error bars, that show the mean concentration +/- SD (Sint-Jans-Molenbeek).

When comparing the results for this station with the background and urban-background location, the results show a more pronounced difference in the pollutant concentrations and the daily profiles during the lockdown for the urban-traffic situation. Therefore, it was chosen to further investigate the changes in patterns of daily concentrations in this station. It is also interesting to calculate the average daily patterns during the lockdown based on the predictions made with the models and compare this with the average daily patterns made with the measured concentrations. Figure 54, shows the daily patterns based on both the predictions and the measurements for the first month after the start of the lockdown.

The mean measured NO concentrations follow the same pattern as the predicted NO-profile. However, the average NO-profile made with the predictions has higher concentrations and a more pronounced peak at 6 a.m. with a concentration of $48.30 \mu\text{g}/\text{m}^3$ compared with the peak at 7 a.m. with the measured values that reaches a concentration of $21.17 \mu\text{g}/\text{m}^3$. In Figure 52, a maximum concentration of $43.28 \mu\text{g}/\text{m}^3$ was observed in the years before the corona pandemic. This means that the model predicts a higher mean peak during the first month of the lockdown than the mean peak in normal years during the same period. As stated before, this could be due to the less favorable weather conditions in this period in 2020 compared with other years. The NO₂-profile constructed with the measured concentrations follows a more clear bimodal pattern than the predicted NO₂-profile and has lower concentrations than predicted. Which is contradictory to the mean NO₂-profile for the years 2015-2019 in Figure 52, where the bimodal pattern is more clear than during the lockdown. The O₃-model predicts lower concentrations but the patterns of the O₃ concentrations are approximately the same: a minimum at 6 a.m. and a maximum in the afternoon. Remarkably, the predicted daily minimum concentration ($27.63 \mu\text{g}/\text{m}^3$) is almost same as the measured value ($28.84 \mu\text{g}/\text{m}^3$). The maximum measured concentration is $84.25 \mu\text{g}/\text{m}^3$ and the maximum predicted concentration is $71.56 \mu\text{g}/\text{m}^3$. It can be noted that the predicted maximum O₃ concentrations reaches a higher value than the calculated mean concentrations for 2015-2019 in Figure 52. So the model was able to predict that the O₃-profile during the lockdown would reach higher concentrations than compared to other years. As mentioned before, the weather conditions during the lockdown were different than in previous years, with more sunlight during the day. This stimulates the ozone formation and therefore the model was able to predict higher concentrations for this period. However, the measured concentrations are higher than predicted meaning that other factors than the changed weather conditions had influence. As stated before, the corona measures can be held responsible for this.

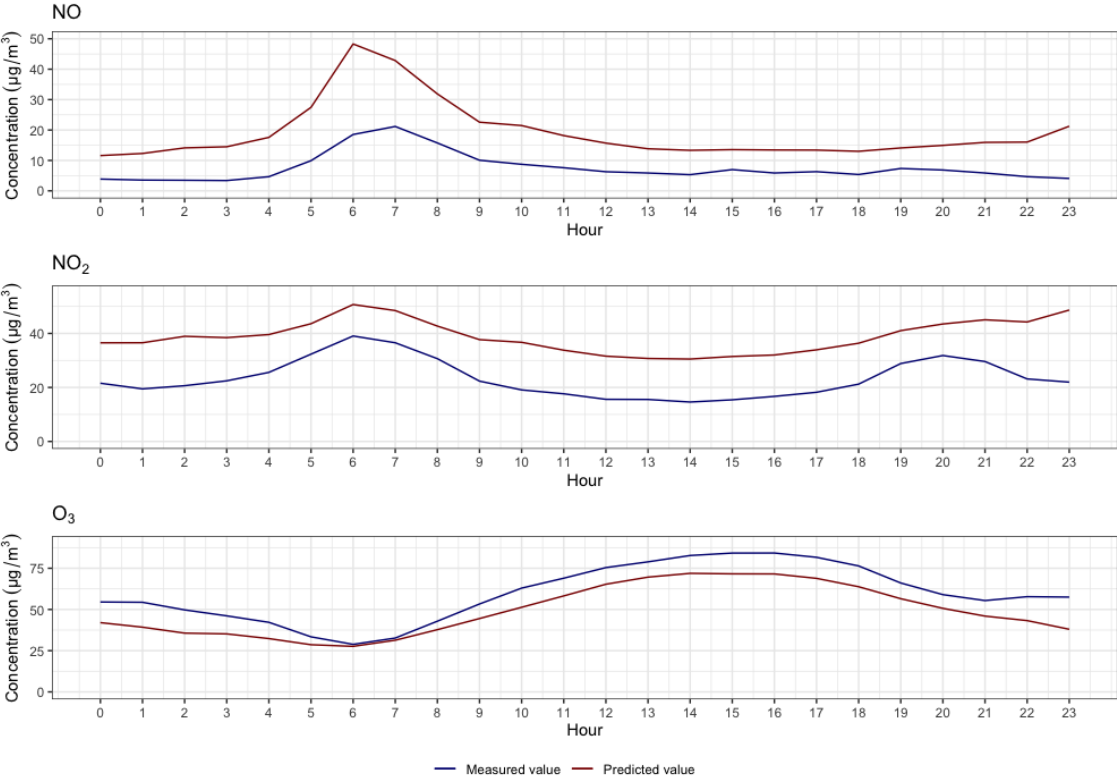


Figure 54: Average daily patterns based on the predictions compared with the average daily patterns based on the measured concentrations for the period 18/03/2020 – 18/04/2020, i.e. the first month of the lockdown (Sint-Jans-Molenbeek).

As for the background station Veurne, the average daily profiles of Tuesday are compared with daily average patterns of a Sunday in Figure 55 for the urban-traffic station. It can be seen that the “normal” average Tuesday profile (A in Figure 55) differs from the “normal” average Sunday profile (C in Figure 55). The NO_x-profiles on a Sunday are more stable compared with a Tuesday. The O₃-profile shows a same increase in concentrations towards the afternoon but the decrease in the morning, like on a Tuesday, isn’t observed. The O₃ concentrations are more stable throughout the evening and night on a Sunday. The difference in the patterns on Sunday can be attributed to the fact that much less traffic is on the roads compared with at Tuesday. Therefore, the increase in concentrations during the peak hours can’t be observed. The patterns seen on a Sunday are quite in line with the patterns seen at the background location.

The average NO profile for a Tuesday in the period 18/03 to 18/04 for the years 2015-2019 shows a very sharp peak at 7 a.m. of 77.98 µg/m³. During the first month of the lockdown the maximum NO concentration on a Tuesday is 34.62 µg/m³ at 6 a.m. (see B in Figure 55). It can also be noted that the NO-profile fluctuates more throughout the rest of the day. The bimodal pattern of NO₂ at an average Tuesday first peaks with 69.04 µg/m³ at 7 a.m. and with 49.35 µg/m³ at 8 p.m. During the lockdown these peaks are also observed but do not attain such high concentrations, namely 43.17 µg/m³ at 7 a.m. and 30.75 µg/m³ at 7 p.m. The O₃-profiles show the same trends for a Tuesday, i.e. a minimum at 6 a.m. and a maximum at 2 p.m. However, the values for the concentrations are higher during the lockdown, namely 24.87 µg/m³ for the minimum and 88.83 µg/m³ for the maximum compared to respectively 16.35 µg/m³ and 69.42 µg/m³ in the same period for the previous years. It can be noted that the NO₂ peaks on a Tuesday aren’t of the same magnitude as was seen in Figure 52.

When comparing the Sunday profiles (C and D in Figure 55), the trends of the profiles are quite the same with stable NO_x-profiles throughout the whole day. The profiles have shifted: the O₃-profile during the lockdown is located at more higher concentrations, and the NO- and NO₂-profiles at lower concentrations. The maximum O₃ concentration during the lockdown is 101.33 µg/m³ compared with 73.61 µg/m³ in previous years. The maximum NO₂ concentration on a Sunday before the lockdown is 44.52 µg/m³ opposed to 19.52 µg/m³ during the lockdown. The corona measures have thus also an effect on the O₃ daily patterns of a Sunday.

It’s interesting to compare these results with the ones for the background station in Figure 37. For that station no remarkable differences were observed between the average profiles on a Tuesday and a Sunday for the years 2015-2019. In the urban-traffic station the Tuesday profiles are strikingly different than the profiles for a Sunday. For the NO_x-profiles no clear change was seen at the background station during the lockdown. Whereas, for the urban-traffic station the profiles have lower concentrations compared with other years. For the O₃-profile the same trend can be observed in the background station and on a Sunday in the urban-traffic station, namely a peak in the afternoon but no clear drop in the morning as on a Tuesday. This again shows the influence of the NO emissions coming from traffic on the O₃ concentrations. Since less NO emissions are released in the background station and on a Sunday in the urban-traffic location during the peak hour in the morning, no clear drop in the O₃ concentrations is observed.

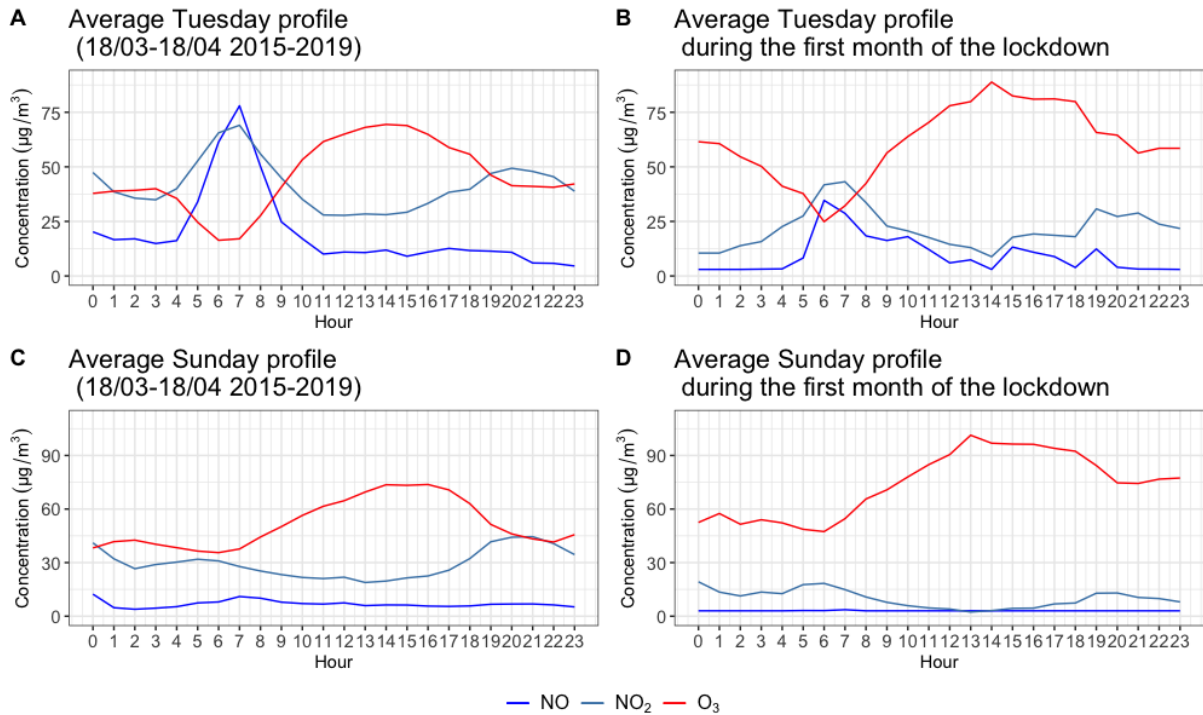


Figure 55: Average daily profiles for a) Tuesday (18/03-18/04 2015-2019), b) Tuesday during the first month of the lockdown, c) Sunday (18/03-18/04 2015-2019) and d) Sunday during the first month of the lockdown (Sint-Jans-Molenbeek).

7.3.4. Urban-traffic location: Brussels, Kunst-Wet

For the last station, situated in the city center of Brussels, again predictions were made with the models for the traffic-related pollutants. Unfortunately, this could only be done for the NO_x compounds since O_3 wasn't measured at this station. It is also essential to mention again that the model predictions for this station are made using data of the weather variables from the station in Sint-Jans-Molenbeek.

The results for NO are given in Figure 56 and Figure 57. Already from the first figure is very clear that the predictions are higher than the measured concentrations with the start of the lockdown. This is confirmed in the second figure with the smoothed values. It is remarkable that the model doesn't predict an increase in the concentrations as the other models did in the other stations. This could be explained by the fact that this station is located in a street canyon and therefore is less susceptible to change in weather conditions. In fact, the predicted NO concentrations at this station show a descending pattern starting from January until the summer. However, it can be remarked that the concentrations are also overestimated by the model in January. Although, the model predicts a decrease during the lockdown, the NO concentrations are in fact much lower. In Figure 58, a difference between the predictions and the measurement for NO_2 can be observed starting from 18th March 2020. Figure 59 shows this difference even more clear. The predicted concentrations do not correspond at all with the observations during the lockdown. A large decrease can be observed in the measurements. With a difference between the smoothed observations and measurement up to $20 \mu\text{g}/\text{m}^3$ in May. The explanation of the difference in predictions and measurements is the same as with the other urban-traffic station Sint-Jans-Molenbeek. However, the impact of the corona measures is even larger in the center of Brussels due to the fact that the reduction in the amount of traffic during the lockdown is more outspoken.

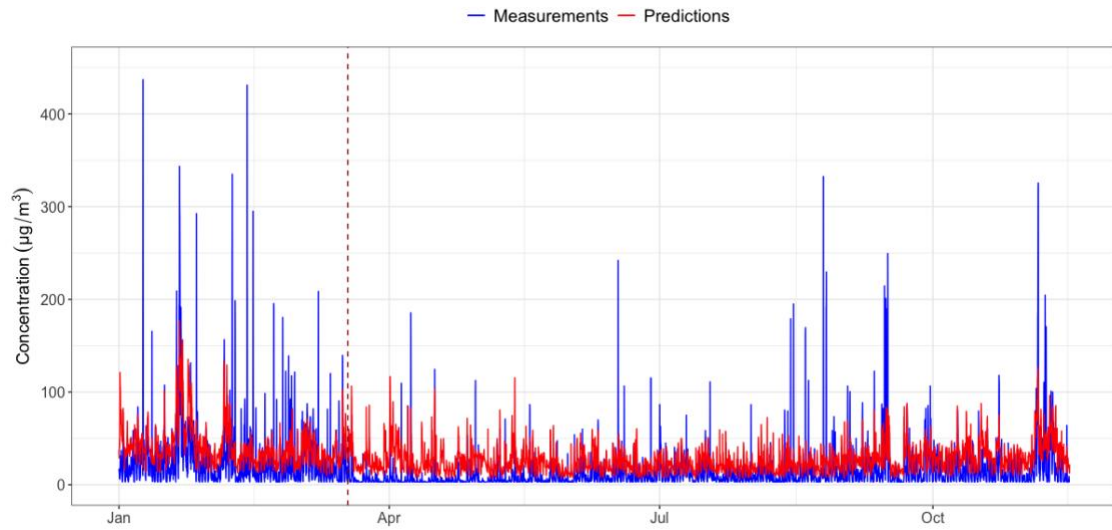


Figure 56: Predicted hourly NO concentrations and measured hourly NO concentrations in 2020 (Kunst-Wet).

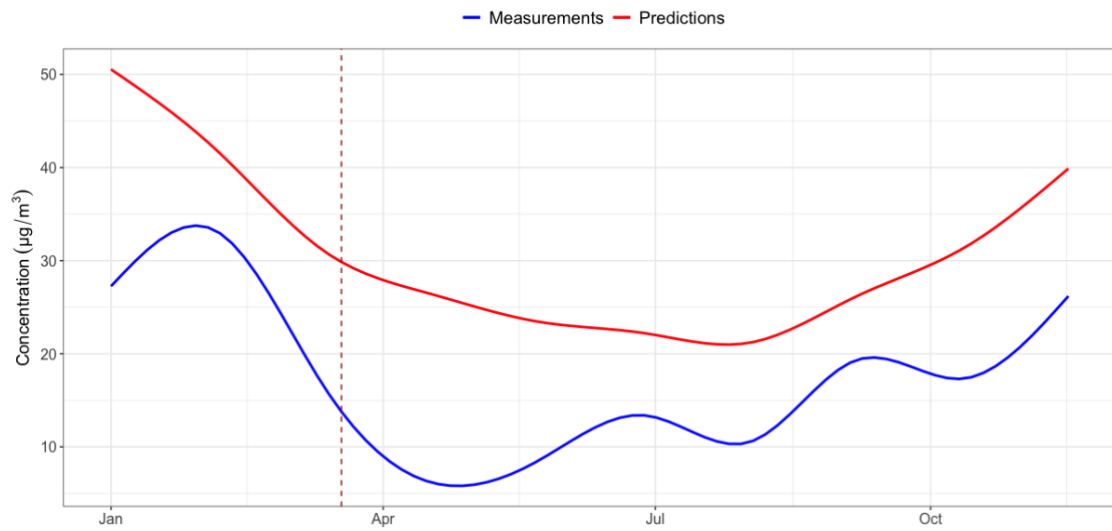


Figure 57: Smoothed predicted hourly NO concentrations and measured hourly NO concentrations in 2020 (Kunst-Wet).

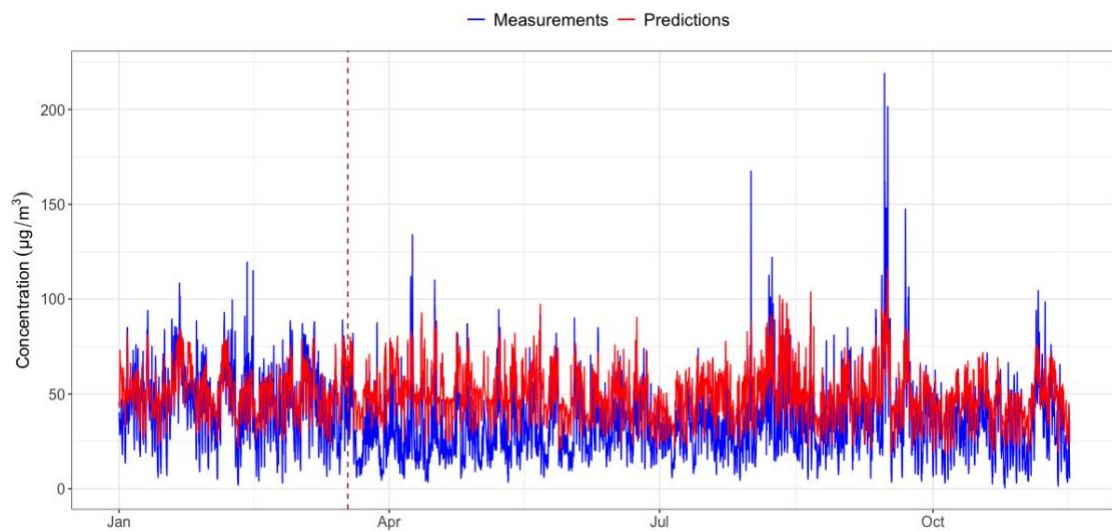


Figure 58: Predicted hourly NO₂ concentrations and measured hourly NO₂ concentrations in 2020 (Kunst-Wet).

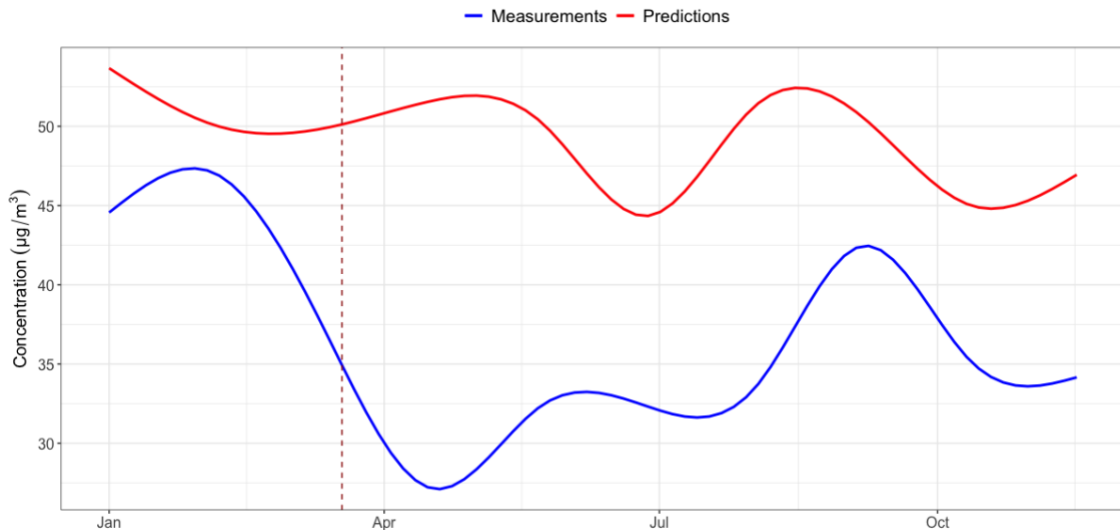


Figure 59: Smoothed predicted hourly NO_2 concentrations and measured hourly NO_2 concentrations in 2020 (Kunst-Wet).

The daily patterns for NO and NO_2 are given in Figure 60, where there are observable differences visible between the average profiles for the period of 18th March until 18th April from the years 2015-2019 and the profiles of that same period in 2020, i.e. the first month of the lockdown. The NO -profile during the lockdown shows a small peak at 7 a.m. with $21.73 \mu\text{g}/\text{m}^3$ and a more stable trend during the rest of the day. In the previous years, the NO -profile shows a less stable pattern but has also a peak at 7 a.m. However this peak reaches a much higher concentration, namely $63.31 \mu\text{g}/\text{m}^3$ and also the concentrations during the rest of the day are higher than during the lockdown. It can be noted that the error bars on the left side of the figure quit large. This indicates that a lot of variations exist on the NO concentrations at this station, especially at the peak hour in the morning. The monitoring station is located near a road that experiences a lot of variation in traffic mostly during rush hours. Therefore it is more likely that extreme values are present in the data for this station at the peak hour, these are included in the error bars. It can also be seen that during the lockdown more variation in the data is present at 7 a.m.

The NO_2 -profile during the lockdown shows a bimodal pattern, just as the profile observed in the years 2015-2019. It can be noted that the peaks aren't from the same magnitude, namely the first peak is more pronounced and reaches $44.77 \mu\text{g}/\text{m}^3$ at 7 a.m. while the second peak only reaches $34.63 \mu\text{g}/\text{m}^3$. The two peaks in the NO_2 -profile of the previous years are relatively from the same magnitude and reach higher values than during the lockdown, namely around $75 \mu\text{g}/\text{m}^3$. It can also be observed that the minimum NO_2 concentrations normally occurs at 3 a.m. with $40.66 \mu\text{g}/\text{m}^3$ and the concentration in the afternoon, between the two peaks, is quite stable around $60 \mu\text{g}/\text{m}^3$. While during the lockdown the concentration after the first peak drops back to around $22 \mu\text{g}/\text{m}^3$ which is equal to the minimum level. The lower concentration during the lockdown can again be attributed to the lower NO emissions coming from traffic and therefore less conversion to NO_2 in the air.

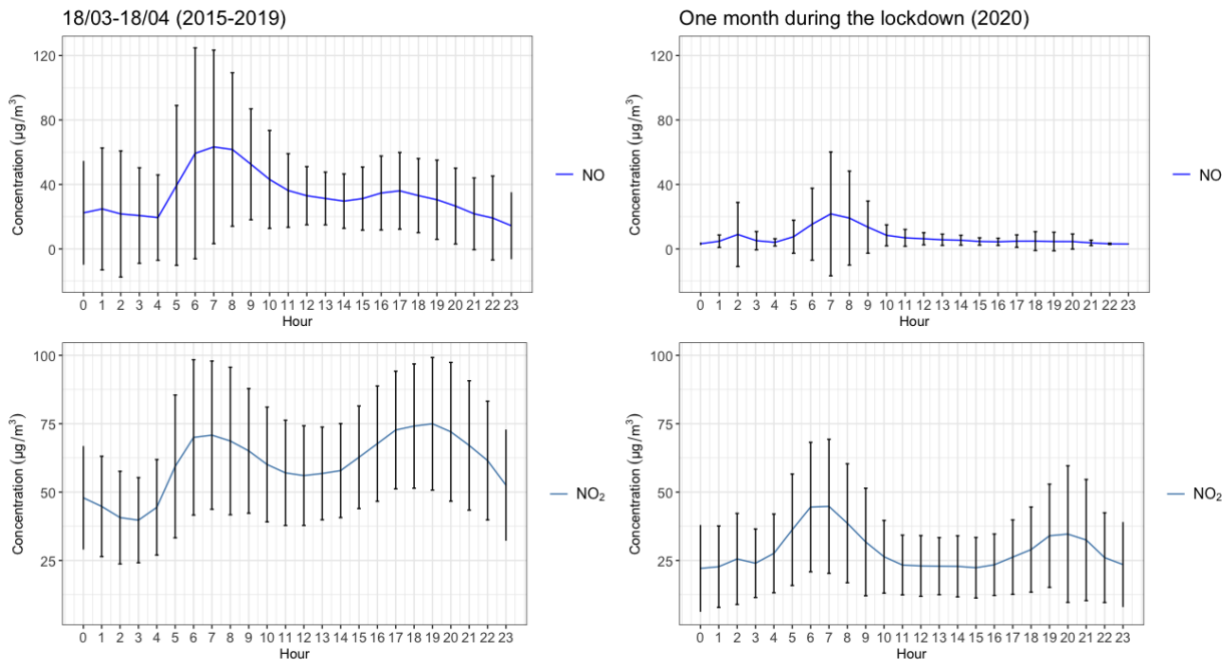


Figure 60: Average daily patterns with error bars, that show the mean concentration +/- SD (Kunst-Wet).

As mentioned before, data was available on the amount of traffic passing by the station at Kunst-Wet per hour. It is interesting to investigate if the corona measures did in fact caused a decrease in the amount of traffic. This can be confirmed with Figure 61. The start of the lockdown is indicated with the dotted line. From that point on, a clear drop in the amount of counts of cars passing at each lane of the road is observed. The amount of cars increases again up to the summer months. During the summer, a decrease can be observed again. This confirms the statements made before that linked the reduction in the amount of traffic with the decrease in NO_x concentrations in the atmosphere and increase in O₃ concentrations.

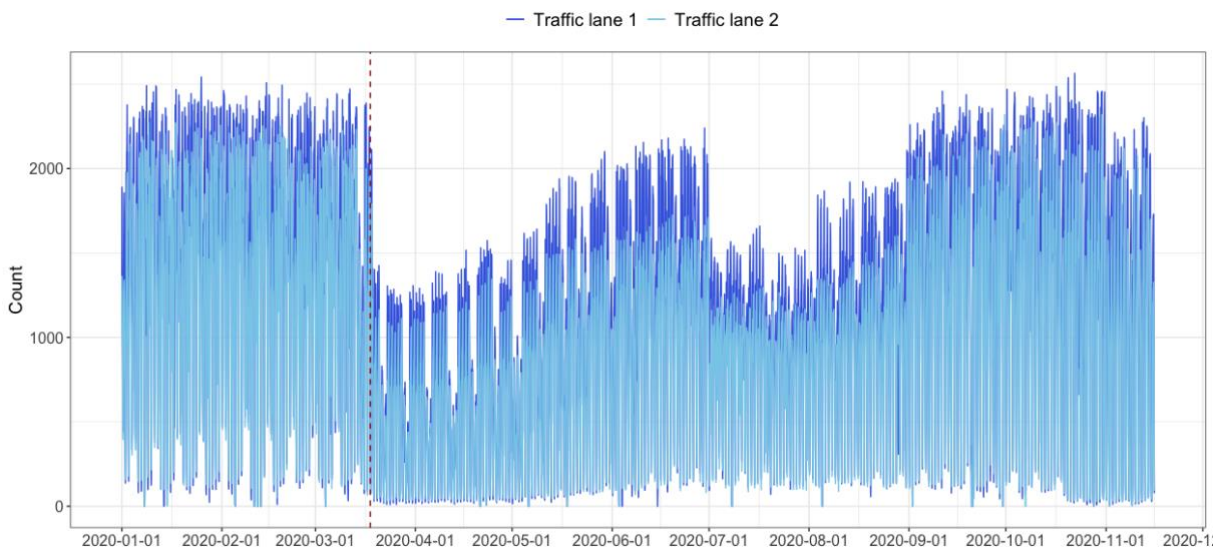


Figure 61: Hourly traffic data of 2020 for the station Kunst-Wet.

8. Conclusion

The aim of this master thesis is to investigate the impact of the corona measures on the concentrations of the traffic-related pollutants NO, NO₂ and O₃ at four different locations, each representing a specific traffic situation. For each pollutant at each location a random forest model is constructed to make predictions of the hourly pollutant concentrations during the lockdown based on weather conditions. The predictions are then used to make a comparison with the measured hourly concentrations in order to detect any changes.

At the background station in Veurne no clear difference is observed between the predicted concentrations and the measured concentrations. The NO_x concentrations increased with the start of the lockdown, i.e. 18th March 2020, and the O₃ concentrations decreased. This can be explained by the fact that the weather conditions were characterized as less favorable for air pollution in the first month of the lockdown. The results for the urban-background station in Ghent show that the predictions made with each model differ from the measurements during the lockdown. Both the NO_x-models predict an increase in the NO_x concentrations as observed in the background station. This increase is seen to a much lesser extent in the measurements. Especially the NO concentrations rather fluctuate during the lockdown than really increase. By contrast, the O₃ concentrations are higher than predicted during the lockdown at this station. The same results are seen in the two urban-traffic locations, one situated in the city center of Brussels and one situated in Sint-Jans-Molenbeek. However, the difference between the predictions and the measurements is more pronounced. These results are in line with the study performed by the VMM. The lower NO concentrations during the lockdown than predicted at these stations can be attributed to the lower NO emissions coming from traffic due to the corona measures. The lower amount of NO causes less conversion with O₃ to NO₂. Hence, the lower NO₂ concentrations and the higher O₃ concentrations.

It can therefore be concluded that the corona measures caused a reduction in the NO_x concentrations during the lockdown and that this reduction is more pronounced in urban-traffic locations. As the background location doesn't experience much traffic in normal conditions, little impact on the amount of traffic passing by the monitoring station is seen during the lockdown and therefore little change in the NO emissions. However, it is confirmed that in the urban-traffic station the amount of traffic did decrease during the lockdown leading to a larger impact of the corona measures on the traffic-related concentrations.

A second objective of this master thesis is to investigate if the daily patterns of the air pollutants during the first month of the lockdown differ from the daily patterns in normal conditions, i.e. the same period in the years 2015-2019. In the background station no clear change was observed in the trend of the daily patterns. For the urban-background and the urban-traffic stations, the NO-profile in normal conditions is characterized with a peak at 7 a.m., i.e. the moment of the morning traffic peak hour. The same trend was seen during the lockdown but the peak didn't reach such high concentrations. This is explained by the lower amount of NO emissions at that time compared with the previous years. The NO₂-profile shows a bimodal pattern in these stations in normal conditions, with a first peak at 7 a.m. and a second peak from the same magnitude at 8 p.m., i.e. respectively the morning and evening peak hours. These peaks are related with the peak in NO concentrations, however, the second peak isn't seen in the NO-profile, which could be explained by a more rapid conversion of NO to NO₂ in the evening.

The NO₂-profile during the lockdown also shows a bimodal pattern at these locations but lower concentrations are observed and the second peak is lower than the first peak. This could imply that the reduction in the amount of traffic during peak hours in the lockdown is larger in the evening. The O₃-profile shows the same trend during the lockdown as in normal condition. A drop in the O₃ concentrations is present at 6 a.m., which is related with the high NO concentrations at that time of the day. Afterwards, there is an increase in the concentrations due to the increasing amount of solar radiation which drives the ozone formation reactions. The O₃-profile has a maximum around 3 p.m. During the lockdown, higher O₃ concentrations are observed and a higher peak in the afternoon. This is attributed to the lower NO concentrations in the atmosphere during the lockdown.

The last objective is to investigate whether the impact of the corona measures on the daily patterns of the air pollutants is different for a week day compared to a weekend day. At the background station, the impact on the daily patterns was the same for a Sunday (a weekend day) and a Tuesday (a week day), i.e. no changes in the NO_x-profiles and the same trend for the O₃-profile but with higher concentrations during the lockdown. The higher concentrations compared with other years are attributed to the higher amount of solar radiation during the first month of the lockdown. Also, the patterns on a Tuesday and a Sunday were in the same line, namely stable NO_x-profiles throughout the day and an increase in the O₃ concentrations starting from 7 a.m. with a maximum in the afternoon. At the urban-traffic location Sint-Jans-Molenbeek, there are noticeable differences between the profiles on a week day and a weekend day. The daily patterns of the pollutants on a Sunday are in line with the patterns observed in the background station. The NO-profile on a Tuesday shows a sharp peak at 7 a.m. The NO₂-profile shows a bimodal pattern with the first peak in the morning and the second (smaller) peak in the evening. The moment of the peaks are related with the traffic peak hours. The O₃-profile shows a drop in the morning and an increase in the concentrations with a maximum in the afternoon. The impact of the corona measures on the daily patterns on a Tuesday and a Sunday are, however, the same. Namely higher O₃ concentrations and lower NO_x concentrations but no clear impact in the trends of the profiles.

9. Bibliography

- AirNow. (2016). *Air Quality Index (AQI) Basics*. <https://doi.org/10.1002/9781119117896.ch4>
- Asman, W. A. H., Sutton, M. A., & Schjørring, J. K. (1998). Ammonia: Emission, atmospheric transport and deposition. *New Phytologist*, 139(1), 27–48. <https://doi.org/10.1046/j.1469-8137.1998.00180.x>
- Atkinson, R. (1998). Atmospheric chemistry of VOCs and NOx. *Atmospheric Environment*, 34, 2063–2101. [https://doi.org/10.1016/0925-4005\(95\)01667-8](https://doi.org/10.1016/0925-4005(95)01667-8)
- Ballesteros-González, K., Sullivan, A. P., & Morales-Betancourt, R. (2020). Estimating the air quality and health impacts of biomass burning in northern South America using a chemical transport model. *Science of the Total Environment*, 739. <https://doi.org/10.1016/j.scitotenv.2020.139755>
- Barletta, B., Meinardi, S., Rowland, F. S., Chan, C. Y., Wang, X., Zou, S., Lo, Y. C., & Blake, D. R. (2005). Volatile organic compounds in 43 Chinese cities. *Atmospheric Environment*, 39(32), 5979–5990. <https://doi.org/10.1016/j.atmosenv.2005.06.029>
- Beeckman, H. (2020). *Files in coronacrisis? 48,5 procent minder auto's op de weg maar hamsteren veroorzaakt wel méér vrachtverkeer | VRT NWS: nieuws*. <https://www.vrt.be/vrtnws/nl/2020/03/26/corona-er-zijn-minder-autos-maar-wel-meer-vrachtwagens-op-de-we/>
- Behera, S. N., & Sharma, M. (2010). Investigating the potential role of ammonia in ion chemistry of fine particulate matter formation for an urban environment. *Science of the Total Environment*, 408(17), 3569–3575. <https://doi.org/10.1016/j.scitotenv.2010.04.017>
- Beliris. (2016). *ARTS-LOI KUNST-WET*.
- Berman, J. D., & Ebisu, K. (2020). Changes in U.S. air pollution during the COVID-19 pandemic. *Science of the Total Environment*, 739, 139864. <https://doi.org/10.1016/j.scitotenv.2020.139864>
- Breiman, L. (1984). *Classification and regression trees*. Chapman & Hall/CSR.
- Breiman, L. (2001). Random forests. *Machine Learning*, 45, 5–32. <https://doi.org/10.1201/9780429469275-8>
- Brimblecombe, P., & Lai, Y. (2021). Diurnal and weekly patterns of primary pollutants in Beijing under COVID-19 restrictions. *Faraday Discussions*. <https://doi.org/10.1039/d0fd00082e>
- Bronsema, B. (2011). *Natuurlijke Ventilatie en Wind*. December. www.rvo.nl
- Broomandi, P., Karaca, F., Nikfal, A., Jahanbakhshi, A., Tamjidi, M., & Kim, J. R. (2020). Impact of covid-19 event on the air quality in Iran. *Aerosol and Air Quality Research*, 20(8), 1793–1804. <https://doi.org/10.4209/aaqr.2020.05.0205>
- Brussel Mobiliteit. (2021). *Brussel Mobiliteit*. <https://mobilite-mobiliteit.brussels/nl>
- Brussels Hoofdstedelijk Gewest. (2018). *Brussel in cijfers*. Visit.Brussels. <https://visit.brussels/nl/article/Brussel-in-cijfers>
- Buchem B.V. (2015). *TENAX-GR Porous Polymer, Resin*. <https://www.buchem.com/product/tenax-porous-polymer-resin/tenax-gr.html>
- CENR. (2000). Atmospheric Ammonia : Sources and Fate A Review of Ongoing Federal Research and. *October, June*.
- Chakure, A. (2019). *Random Forest Regression*. Medium. <https://medium.com/swlh/random-forest-and-its-implementation-71824ced454f>
- Chen, Q. X., Huang, C. L., Yuan, Y., & Tan, H. P. (2020). Influence of covid-19 event on air quality and their association in mainland China. *Aerosol and Air Quality Research*, 20(7), 1541–1551. <https://doi.org/10.4209/aaqr.2020.05.0224>
- Chromatotec group. (2009). *airmo BTX 1000*. www.chromatotec.com
- Chromatotec group. (2016). *airmo BTX 1000*. www.chromatotec.com
- Cole, M. A., Elliott, R. J. R., & Liu, B. (2020). The Impact of the Wuhan Covid-19 Lockdown on Air Pollution and Health: A Machine Learning and Augmented Synthetic Control Approach. *Environmental and Resource Economics*, 76(4), 553–580. <https://doi.org/10.1007/s10640-020-00483-4>

- Daly, A., & Zannetti, P. (2007). An Introduction to Air Pollution – Definitions , Classifications , and History. *Science And Technology*, 1–14.
- De Leeuw, F. A. A. M. (2002). A set of emission indicators for long-range transboundary air pollution. *Environmental Science and Policy*, 5(2), 135–145.
[https://doi.org/10.1016/S1462-9011\(01\)00042-9](https://doi.org/10.1016/S1462-9011(01)00042-9)
- Departement Omgeving Vlaanderen. (2019). *Luchtbeleidsplan 2030*.
- DG Sante. (2015). *Evaluation and fitness check (fc) roadmap*. 1(2), 1–8.
- ECE. (2019). *Economic and Social Council Economic Commission for Europe Executive Body for the Convention on Long-range*. December.
- ECMWF. (2021). *Total cloud cover*.
https://www.ecmwf.int/en/forecasts/charts/catalogue/medium-clouds?facets=undefined&time=2021022500,0,2021022500&projection=classical_arctic
- EEA. (2008). *Tropospheric ozone: background information — European Environment Agency*.
<https://www.eea.europa.eu/publications/TOP08-98/page004.html>
- EEA. (2020). Air quality in Europe - 2020 report. In *EEA Report* (Issue No 09/2020).
<https://www.eea.europa.eu//publications/air-quality-in-europe-2020-report>
- EU. (2004). *Richtlijn 2004/107/EG*. 6, 34–44.
- EU. (2008). *Richtlijn 2008/50/EG*. 1–44.
- European Commission. (n.d.). *Air - Policies - Environment - European Commission*. Retrieved March 3, 2021, from https://ec.europa.eu/environment/air/index_en.htm
- European Commission. (2013). *Environment: New policy package to clean up Europe's air*. 18 December, 3.
- European Commission. (2019). *REPORT FROM THE COMMISSION TO THE EUROPEAN PARLIAMENT, THE COUNCIL, THE EUROPEAN ECONOMIC AND SOCIAL COMMITTEE AND THE COMMITTEE OF THE REGIONS*.
- European Commission. (2020a). *Een Europese Green Deal | Europese Commissie*. A European Green Deal. https://ec.europa.eu/info/strategy/priorities-2019-2024/european-green-deal_nl
- European Commission. (2020b). *Proposal for a DECISION OF THE EUROPEAN PARLIAMENT AND OF THE COUNCIL on a General Union Environment Action Programme to 2030*. 0300, 34.
- European Environment Agency (EEA). (2013). *Air quality in Europe — 2013 report* (Issue 9).
<http://www.eea.europa.eu/publications/air-quality-in-europe-2013>
- European Environment Agency (EEA). (2020). *Air pollution goes down as Europe takes hard measures to combat coronavirus — European Environment Agency*.
<https://www.eea.europa.eu/highlights/air-pollution-goes-down-as>
- European Parliament and Council. (2016). DIRECTIVE (EU) 2016/2284 OF THE EUROPEAN PARLIAMENT AND OF THE COUNCIL of 14 December 2016 on on the reduction of national emissions of certain atmospheric pollutants, amending Directive 2003/35/EC and repealing Directive 2001/81/EC. *Official Journal of the European Union*, L 344(17.12.2016), 1–31.
- European Parliament, & Council of the European Union. (2001). Directive 2001/81/EC on national emission ceilings for atmospheric pollutants. *Official Journal of the European Communities*, L 309, 22–30.
- Europese Unie. (2021). *Europees Parlement - EUROPA | Europese Unie*.
https://europa.eu/european-union/about-eu/institutions-bodies/european-parliament_nl
- Fernando, J. (2020). *R-Squared Definition*. Investopedia.
<https://www.investopedia.com/terms/r/r-squared.asp>
- Finlayson-Pitts, B. J., & Pitts, J. N. (1993). Atmospheric chemistry of tropospheric ozone formation: Scientific and regulatory implications. *Air and Waste*, 43(8), 1091–1100.
<https://doi.org/10.1080/1073161X.1993.10467187>
- Fuhrer, J., Skärby, L., & Ashmore, M. R. (1997). Critical levels for ozone effects on vegetation in Europe. *Environmental Pollution*, 97(1–2), 91–106. [https://doi.org/10.1016/S0269-7491\(97\)00067-5](https://doi.org/10.1016/S0269-7491(97)00067-5)
- Google. (2019). *Reigersstraat - Google Maps*.

- <https://www.google.be/maps/@51.016178,2.5824676,3a,75y,294.96h,98.8t/data=!3m6!1e1!3m4!1sjZgAGNNsMp17EINfBsnYrg!2e0!7i13312!8i6656>
- Google Maps. (n.d.). *Meetstation Houtem Veurne*. Retrieved February 23, 2021, from <https://www.google.com/maps/place/Meetstation+Houtem+Veurne/@51.0139089,2.5763349,14z/data=!4m19!1m13!4m12!1m3!2m2!1d2.5490696!2d51.0890521!1m6!1m2!1s0x47dc95d42c5848f9:0xcc052efa2e6e171c!2sMeetstation+Houtem+Veurne,+Houtem+Ring sloot,+8630+Veurne!2m2!1d2>.
- Grange, S. K. (2020). *Package 'rmweather'*. <https://doi.org/10.5194/acp-18-6223-2018>
- Gross, A. (2020). *Binary search trees and recursion*. Gitconnected. <https://doi.org/10.1017/cbo9780511804793.013>
- Gualano, M. R., Lo Moro, G., Voglino, G., Bert, F., & Siliquini, R. (2020). Effects of COVID-19 lockdown on mental health and sleep disturbances in Italy. *International Journal of Environmental Research and Public Health*, 17(13), 1–13. <https://doi.org/10.3390/ijerph17134779>
- Guan, W., Ni, Z., Hu, Y., Liang, W., Ou, C., He, J., Liu, L., Shan, H., Lei, C., Hui, D. S. C., Du, B., Li, L., Zeng, G., Yuen, K.-Y., Chen, R., Tang, C., Wang, T., Chen, P., Xiang, J., ... Zhong, N. (2020). Clinical Characteristics of Coronavirus Disease 2019 in China. *New England Journal of Medicine*, 382(18), 1708–1720. <https://doi.org/10.1056/nejmoa2002032>
- Harrison, R. M. (2005). *Outdoor Air*. A, 1–2. http://www.who.int/phe/health_topics/outdoorair/databases/en/
- Holtzlag, A. A. M., Svensson, G., Baas, P., Basu, S., Beare, B., Beljaars, A. C. M., Bosveld, F. C., Cuxart, J., Lindvall, J., Steeneveld, G. J., Tjernström, M., & Van De Wiel, B. J. H. (2013). Stable atmospheric boundary layers and diurnal cycles: Challenges for weather and climate models. *Bulletin of the American Meteorological Society*, 94(11), 1691–1706. <https://doi.org/10.1175/BAMS-D-11-00187.1>
- i-CITY. (n.d.). *Lage Emissie Zone | Stad Brussel*. Retrieved March 1, 2021, from <https://www.brussel.be/lez>
- Informatie Vlaanderen. (2020a). *Gent | Vlaanderen.be*. <https://www.vlaanderen.be/gemeenten-en-provincies/provincie-oost-vlaanderen/gent>
- Informatie Vlaanderen. (2020b). *Veurne | Vlaanderen.be*. <https://www.vlaanderen.be/gemeenten-en-provincies/provincie-west-vlaanderen/veurne>
- irCELine. (2019). *BelAQI Index*. <https://www.irceline.be/en/air-quality/measurements/belaqi-air-quality-index/information>
- irCELine. (n.d.). *Interactieve viewer*. Retrieved February 23, 2021, from <https://www.irceline.be/nl/luchtkwaliteit/metingen/meetstations>
- irCELine. (2021). *Interactieve viewer*. <https://www.irceline.be/nl/luchtkwaliteit/metingen/meetstations>
- IVL. (2015). *Diffusive sampling*. <https://doi.org/10.1080/1047322X.1998.10389145>
- James, G., Witten, D., Hastie, T., & Tibishirani, R. (2013). An Introduction to Statistical Learning with Applications in R. *Springer Texts in Statistics*, 426. <http://books.google.com/books?id=9tv0tal8l6YC>
- Kampa, M., & Castanas, E. (2008). Human health effects of air pollution. *Environmental Pollution*, 151(2), 362–367. <https://doi.org/10.1016/j.envpol.2007.06.012>
- Kerimray, A., Baimatova, N., Ibragimova, O. P., Bukenov, B., Kenessov, B., Plotitsyn, P., & Karaca, F. (2020). Assessing air quality changes in large cities during COVID-19 lockdowns: The impacts of traffic-free urban conditions in Almaty, Kazakhstan. *Science of the Total Environment*, 730, 139179. <https://doi.org/10.1016/j.scitotenv.2020.139179>
- Krupa, S. V., & Manning, W. J. (1988). Atmospheric ozone: Formation and effects on vegetation. *Environmental Pollution*, 50(1–2), 101–137. [https://doi.org/10.1016/0269-7491\(88\)90187-X](https://doi.org/10.1016/0269-7491(88)90187-X)
- Lai, C., Shih, T., Ko, W., Tang, H., & Hsueh, P. (2020). International Journal of Antimicrobial Agents Severe acute respiratory syndrome coronavirus 2 (SARS-CoV-2) and coronavirus disease-2019 (COVID-19): The epidemic and the challenges. *International Journal of Antimicrobial Agents*, 55(3), 105924. <https://doi.org/10.1016/j.ijantimicag.2020.105924>

- Lee, B. K., Jun, N. Y., & Lee, H. K. (2005). Analysis of impacts on urban air quality by restricting the operation of passenger vehicles during Asian Game events in Busan, Korea. *Atmospheric Environment*, 39(12), 2323–2338. <https://doi.org/10.1016/j.atmosenv.2004.11.044>
- Lee, D. S., Holland, M. R., & Falla, N. (1996). The potential impact of ozone on materials in the U.K. *Pergamon*.
- Leelossy, Á., Molnár Jr., F. M., Izsák, F., Ágnes, H., Lagzi, I., & Mészáros, R. (2014). Dispersion modeling of air pollutants in the atmosphere : a review. *Central European Journal of Geosciences*, 6(3). <https://doi.org/10.2478/s13533-012-0188-6>
- Lelieveld, J., & Dentener, F. J. (2000). What controls tropospheric ozone? *Journal of Geophysical Research Atmospheres*, 105(D3), 3531–3551. <https://doi.org/10.1029/1999JD901011>
- Lelieveld, J., Klingmüller, K., Pozzer, A., Pöschl, U., Fnais, M., Daiber, A., & Münzel, T. (2019). Cardiovascular disease burden from ambient air pollution in Europe reassessed using novel hazard ratio functions. *European Heart Journal*, 40(20), 1590–1596. <https://doi.org/10.1093/eurheartj/ehz135>
- Liao, T., Gui, K., Jiang, W., Wang, S., Wang, B., Zeng, Z., Che, H., Wang, Y., & Sun, Y. (2018). Air stagnation and its impact on air quality during winter in Sichuan and Chongqing, southwestern China. *Science of the Total Environment*, 635, 576–585. <https://doi.org/10.1016/j.scitotenv.2018.04.122>
- Mallet, V., & Sportisse, B. (2008). Air quality modeling: From deterministic to stochastic approaches. *Computers and Mathematics with Applications*, 55(10), 2329–2337. <https://doi.org/10.1016/j.camwa.2007.11.004>
- Metro. (2020). *Zo kreeg het coronavirus België in zijn greep | Metro*. <https://nl.metrotime.be/2020/05/19/must-read/zo-kreeg-het-coronavirus-belgie-in-zijn-greep/>
- Molnar, C. (2020). *5.5 Permutation Feature Importance | Interpretable Machine Learning*. <https://christophm.github.io/interpretable-ml-book/feature-importance.html>
- Nakada, L. Y. K., & Urban, R. C. (2020). COVID-19 pandemic: Impacts on the air quality during the partial lockdown in São Paulo state, Brazil. *Science of the Total Environment*, 730, 139087. <https://doi.org/10.1016/j.scitotenv.2020.139087>
- NoodweerBenelux. (2021). *Lagedruk en hogedrukgebieden*. <https://www.noodweer.be/lagedrukgebieden-en-hogedrukgebieden/>
- Pinder, R W, Gilliland, A. B., & Dennis, R. L. (2008). Environmental impact of atmospheric NH 3 emissions under present and future conditions in the eastern United States. *Geophysical*, 35(April 2008), 1–6. <https://doi.org/10.1029/2008GL033732>
- Pinder, Robert W., Adams, P. J., & Pandis, S. N. (2007). Ammonia emission controls as a cost-effective strategy for reducing atmospheric particulate matter in the Eastern United States. *Environmental Science and Technology*, 41(2), 380–386. <https://doi.org/10.1021/es060379a>
- Pott, D. A., Marais, E. A., Boesch, H., Pope, R. J., & Lee, J. (2021). *Diagnosing air quality changes in the UK during the COVID-19 lockdown using TROPOMI and GEOS-Chem*. October, 37–41.
- Pronobis, M. (2020). *Environmentally Oriented Modernization of Power Boilers* (Issue 2). Elsevier. <https://doi.org/10.1016/B978-0-12-819921-3/00004-2>
- Rai, R., Rajput, M., Agrawal, M., & Agrawal, S. B. (2011). Gaseous Air Pollutants : a Review on Current and Future Trends of Emissions and Impact on Agriculture. *Journal of Scientific Research*, 55(771), 1.
- Ren, X. (2020). Pandemic and lockdown: a territorial approach to COVID-19 in China, Italy and the United States. *Eurasian Geography and Economics*, 00(00), 1–12. <https://doi.org/10.1080/15387216.2020.1762103>
- Rijksoverheid. (2019). *IBO Luchtkwaliteit*. 1–87.
- Sasquatch Station. (2017). *Wind Page*. <https://www.sasquatchstation.com/Wind.php>
- Schifer, L. D., Heald, C. L., Nowak, J., & Holloway, J. (2014). An investigation of ammonia and inorganic particulate matter in California during the CalNex campaign. *Journal of Geophysical Research : Atmospheres*, 1883–1902. <https://doi.org/10.1002/2013JD020765>. Received

- Sharma, N., & Agarwal, A. K. (2018). *Air pollution and Control*. Springer.
https://doi.org/10.1007/978-981-10-7185-0_6
- Sitaras, I. E., & Siskos, P. A. (2008). The role of primary and secondary air pollutants in atmospheric pollution: Athens urban area as a case study. *Environmental Chemistry Letters*, 6(2), 59–69. <https://doi.org/10.1007/s10311-007-0123-0>
- Stad Gent. (2020). *Mobiliteitsplan, Circulatieplan en Parkeerplan Gent | Stad Gent*.
<https://stad.gent/nl/mobiliteit-openbare-werken/mobiliteit/plannen-projecten-subsidies-cijfers-scholenwerking/mobiliteitsplan-circulatieplan-en-parkeerplan-gent>
- Stull, R. B. (1988). An introduction to boundary layer meteorology. In *An introduction to boundary layer meteorology*. Kluwer Academic; Atmospheric Sciences Library, 13.
<https://doi.org/10.1007/978-94-009-3027-8>
- Synspec. (2019). *GC955 SYN SPEC BENZENE / BTEX ANALYSER*.
- Teledyne Technologies Incorporated. (2021). *T400*. <http://www.teledyne-api.com/products/oxygen-compound-instruments/t400>
- Thermo Fisher Scientific Inc. (n.d.). *Model 42i (NO-NO2-NOx)*. Retrieved April 1, 2021, from <https://www.thermofisher.com/order/catalog/product/42I#/42I>
- Thermo Fisher Scientific Inc. (2007). *Model 42. 2*.
- Tom Mitchell. (1997). Machine Learning. In McGraw Hill (Ed.), *McGraw Hill*.
<http://www.cs.cmu.edu/afs/cs.cmu.edu/user/mitchell/ftp/mlbook.html>
- Trinh, T. T., Trinh, T. T., Le, T. T., Nguyen, T. D. H., & Tu, B. M. (2019). Temperature inversion and air pollution relationship, and its effects on human health in Hanoi City, Vietnam. *Environmental Geochemistry and Health*, 41(2), 929–937. <https://doi.org/10.1007/s10653-018-0190-0>
- U.S. Environmental Protection Agency. (2018). *Technical Assistance Document for the Reporting of Daily Air Quality – the Air Quality Index (AQI)*.
<https://airnowtest.epa.gov/sites/default/files/2018-05/aqi-technical-assistance-document-may2016.pdf>
- United Nations. (2018). *Decision 2018 / 5 Long-term strategy for the Convention on Long-range Transboundary Air Pollution for 2020 – 2030 and beyond Annex Long-term strategy for the Convention on Long-range Transboundary Air Pollution for 2020 – 2030 and beyond I. Introduction. c, 1–15*.
- United Nations. (2020). *The Sustainable Development Goals Report 2020*. 4–5.
<https://doi.org/10.18356/2282dd98-en>
- Universiteit Gent. (2020). *Organisatie en cijfers — Universiteit Gent*.
<https://www.ugent.be/nl/univgent/waarvoor-staat-ugent>
- Van Langenhove, H., & Walgraeve, C. (2019). *Milieuchemie: organisch Inleiding tot de eco-chemie*.
- Vancraeynest, L. (2013). MIRA Milieurapport Vlaanderen, Themabeschrijving Fotochemische luchtverontreiniging. *Milieurapport Vlaanderen*, 28.
- Varian, H. R. (2014). Big data: New tricks for econometrics. *Journal of Economic Perspectives*, 28(2), 3–28. <https://doi.org/10.1257/jep.28.2.3>
- Vlaamse Milieumaatschappij. (n.d.). *Methodiek NOx-meting*. Retrieved May 17, 2021, from <https://www.vmm.be/data/zwaveldioxide-stikstofoxiden-koolstofmonoxide-en-benzeen/methodiek-nox-meting>
- Vlaamse Milieumaatschappij. (2020a). *Jaarrapport Lucht - Effecten van luchtvervuiling op gezondheid en ecosystemen*.
- Vlaamse Milieumaatschappij. (2020b). *Jaarrapport Lucht - Emissies en concentraties van luchtverontreinigende stoffen*.
- VMM. (2011). *NO2 -meetcampagne met passieve samplers in steden in 2010 (Issue 2)*.
- VMM. (2013a). *Luchtkwaliteit in het Vlaamse Gewest. Jaarverslag Immissiemeetnetten – 2013*.
- VMM. (2013b). *Luchtkwaliteit in Vlaanderen – Zure regen in Vlaanderen in 2011*.
- VMM. (2016). *Luchtkwaliteit in het Vlaamse Gewest. Jaarverslag Immissiemeetnetten – 2016 Bijlagen*.
- VMM. (2017a). *Jaarverslag Immissiemeetnetten – 2016*.
- VMM. (2017b). *Over VMM — Vlaamse Milieumaatschappij*. VMM. <https://www.vmm.be/over->

vmm

- VMM. (2019). *2019_Algemene informatie*.
- VMM. (2020a). *Het effect van de COVID-19 maatregelen op de luchtkwaliteit in België een inschatting met een Random Forest model*.
- VMM. (2020b). *Uitstoot En Luchtkwaliteit in Vlaanderen: Evaluatie 2020 - Samenvatting*.
<https://www.vmm.be/publicaties/lucht-2020/uitstoot-en-luchtkwaliteit-in-vlaanderen-evaluatie-2020>
- VMM. (2021). *Actuele luchtkwaliteit — Vlaamse Milieumaatschappij*.
<https://www.vmm.be/data/actuele-luchtkwaliteit>
- Vuong, Q. T., Thang, P. Q., Park, M. K., & Choi, S. D. (2020). Effects of the COVID-19 lockdown on criteria air pollutants in the city of Daegu, the epicenter of South Korea's outbreak. *Environmental Science and Pollution Research*, 27(36), 45983–45991.
<https://doi.org/10.1007/s11356-020-11360-4>
- Wang, L., Li, M., Yu, S., Chen, X., Li, Z., Zhang, Y., Jiang, L., Xia, Y., Li, J., Liu, W., Li, P., Lichtfouse, E., Rosenfeld, D., & Seinfeld, J. H. (2020). Unexpected rise of ozone in urban and rural areas, and sulfur dioxide in rural areas during the coronavirus city lockdown in Hangzhou, China: implications for air quality. *Environmental Chemistry Letters*, 18(5), 1713–1723.
<https://doi.org/10.1007/s10311-020-01028-3>
- Wang, S., Zhang, Y., Ma, J., Zhu, S., Shen, J., Wang, P., & Zhang, H. (2021). Responses of decline in air pollution and recovery associated with COVID-19 lockdown in the Pearl River Delta. *Science of the Total Environment*, 756, 143868.
<https://doi.org/10.1016/j.scitotenv.2020.143868>
- WHO. (1997). *Guidelines for Air Quality*.
- WHO. (2018). *Ambient (outdoor) air pollution*. [https://www.who.int/en/news-room/fact-sheets/detail/ambient-\(outdoor\)-air-quality-and-health](https://www.who.int/en/news-room/fact-sheets/detail/ambient-(outdoor)-air-quality-and-health). [https://www.who.int/news-room/fact-sheets/detail/ambient-\(outdoor\)-air-quality-and-health](https://www.who.int/news-room/fact-sheets/detail/ambient-(outdoor)-air-quality-and-health)
- WHO. (2020). Coronavirus Disease 2019 Situation Report 51 - 11th March 2020. *WHO Bulletin*, 2019(March), 2633. <https://www.who.int/emergencies/diseases/novel-coronavirus-2019>
- World Health Organization. (2005). *WHO Air quality guidelines for particulate matter, ozone, nitrogen dioxide and sulfur dioxide*. <https://doi.org/10.1007/s12011-019-01864-7>
- World Health Organization. (2013). Health risks of air pollution in Europe – HRAPIE project. *World Health Organization (WHO)*, 60. <http://tinyurl.com/oe8wmc6%0A>
- Xu, K., Cui, K., Young, L. H., Wang, Y. F., Hsieh, Y. K., Wan, S., & Zhang, J. (2020). Air quality index, indicator air pollutants and impact of covid-19 event on the air quality near central china. *Aerosol and Air Quality Research*, 20(6), 1204–1221.
<https://doi.org/10.4209/aaqr.2020.04.0139>
- Yadav, R., Korhale, N., Anand, V., Rathod, A., Bano, S., Shinde, R., Latha, R., Sahu, S. K., Murthy, B. S., & Beig, G. (2020). Urban Climate COVID-19 lockdown and air quality of SAFAR-India metro cities. *Urban Climate*, 34(October), 100729.
<https://doi.org/10.1016/j.uclim.2020.100729>
- Zhang, Q., Jiang, X., Tong, D., Davis, S. J., Zhao, H., Geng, G., Feng, T., Zheng, B., Lu, Z., Streets, D. G., Ni, R., Brauer, M., Van Donkelaar, A., Martin, R. V., Huo, H., Liu, Z., Pan, D., Kan, H., Yan, Y., ... Guan, D. (2017). Transboundary health impacts of transported global air pollution and international trade. *Nature*, 543(7647), 705–709. <https://doi.org/10.1038/nature21712>
- Zhou, Y., Wu, Y., Yang, L., Fu, L., He, K., Wang, S., Hao, J., Chen, J., & Li, C. (2010). The impact of transportation control measures on emission reductions during the 2008 Olympic Games in Beijing, China. *Atmospheric Environment*, 44(3), 285–293.
<https://doi.org/10.1016/j.atmosenv.2009.10.040>